A PHENOMENOLOGICAL TREATMENT OF THERMAL EXPANSION IN CRYSTALS OF THE LOWER SYMMETRY CLASSES AND THE CRYSTAL STRUCTURES OF $CaCoSi_2O_6$ AND $CaNiSi_2O_6$

by

John L. Schlenker

Dissertation submitted to the Graduate Faculty of the

Virginia Polytechnic Institute and State University

in partial fulfillment of the requirements for the degree of

DOCTOR OF PHILOSOPHY

in

Geological Sciences

APPROVED

G.V. Gibbs, Chairman

F.K. Ross

P.H. Ribbe

J.C. Schug

M.B. Boisen

July, 1976

Blacksburg, Virginia

ACKNOWLEDGMENTS

The author wishes to thank Dr. G.V. Gibbs for his interest, aid, and encouragement during all aspects of this work. I also wish to express my appreciation to Dr. Monte B. Boisen, Jr. of the Department of Mathematics for his helpful discussions and advice with regard to the material contained in Chapter One and to Dr. Frederick K. Ross of the Department of Chemistry for his help with the material contained in Chapter Two.

I wish to thank Mrs. Ramonda Haycocks for typing Appendices A and B and the major part of Chapter One, Mrs. Margie Strickler for typing Chapter Two, and Ms. Gail Walbridge for typing the initial rough draft. All graphs and drawings were made by Mrs. Sharon Chiang and Dr. J. Alexander Speer. They are also thanked.

TABLE OF CONTENTS

TABLE OF CONTENTS, continued

TABLE OF CONTENTS, continued

LIST OF TABLES

LIST OF TABLES, continued

LIST OF FIGURES

LIST OF FIGURES, continued

LIST OF FIGURES, continued

INTRODUCTION

Appendices A and B of this dissertation are short reviews of the theory of stress and strain. They contain nothing new. Their sole purpose is to provide an introduction to the material presented in chapter one. Chapter one constitutes the bulk of the dissertation. It contains a detailed analysis of procedures which have been utilized to compute thermal expansion coefficients of single crystals. These are considered in roughly the historical order of their appearance. Four new sets of expressions are developed. Two of these are applicable to crystals of monoclinic and higher symmetry while the remaining two are exact linear Lagrangian and Eulerian formulations applicable to all crystal systems. The exact linear Lagrangian form is given in Born and Huang (1968) but in a very abstract form. It was redeveloped, apparently independently, by Ohashi and Burnham (1973) and presented in a less abstract way. It is presented here in a way which is in closest accord with the fundamental definition of the thermal expansion tensor. The approximate linear Eulerian thermal expansion coefficients developed here are then used to compute thermal expansion coefficients of indialite, emerald, and beryl and of the clinopyroxenes: spodumene, jadeite, acmite, ureyite, hedenbergite, and diopside. The results agree, in general, with those arrived at using the Ohashi-Burnham equations.

Chapter two is concerned with a refinement of the crystal structures of the synthetic clinopyroxenes $CaCoSi_2O_6$ and $CaNiSi_2O_6$.

CHAPTER I

A PHENOMENOLOGICAL TREATMENT OF THERMAL EXPANSION IN CRYSTALS WITH APPLICATION TO MINERALS

Introduction

From an intuitive point of view, thermal expansion appears to be one of the simplest physical properties of a crystal. It is a phenomenon that can be directly observed and one that may be interpreted in terms of simple mechanical models (Megaw, 1973), however, this apparent simplicity is deceptive. This is true not only because a correct theoretical treatment of the phenomenon, in terms of the anharmonic model, is exceedingly complex, but also because there is a considerable lack of uniformity of procedures and confusion about definitions in even the more elementary aspects of the subject.

Basic Theory

When a material is heated from a temperature T_o to a temperature T a mapping is defined (one-to-one onto) in which a material point initially occupying the position (X_1,X_2,X_3) at temperature T_o moves until it is located at the position (x_1,x_2,x_3) at temperature T (see Appendix B). The ith component of the displacement is given by

$$u_i = x_i - X_i \tag{1-1}$$

where i = 1,2,3. The deformation (thermal strain) which a substance undergoes on heating may be succinctly summarized in mathematical form by means of a strain tensor of which there are several kinds, for example:

(1-2) the *finite Lagrangian (Green's) strain tensor* defined as

$$L_{ij} = \frac{1}{2}\left(\frac{\partial u_i}{\partial X_j} + \frac{\partial u_j}{\partial X_i} + \frac{\partial u_k}{\partial X_i}\frac{\partial u_k}{\partial X_j}\right) ,$$

(1-3) the *finite Eulerian (Almansi's) strain tensor* defined as

$$E_{ij} = \left(\frac{1}{2}\frac{\partial u_i}{\partial x_j} + \frac{\partial u_j}{\partial x_i} + \frac{\partial u_k}{\partial x_i}\frac{\partial u_k}{\partial x_j}\right) ,$$

(1-4) the *linear Lagrangian strain tensor* defined as

$$\ell_{ij} = \frac{1}{2}\left(\frac{\partial u_i}{\partial X_j} + \frac{\partial u_j}{\partial X_i}\right) ,$$

and

(1-5) the *linear Eulerian strain tensor* defined as

$$e_{ij} = \frac{1}{2}\left(\frac{\partial u_i}{\partial x_j} + \frac{\partial u_j}{\partial x_i}\right) .$$

Let η_{ij} represent the components of an arbitrary strain tensor without specifying the type. The thermal expansion property of the crystal (which is a property just as characteristic of the substance as color, hardness, etc.) is described by six coefficients α_{ij} ($\alpha_{ij} = \alpha_{ji}$) defined by the equations

(1-6) $\alpha_{ij}(T) = \partial\eta_{ij}(T)/\partial T$

(Smith, 1958) under conditions of constant stress. Other constraints may be significant in some cases. In addition the $\alpha_{ij}(T)$ are usually measured under conditions of zero stress. Naturally there are as many different types of thermal expansion as there are types of strain, for example,

(1-7) $\Gamma_{ij} = (\partial L_{ij}/\partial T)_{\sigma}$

and

(1-8) $E'_{ij} = (\partial E_{ij}/\partial T)_{\sigma}$.

Since the Γ_{ij} and E'_{ij} are obtained by taking the derivatives of the corresponding elements of the finite Eulerian and Lagrangian strain tensors respectively they can be referred to as the finite Lagrangian and Eulerian thermal expansion coefficients of the medium.

Thermal expansion is often referred to as a tensor-scalar property because it relates a dependent tensor quantity (i.e. the $d\eta_{ij}$ in the expression $d\eta_{ij} = \alpha_{ij}dT$) to an independent scalar property dT. The rank of a tensor property involved in a property equation is given by a simple rule (McMillan, 1968)

(1-9) Rank of independent-variable tensor +
Rank of dependent quantity tensor =
Rank of property tensor.

Since the temperature, a scalar, is a tensor of zero rank and since strain is a second rank tensor (nine components) we have from equation (1-9)

(1-10) Rank of property tensor (i.e. the thermal expansion tensor)
= 0 + 2 = 2

Because a crystal is a complex thermodynamic system it is not permissible to treat one physical property as if it is isolated from all others (Bhagavantam, 1966). This is also true for the thermal expansion property. For a nonmagnetic crystal, that is, for a crystal whose magnetic susceptibilities are zero, the thermodynamic state is fixed by the applied stress, [σ], a second rank tensor, the applied electric field, [E], a first rank tensor or vector, and the temperature, T, a

zero rank tensor or scalar. These 13 parameters constitute the independent thermodynamic variables for the system. All remaining thermodynamic parameters, such as internal energy, U, a scalar, the dielectric displacement, [D], a vector, the entropy, S, a scalar, and the strain, [η], a second rank tensor, are to be regarded as dependent functions of these 13 independent variables. For example, for the strain we have

$$(1\text{-}11)\quad \eta_{ij} = \eta_{ij}(\sigma_{11}, \sigma_{12}, \sigma_{13}, \sigma_{21}, \sigma_{22}, \sigma_{23}, \sigma_{31}\ \sigma_{32}, \sigma_{33}, E_1, E_2, E_3, T)$$

(nine equations). The total derivative of eq. (1-11) is

$$(1\text{-}12)\quad d\eta_{ij} = \left(\frac{\partial \eta_{ij}}{\partial \sigma_{kl}}\right)_{E,T} d\sigma_{kl} + \left(\frac{\partial \eta_{ij}}{\partial E_k}\right)_{\sigma,T} dE_k + \left(\frac{\partial \eta_{ij}}{\partial T}\right)_{E,\sigma} dT\ .$$

Under conditions of zero stress, $\sigma_{ij} = 0$, eq. (1-12) becomes

$$(1\text{-}13)\quad d\eta_{ij} = d^T_{kij} dE_k + \alpha^E_{ij} dT$$

where the $d^T_{kij} = (\partial \eta_{ij}/\partial E_k)_T$ are the piezoelectric coefficients and the $\alpha^E_{ij} = (\partial \eta_{ij}/\partial T)_E$ are the thermal expansion coefficients under the conditions of constant electric field. On differentiating eq. (1-13) with respect to temperature at constant dielectric displacement and setting $(\partial \eta_{ij}/\partial T)_D = \alpha^D_{ij}$ we obtain

$$(1\text{-}14)\quad \alpha^D_{ij} = d^T_{kij}\left(\frac{\partial E_k}{\partial T}\right)_D + \alpha^E_{ij}$$

The dielectric displacement is given implicitly by

$$(1\text{-}15)\quad D_i = D_i(\sigma_{11}, \sigma_{12}, \sigma_{13}, \sigma_{21}, \sigma_{22}, \sigma_{23}, \sigma_{31}, \sigma_{32}, \sigma_{33}, E_1, E_2, E_3, T)\ ,$$

and the total differential is at zero stress is

$$(1\text{-}16)\quad dD_i = \left(\frac{\partial D_i}{\partial E_k}\right)_T dE_k + \left(\frac{\partial D_i}{\partial T}\right)_E dT = \kappa_{ij}^T dE_k + p_i^E dT$$

where the κ_{ij}^T are the isothermal permittivities and the p_i^E the pyroelectric coefficients of the crystal respectively.

On differentiating equation (1-16) with respect to temperature at constant $\underset{\sim}{D}$ we obtain

$$(1\text{-}17)\quad \left(\frac{\partial D_i}{\partial T}\right)_D = 0 = \kappa_{ij}^T \left(\frac{\partial E_j}{\partial T}\right)_D + p_i^E$$

or

$$(1\text{-}18)\quad \left(\frac{\partial E_j}{\partial T}\right)_D = -p_i^E \beta_{ij}^T$$

where,

$$(1\text{-}19)\quad \beta_{ij}^T = \frac{\text{cofactor } \kappa_{ij}^T}{\text{Det}\left[\kappa_{ij}^T\right]} ,$$

is termed the dielectric impermeability tensor. Substituting into (1-14) gives

$$(1\text{-}20)\quad \alpha_{ij}^E = d_{kij}^T \beta_{k\ell}^T p_\ell^E + \alpha_{ij}^D \qquad \text{(see Nye, 1957)}$$

Equation (1-20) indicates that a false contribution to thermal expansion (analogous to the false pyroelectric effect of the first kind) can occur in crystals which are pyro- and piezoelectric (Cady, 1946). When a pyroelectric crystal is heated, a change in its polarization occurs and as a result "bound" charge appears on the surface of the crystal. This charge is referred to as "bound" because it cannot be conducted away by a conductor -- it is "bound" to the "molecules" of the dielectric. No "free" charge appears as a result of this polarization. Therefore, $\underset{\sim}{D}$, the dielectric displacement in the crystal must

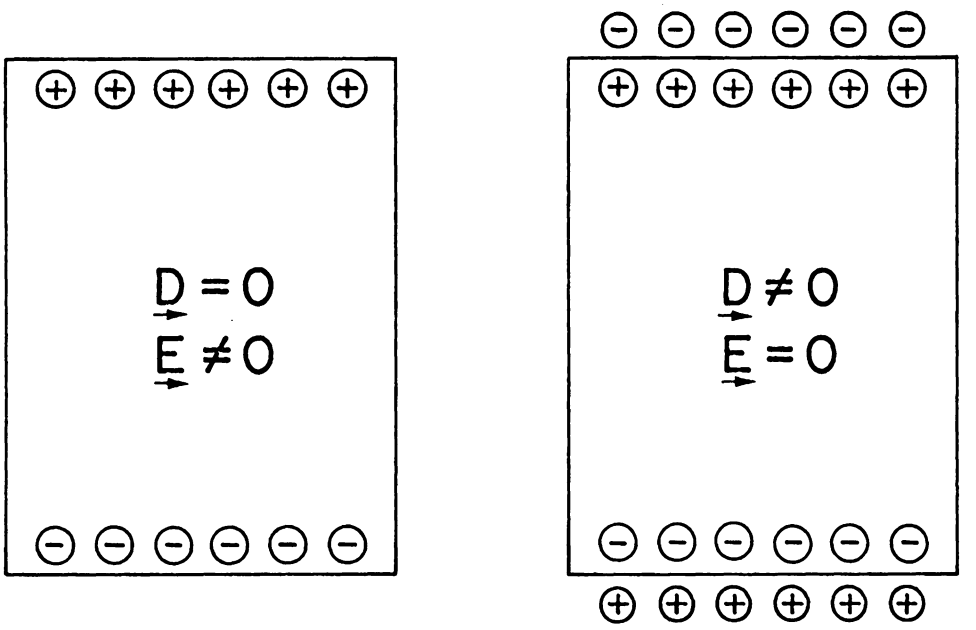

Figure 1-1: Conditions for determining α_{ij}^{D} and α_{ij}^{E}. On being heated from T_o to a temperature T a pyroelectric crystal (left) undergoes a polarization change which manifests itself as a bound surface charge on the ends of the crystal. The dielectric displacement, but not the electric field, in the interior of the crystal is zero under these conditions. If the changes in the dimensions of the crystal are used to determine the thermal expansion, coefficients of the type α_{ij}^{D} will be obtained. On the right, the same crystal after having been maintained at the elevated temperature T for a period of time. The polarization charges have been neutralized through collection of dust particles from the air and via internal conduction in the crystal. The electric field, but not the dielectric displacement, in the interior of the crystal is now zero. If the changes in the dimensions of the crystal are used to determine the thermal expansion, coefficients of the type α_{ij}^{E} will be obtained. These two types of coefficient are related through the expression $\alpha_{ij}^{E} = d_{kij}^{T}\ \beta_{k\ell}^{T}\ P_{\ell}^{E} + \alpha_{ij}^{D}$ (see text).

be zero under these conditions since "lines of [dielectric] displacement" can originate and terminate only on free charges (Winch, 1957). Therefore, unless these surface charges are neutralized (which is the same as saying that the crystal is short circuited so that $\underset{\rightarrow}{E}$ (and not $\underset{\rightarrow}{D}$) is zero in the crystal), $\underset{\rightarrow}{E}$ will not be constant during the experiment and a correction (the term $d^{T}_{kij}\beta_{k\ell}p^{E}_{\ell}$ in equation (1-20)) must be made in order to determine α^{E}_{ij} (Cady (1946) refers to α^{E}_{ij} rather than α^{D}_{ij} as the "true" thermal expansion). It seems worthwhile to point out that it is a short circuiting process which is occurring when pyroelectric crystals collect dust in museum collections. The polarized ends attract tiny charged dust particles from the air which neutralize the bound surface charge on the crystal (making $\underset{\rightarrow}{E} = 0$ in the interior). One can conclude from this that the conditions under which the thermal expansion coefficients are being measured (constant $\underset{\rightarrow}{D}$ or constant $\underset{\rightarrow}{E}$) could depend on the period of time the crystal has been maintained at the temperature at which the measurements are being carried out. The essential question is whether or not the bound surface charge caused by the heating has become neutralized. Fortunately, since $dp/\kappa \simeq 10^{-2}\alpha$ (Nye, 1957) this effect is small and can probably be neglected except in the most accurate work. The net result is that thermal expansion can, in practice if not in theory, be regarded as an isolated phenomenon.

Early Methods of Calculating the Thermal Expansion Coefficients of Cubic, Tetragonal, Hexagonal, and Orthorhombic Crystals

The thermal expansion coefficient of a material in a given

direction may be defined as the rate of change of strain in that direction per unit temperature change. As noted previously, for each type of strain that has been defined there is a corresponding type of thermal expansion coefficient obtained by taking the derivative of that strain with respect to temperature. Among the types of one dimensional strain that are used (Mase, 1970) are the "conventional engineering strain" defined as

$$(1\text{-}21) \quad e = (\ell - \ell_o)/\ell_o$$

and the "natural (logarithmic) strain" defined as

$$(1\text{-}22) \quad \varepsilon' = \ell n(\ell/\ell_o)$$

where ℓ_o and ℓ represent the length of a given line segment in the medium at the temperature T_o and T respectively. The corresponding thermal expansion coefficients are therefore

$$(1\text{-}23) \quad \lambda(T) = \frac{de}{dT} = \frac{1}{\ell_o} \frac{d\ell(T)}{dT}$$

and

$$(1\text{-}24) \quad \varepsilon(T) = \frac{d\varepsilon'}{dT} = \frac{1}{\ell(T)} \frac{d\ell(T)}{dT} \quad .$$

Thermal expansion coefficients of the type $\lambda(T)$ were termed "true" thermal expansion coefficients by Eucken and Dannohl (Connell and Martin, 1939) and "instantaneous linear thermal expansion coefficient[s]" by Kempter and Elliott (1959). Kempter and Elliott refer to thermal expansion coefficients of the type $\varepsilon(T)$ as "true linear thermal expansion coefficient[s]."

It may be shown from symmetry considerations that the thermal expansion coefficient for a crystal with orthogonal axes (including

hexagonal crystals where $\hat{j}$ is to be taken along [120]) has the form

$$(1\text{-}25)\quad \begin{bmatrix} \alpha_{11}(T) & \alpha_{12}(T) & \alpha_{13}(T) \\ \alpha_{21}(T) & \alpha_{22}(T) & \alpha_{23}(T) \\ \alpha_{31}(T) & \alpha_{32}(T) & \alpha_{33}(T) \end{bmatrix} = \begin{bmatrix} \alpha_1(T) & 0 & 0 \\ 0 & \alpha_2(T) & 0 \\ 0 & 0 & \alpha_3(T) \end{bmatrix}$$

where $\alpha_1(T)$, $\alpha_2(T)$, and $\alpha_3(T)$ represent the expansions along a_1, a_2 and a_3 (with $\alpha_1(T) = \alpha_2(T) = \alpha_3(T)$) for cubic crystals, along a_1, a_2 and c (with $\alpha_1(T) = \alpha_2(T) \neq \alpha_3(T)$) for tetragonal crystals, along a_1, [120], and c for hexagonal crystals (with $\alpha_1(T) = \alpha_2(T) \neq \alpha_3(T)$), and along a, b, and c (with $\alpha_1(T) \neq \alpha_2(T) \neq \alpha_3(T)$) for orthorhombic crystals.

In these crystal systems the principal directions of thermal expansion coincide with the crystal axes. In the above the symbol $\neq$ (not equal to) means non-equivalent. Accidental equality is possible.

If we let a_o, b_o, and c_o be the length of the crystallographic axes at T_o and $a(T)$, $b(T)$, and $c(T)$ be the length of these same axes T then, by utilizing equations (1-23) and (1-24) it becomes possible to immediately write expressions for the thermal expansion coefficient of those systems with orthogonal axes. We have

$$(1\text{-}26)\quad \lambda_1(T) = \frac{1}{a_o}\frac{da(T)}{dT},$$

$$(1\text{-}27)\quad \lambda_2(T) = \frac{1}{b_o}\frac{db(T)}{dT},$$

$$(1\text{-}28)\quad \lambda_3(T) = \frac{1}{c_o}\frac{dc(T)}{dT},$$

$$(1\text{-}29)\quad \varepsilon_1(T) = \frac{1}{a(T)}\frac{da(T)}{dT} = \frac{d}{dT}[\ell n a(T)],$$

$$(1\text{-}30)\quad \varepsilon_2(T) = \frac{1}{b(T)}\frac{db(T)}{dT} = \frac{d}{dT}[\ell nb(T)] \ ,$$

and

$$(1\text{-}31)\quad \varepsilon_3(T) = \frac{1}{c(T)}\frac{dc(T)}{dT} = \frac{d}{dT}[\ell nc(T)] \ .$$

In the above (for the sake of simplicity) we are using a to denote a_1 (cubic and tetragonal and hexagonal); and a (orthorhombic); b to denote a_2 (cubic and tetragonal), [120] (hexagonal), and b (orthorhombic); and c to denote a_3 (cubic) and c (tetragonal and hexagonal and orthorhombic). Expressions of the type given in equations (1-26) to (1-31) came into use immediately after the development of high temperature x-ray diffraction apparatus in the early nineteen thirties. Their use has continued to the present day. This approach was not extended to nonorthogonal systems until recently (Schlenker, Gibbs, and Boisen, 1975).

In order to use the preceeding expressions to calculate the $\lambda_i(T)$ or $\varepsilon_i(T)$ the cell parameters of the crystal must be first expressed as functions of temperature. Owen and Roberts (1936), Stokes and Wilson (1941), Kempter and Elliott (1959), and Pathok and Panda (1960a, 1960b) use power series expansions of T for this purpose. For example we can write the expression for the length of the a-axis as a function of T in the form

$$(1\text{-}32)\quad a(T) = [d_o + d_1T + d_2T^2 + \cdots] \text{ Å} \ .$$

This means that

$$(1\text{-}33)\quad \lambda_1(T) = \frac{1}{a_o}\frac{da(T)}{dT} = \frac{d_1 + 2d_2T + \cdots}{d_o + d_1T_o + d_2T_o^{\,2} + \cdots}$$

where a_o is the length of the cell edge at some arbitrarily selected

reference temperature T_o ($a_o = d_o + d_1T_o + d_2T_o^2 + \cdots$). As a specific example of such an approach let us consider the determination of the thermal expansion coefficient of lead metal by Stokes and Wilson (1941). Their expression for the length of the a-axis in lead was

(1-34) $a = [4.93687 + 138.98 \times 10^{-6}T\ (°C) + 60.16 \times 10^{-9}T^2\ (°C)]$ Å.

They selected a reference temperature, T_o, of 0°C ($a_o = 4.93687$ Å) so that

(1-35) $\lambda_1(T) = [28.15 \times 10^{-6} + 23.6 \times 10^{-9}T\ (°C)]\ (°C)^{-1}$.

Their results are shown in Figures (1-2) and (1-3).

A similar study by Kempter and Elliott (1959) for UN, UO_2, $UO_2 \cdot ThO_2$, and ThO_2 gave the following results:

(1-36) $$\lambda_1(T) = \frac{3.657 \times 10^{-5} + 10.75 \times 10^{-9}T\ (°C)}{4.8897}\ (°C)^{-1}$$

for uranium nitride (UN),

(1-37) $$\lambda_1(T) = \frac{4.511 \times 10^{-5} + 24.17 \times 10^{-9}T\ (°C)}{5.4686}\ (°C)^{-1}$$

for uranium oxide (UO_2), and

(1-38) $$\lambda_1(T) = \frac{4.570 \times 10^{-5} + 12.55 \times 10^{-9}T\ (°C)}{5.5971}\ (°C)^{-1}$$

for uranium thorium oxide ($UO_2 \cdot ThO_2$). Their reference temperature T_o was 26°C and the results are considered valid between 26 and 1000 degrees Celsius. These results are typical. No examples were found where this method was applied to tetragonal or orthorhombic crystals; however, it was applied to cadmium, osmium, and ruthenium (all hexagonal) by Owen and Roberts (1936) using a reference temperature of 20°C.

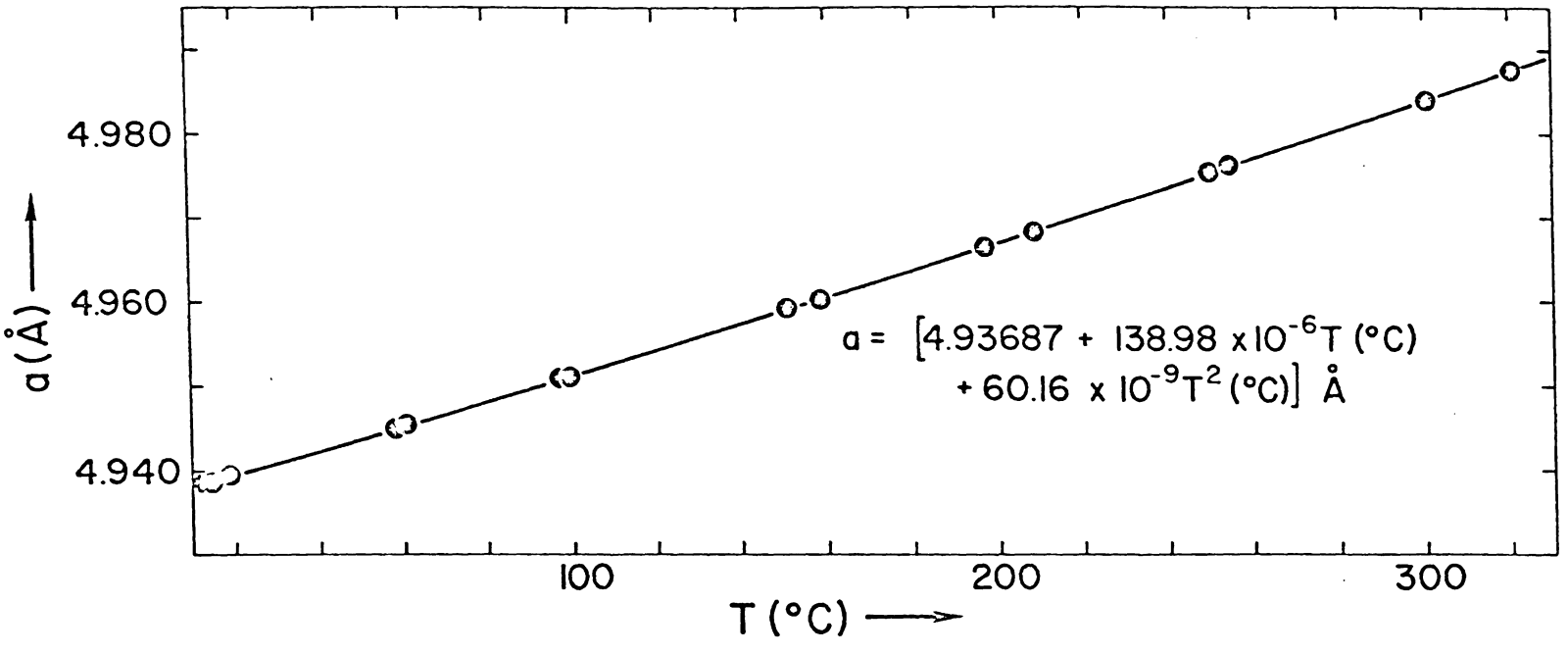

Figure 1-2: Cell parameters of lead metal (cubic) as a function of temperature (based on the x-ray data of Stokes and Wilson (1941)).

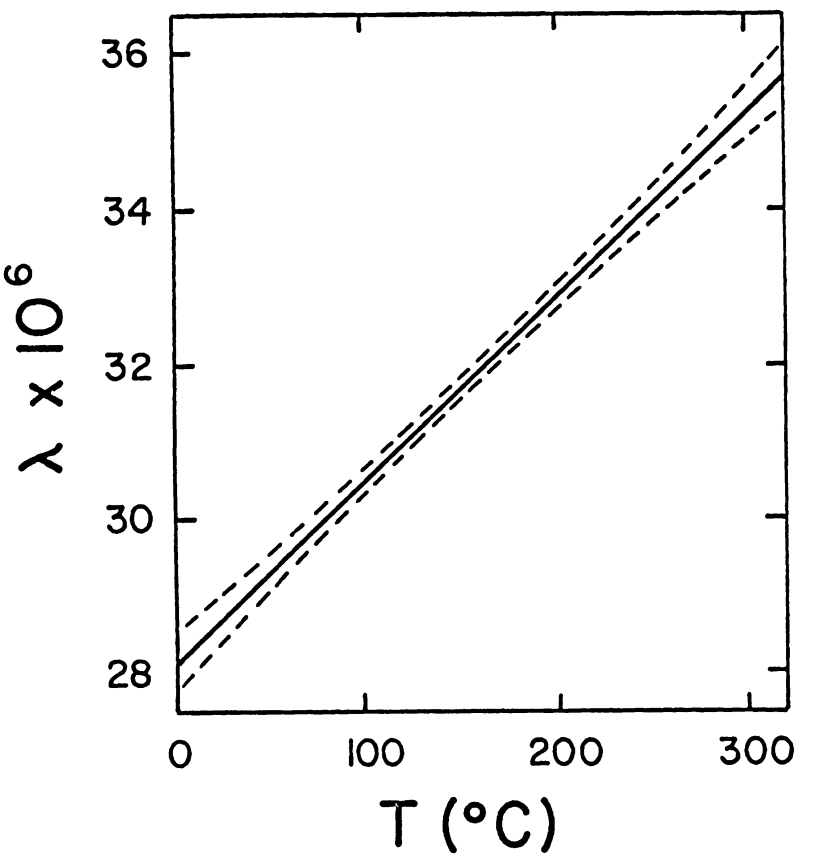

Figure 1-3: Linear Lagrangian thermal expansion coefficient of lead metal calculated using the expression

$$\lambda_1 = \frac{1}{a_o} \frac{da(T)}{dT}$$

where a_o is the length of the cell edge at 0°C (a_o = 4.93687 Å). The calculation is based on the data and expression for a(T) given in Figure 1-2 (after Stokes and Wilson, 1941).

This illustrates one of the drawbacks with thermal expansion coefficients of the type $\lambda_i(T)$. The choice of T_o is arbitrary and there is no general agreement or convention as to what reference temperature should be used. This means that the magnitudes of the $\lambda_i(T)$ which are obtained are not unique. In addition there is no general agreement as to how the necessary derivatives, i.e. da(T)/dT, should be obtained from the experimental data. At least three procedures are in general use. These are

(1) Measure values of α at T_o and T. Subtract the values of a and divide by the temperature interval ($\Delta T = T - T_o$). This method was used by Wilson (1941) and is closely related to the method developed by Ohashi and Burnham (1973). It yields mean values for the thermal expansion coefficients which should be plotted at the mean value of the temperature interval.

(2) A variation of the first procedure, used by Owen and Richards (1936) and by Deshpande and Mudholker (1960), obtains mean values of the derivative over small temperature intervals from a carefully drawn graph of a versus T.

(3) The method previously discussed where the cell parameters are expressed as power series expansions in T. The necessary derivatives may then be obtained analytically.

A comparison of procedures two and three was made by Deshpande and Mudholker (1961) using potassium chlorate, $KClO_3$. Their results

are shown in Figure (1-4). Curve I was obtained by method two while curves II and III were obtained by the third method. Curves II and III differ because a quadratic expression of the form

$$(1\text{-}39) \quad a(T) = d_o + d_1 T + d_2 T^2$$

was used to calculate curve II while curve III was calculated from an expression of the form

$$(1\text{-}40) \quad a(T) = d_o + d_1 T + d_2 T^2 + d_3 T^3 \ .$$

Note that the arbitrary use of a quadratic function for a(T), curve II, forces the thermal expansion coefficient to be linear which may or may not be the correct result. Curves I and III show good agreement.

The Matrix Method of W.L. Bond (1945)

In their original form none of the methods discussed to this point can be used to calculate thermal expansion coefficients for the non-orthogonal crystals (monoclinic and triclinic). Prior to the development of the Ohashi-Burnham method (1973), this was accomplished by means of a method originally developed by W.L. Bond (1945, unpublished). This technique was originally used with slabs cut, with preselected orientations, from single crystals. It is discussed in this form by Nye (1957). It is presented in a form suitable for use with x-ray data, by Bouvaist and Weigel (1970). This is the form which will be discussed here.

The characteristic feature of all deformations resulting from a change in temperature is that they are homogeneous (often called affine, i.e., deformations in which straight lines remain straight,

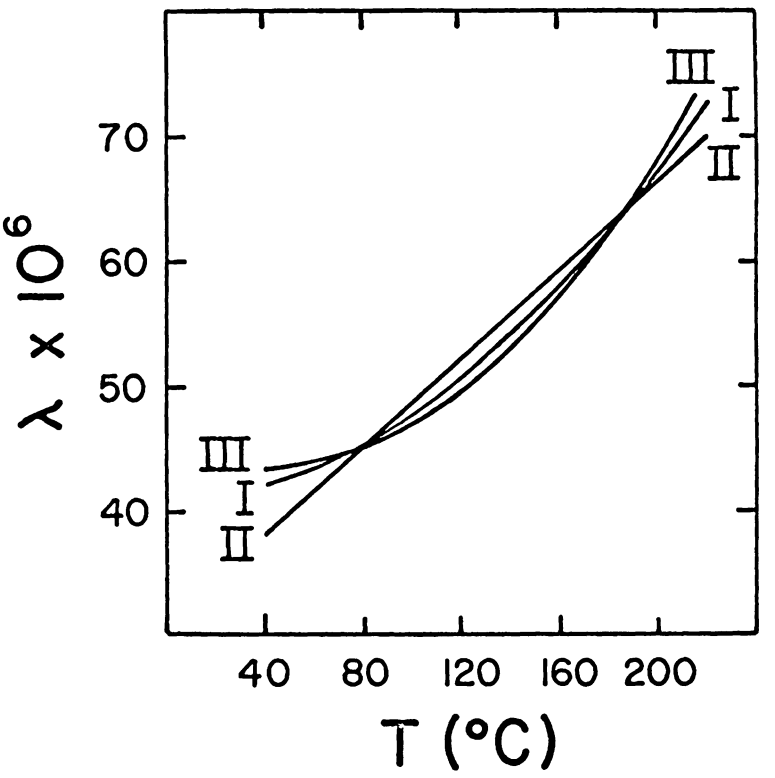

Figure 1-4: A comparison of two procedures for computing thermal expansion coefficients from x-ray data (see text for discussion). The substance used in the test was potassium chlorate ($KClO_3$, cubic). (After Deshpande and Mudholker, 1961).

planes remain planes, and spheres are transformed into triaxial ellipsoids). Such deformations may be described mathematically by equations of the form

$$(1\text{-}41) \quad u_i = I_{ij} X_j$$

or

$$(1\text{-}42) \quad u_i = J_{ij} x_j$$

where I_{ij} and J_{ij} are constants. Here we will assume we are dealing with pure deformations, that is, no rotation of the medium occurs. This requires that the components of the linear Lagrangian and Eulerian strain tensor take the forms

$$(1\text{-}43) \quad \ell_{ij} = \frac{1}{2}\left(\frac{\partial u_i}{\partial X_j} + \frac{\partial u_j}{\partial X_i}\right) = \frac{1}{2}(I_{ij} + I_{ji})$$

and

$$(1\text{-}44) \quad e_{ij} = \frac{1}{2}\left(\frac{\partial u_i}{\partial x_j} + \frac{\partial u_j}{\partial x_i}\right) = \frac{1}{2}(J_{ij} + J_{ji}) \ .$$

Consider a line segment in the medium with initial length ℓ_o, initial direction cosines (n_1, n_2, n_3), final length ℓ, and final direction cosines $(\bar{n}_1, \bar{n}_2, \bar{n}_3)$. We will then have

$$(1\text{-}45) \quad X_i = \ell_o n_i$$

and

$$(1\text{-}46) \quad x_i = \ell \bar{n}_i \ .$$

Using equations (1-1) and (1-41) we can write

$$(1\text{-}47) \quad x_k = X_k + I_{ki} X_i = (\delta_{ki} + I_{ki}) X_i = (\delta_{ki} + I_{ki}) n_i \ell_o$$

$$= (\delta_{kj} + I_{kj}) n_j \ell_o \ .$$

Forming the dot product

$$(1\text{-}48)\quad \underset{\sim}{x}\cdot\underset{\sim}{x} = x_k x_k = n_k n_k \ell^2 = \ell^2 = (\delta_{ki} + I_{ki})(\delta_{kj} + I_{kj}) n_i n_j \ell_o^2$$

$$= (\delta_{ki}\delta_{kj} + \delta_{ki}I_{kj} + I_{ki}\delta_{kj} + I_{ki}I_{kj}) n_i n_j \ell_o^2$$

$$= (\delta_{ij} + I_{ij} + I_{ji} + I_{ki}I_{kj}) n_i n_j \ell_o^2$$

$$= \ell_o^2 + (I_{ij} + I_{ji} + I_{ki}I_{kj}) n_i n_j \ell_o^2$$

and rearranging, we obtain

$$(1\text{-}49)\quad \frac{\ell^2 - \ell_o^2}{\ell_o^2} = (I_{ij} + I_{ji} + I_{ki}I_{kj}) n_i n_j$$

or

$$(1\text{-}50)\quad \frac{\ell - \ell_o}{\ell_o} = \frac{(I_{ij} + I_{ji} + I_{ki}I_{kj}) n_i n_j}{1 + \sqrt{1 + (I_{ij} + I_{ji} + I_{ki}I_{kj}) n_i n_j}}$$

$$\simeq \frac{1}{2}(I_{ij} + I_{ji}) n_i n_j$$

if $I_{ij} \ll 1$. From equations (1-43) and (1-50) we see that

$$(1\text{-}51)\quad \frac{\ell - \ell_o}{\ell_o} \simeq \ell_{ij} n_i n_j \ .$$

In a similar way it is possible to start from equations (1-1) and (1-42) and show that

$$(1\text{-}52)\quad \frac{\ell - \ell_o}{\ell} = \frac{(J_{ij} + J_{ji} + J_{ki}J_{kj}) \bar{n}_i \bar{n}_j}{1 + \sqrt{1 + (J_{ij} + J_{ji} + J_{ki}J_{kj}) \bar{n}_i \bar{n}_j}}$$

$$\simeq \frac{1}{2}(J_{ij} + J_{ji}) \bar{n}_i \bar{n}_j = e_{ij} \bar{n}_i \bar{n}_j$$

if $J_{ij} \ll 1$.

It is possible to derive equations (1-51) and (1-52) in a somewhat different way. Consider the displacement of a material particle initially located at

$$(1\text{-}53)\quad \underset{\rightarrow}{X} = \ell_o(n_1\hat{i} + n_2\hat{j} + n_3\hat{k})$$

where

$$(1\text{-}54)\quad |\underset{\rightarrow}{X}| = \ell_o \ .$$

If the particle is displaced by an amount

$$(1\text{-}55)\quad \underset{\rightarrow}{u} = u_1\hat{i} + u_2\hat{j} + u_3\hat{k}$$

(where $u_i = \ell_{ij}X_j = \ell_{ij}n_j\ell_o$) during deformation, then

$$(1\text{-}56)\quad \frac{\underset{\rightarrow}{u}\cdot\underset{\rightarrow}{X}}{\underset{\rightarrow}{X}\cdot\underset{\rightarrow}{X}} = \frac{\ell_{ij}n_j\ell_o\cdot\ell_o n_i}{\ell_o^{\,2}} = \ell_{ij}n_i n_j \ .$$

But according to equation (1-1), $\underset{\rightarrow}{u}$ is defined to be

$$(1\text{-}57)\quad \underset{\rightarrow}{u} = \underset{\rightarrow}{x} - \underset{\rightarrow}{X}$$

so that

$$(1\text{-}58)\quad u_i = x_i - X_i = \ell\bar{n}_i - \ell_o n_i \ .$$

Hence

$$(1\text{-}59)\quad \frac{\underset{\rightarrow}{u}\cdot\underset{\rightarrow}{X}}{\ell_o^{\,2}} = \frac{(\ell\bar{n}_i - \ell_o n_i)\ell_o n_i}{\ell_o^{\,2}} = \frac{\bar{n}_i n_i\ell - n_i n_i\ell_o}{\ell_o}$$

This means that

$$(1\text{-}60)\quad \frac{\bar{n}_i n_i\ell - \ell_o}{\ell_o} = \ell_{ij}n_i n_j \ .$$

Since the deformation is small we make the approximation

$$(1\text{-}61)\quad n_i \simeq \bar{n}_i$$

so that equation (1-51) results. In a similar way, by starting with $\frac{\vec{u}\cdot\vec{x}}{\vec{x}\cdot\vec{x}}$, we may obtain equation (1-52).

Taking the derivatives of equations (1-51) and (1-52) with respect to temperature, we obtain

$$(1\text{-}62)\quad \frac{1}{\ell_o}\frac{d\ell(T)}{dT} \simeq \frac{d\ell_{ij}(T)}{dT} n_i n_j = \lambda_{ij}(T) n_i n_j$$

and

$$(1\text{-}63)\quad \frac{\ell_o}{\ell^2(T)}\frac{d\ell(T)}{dT} = \frac{de_{ij}(T)}{dT}\bar{n}_i(T)\bar{n}_j(T) + 2e_{ij}(T)\bar{n}_i(T)\frac{d\bar{n}_j(T)}{dT} \quad .$$

On making the usual assumptions of linear strain theory ($\ell \simeq \ell_o$ and $d\bar{n}_i(T)/dT \simeq o$), equation (1-63) becomes

$$(1\text{-}64)\quad \frac{1}{\ell(T)}\frac{d\ell(T)}{dT} \simeq \frac{de_{ij}(T)}{dT}\bar{n}_i(T)\bar{n}_j(T) = \varepsilon_{ij}(T)\bar{n}_i(T)\bar{n}_j(T) \quad .$$

Equations (1-62) and (1-64) are very important for what follows.

Consider a plane in the crystal with Bragg diffraction indices $(hk\ell)$. If we denote the normals to the plane $(hk\ell)$, at T_o, by (n_1,n_2,n_3), the d-spacing of this plane by $d_{(hk\ell)}(T_o)$, the normals to the same plane at T by $(\bar{n}_1,\bar{n}_2,\bar{n}_3)$, and the d-spacing by $d_{(hk\ell)}(T)$ then we can write, using equations (1-62) and (1-64)

$$(1\text{-}65)\quad \frac{1}{d_{(hk\ell)}(T_o)}\frac{d[d_{(hk\ell)}(T)]}{dT} = \lambda_{ij}(T) n_i n_j$$

and

$$(1\text{-}66)\quad \frac{1}{d_{(hk\ell)}(T)}\frac{d[d_{(hk\ell)}(T)]}{dT} = \varepsilon_{ij}(T)\bar{n}_i(T)\bar{n}_j(T)$$

(Bouvaist and Weigel, 1970).

We know from the Bragg law that

$$(1\text{-}67)\quad d_{(hk\ell)} = \frac{\lambda}{2\sin\theta}$$

so that

$$(1\text{-}68)\quad \frac{d[d_{(hk\ell)}(T)]}{dT} = -\frac{\lambda\cos\theta(T)}{2\sin^2\theta(T)}\frac{d\theta(T)}{dT} \quad .$$

Therefore, we can write

$$(1\text{-}69)\quad A(hk\ell,T) = \frac{1}{d_{(hk\ell)}(T)}\frac{d[d_{(hk\ell)}(T)]}{dT}$$

$$= -\frac{\lambda\cos\theta(T)}{2\sin^2\theta(T)} \cdot \frac{2\sin\theta(T)}{\lambda} = -\cot\theta(T)\frac{d\theta(T)}{dT}$$

This approach appears to have been developed by Gott (1942). This means that equation (1-66) can be written as

$$(1\text{-}70)\quad A(hk\ell,T) = -\cot\theta_{(hk\ell)}(T)\frac{d\theta_{(hk\ell)}(T)}{dT} = \varepsilon_{ij}(T)\bar{n}_i(T)\bar{n}_j(T) \quad .$$

The expression $\cot\theta_{(hk\ell)}(T)[d\theta_{(hk\ell)}(T)/dT]$ is now to be evaluated for as many planes as possible. We will then have a set of simultaneous equations of the form

$$(1\text{-}71)\quad A(h_1k_1\ell_1) = n_i(h_1k_1\ell_1)n_j(h_1k_1\ell_1)\varepsilon_{ij},$$

$$A(h_2k_2\ell_2) = n_i(h_2k_2\ell_2)n_j(h_2k_2\ell_2)\varepsilon_{ij},$$

$$. . . . . .,$$

and

$$A(h_nk_n\ell_n) = n_i(h_nk_n\ell_n)n_j(h_nk_n\ell_n)\varepsilon_{ij}.$$

For a monoclinic crystal we must have $n \geq 4$ and for a triclinic crystal $n \geq 6$. We can rewrite the above expressions as

$$(1\text{-}72)\quad V_1 = n_i(h_1k_1\ell_1)n_j(h_1k_1\ell_1)\varepsilon_{ij} - A(h_1k_1\ell_1),$$

$$V_2 = n_i(h_2k_2\ell_2)n_j(h_2k_2\ell_2)\varepsilon_{ij} - A(h_2k_2\ell_2),$$

. . . . . ,

and

$$V_n = n_i(h_nk_n\ell_n)n_j(h_nk_n\ell_n)\varepsilon_{ij} - A(h_nk_n\ell_n)$$

The principle of least squares, which states that

$$(1\text{-}73) \quad \sum_{i=1}^{n} V_i^2 = V_1^2 + V_2^2 + \ldots + V_n^2$$

should be a minimum, may then be used to find the values of the ε_{ij}.

The problem of evaluating the term $-\cot\theta d\theta/dT$ for each plane still remains. In practice this is done as follows. On integrating equation (1-69) between T_o and T we obtain

$$(1\text{-}74) \quad \int_{T_o}^{T} \frac{1}{d_{(hk\ell)}(T)} \frac{d[d_{(hk\ell)}(T)]}{dT} dT = \int_{d_{(hk\ell)}(T_o)}^{d_{(hk\ell)}(T)} d[\ell n(d_{(hk\ell)})]$$

$$= -\int_{T_o}^{T} \cot\theta \frac{d\theta}{dT} dT = -\int_{\theta_o}^{\theta} \cot\theta d\theta \ .$$

This gives

$$(1\text{-}75) \quad \ell n \frac{d_{(hk\ell)}(T)}{d_{(hk\ell)}(T_o)} = -\ell n \frac{\sin\theta}{\sin\theta_o} = \ell n \frac{\sin\theta_o}{\sin\theta} \ .$$

Taking the antilog of both sides and subtracting one gives

$$(1\text{-}76) \quad \frac{d_{(hk\ell)}(T) - d_{(hk\ell)}(T_o)}{d_{(hk\ell)}(T_o)} = \frac{\sin\theta_o - \sin\theta}{\sin\theta}$$

On letting

$$(1\text{-}77)\quad \Delta d_{(hk\ell)} = d_{(hk\ell)}(T) - d_{(hk\ell)}(T_o)$$

and on realizing that

$$(1\text{-}78)\quad \sin\theta_o = \sin(\theta - \Delta\theta) = \sin\theta\cos\Delta\theta - \cos\theta\sin\Delta\theta$$
$$= -\cos\theta\sin\Delta\theta \simeq -\cos\theta\Delta\theta$$

($\Delta\theta$ is small). We can write (1-69) as

$$(1\text{-}79)\quad \frac{1}{d_{(hk\ell)}(T_o)} \frac{\Delta d_{(hk\ell)}}{\Delta T} \simeq -\cot\theta_{(hk\ell)} \frac{\Delta\theta(hk\ell)}{T}$$

The approximation is then made that

$$(1\text{-}80)\quad A(hk\ell) \simeq -\cot\theta_{(hk\ell)} \Delta\theta_{(hk\ell)}/\Delta T \ .$$

This approach is satisfactory because the $\theta_{(hk\ell)}$ are slowly varying functions of temperature. Therefore approximating $d\theta/dT$ with $\Delta\theta/\Delta T$ does not introduce a large amount of error. Nevertheless the method is a kind of finite differencing approach and as such yields only mean values of the thermal expansion coefficients. Note that although (1-70) has been formulated in terms of the $\varepsilon_{ij}(T)$ because such a formulation arises naturally from equations (1-66) and (1-68). No distinction is made by Bond, Nye or Bouvaist and Weigel between the $\lambda_{ij}(T)$ and the $\varepsilon_{ij}(T)$. This is justified if the spacial and material displacement gradients are small since in such a situation we have $\ell_{ij} \simeq e_{ij}$.

The Ohashi-Burnham Method (1973)

This method represents a significant advance over the technique developed by Bond (1945). It makes direct use of refined cell

parameters which are readily available. It has the disadvantage, however, of being a finite differencing technique which yields only mean values of the thermal expansion coefficients.

Consider the coordinate system shown in Figure (1-5). Let us choose a vector $\underset{\rightarrow}{r}$ in this coordinate system. In terms of spherical coordinates the c-ordinates of the end point of the vector will be (r,ϕ,ρ). In terms of $\hat{i}$, $\hat{j}$ and $\hat{k}$ we may write

(1-81) $\underset{\rightarrow}{r} = r\sin\rho\sin\phi\hat{i} + r\sin\rho\cos\phi\hat{j} + r\cos\rho\hat{k}$

Let us now consider a triclinic crystal oriented so as to have $\underset{\rightarrow}{c}$ parallel to X_3 or $\hat{k}$ and $\underset{\rightarrow}{a}^*$ parallel to X_1 or $\hat{i}$. This is the orientation suggested by the IRE (Institute of Radio Engineers). The third axis is chosen so as to have a right handed coordinate system. This is illustrated by Figure (1-6). We wish to express $\underset{\rightarrow}{a}$, $\underset{\rightarrow}{b}$ and $\underset{\rightarrow}{c}$ in terms of the unit vectors $\hat{i}$, $\hat{j}$ and $\hat{k}$. We begin with $\underset{\rightarrow}{c}$, for which $\rho = 0$ and $\phi = 0$, therefore we obtain

(1-82) $\underset{\rightarrow}{c} = c\sin 0\sin 0\hat{i} + c\sin 0\cos 0\hat{j} + c\cos 0\hat{k}$

or

(1-83) $c = c\hat{k}$.

We know that $\underset{\rightarrow}{b}$ is perpendicular to $\underset{\rightarrow}{a}^*$ and must therefore lie in the X_2X_3 plane. Therefore for $\underset{\rightarrow}{b}$ we have $\rho = \alpha$ and $\phi = 0$. This is illustrated in Figure (1-6). This means that

(1-84) $\underset{\rightarrow}{b} = b\sin\alpha\sin 0\hat{i} + b\sin\alpha\cos 0\hat{j} + b\cos\alpha\hat{k}$

or

(1-85) $\underset{\rightarrow}{b} = b\sin\alpha\hat{j} + b\cos\alpha\hat{k}$.

The resolution of $\underset{\rightarrow}{a}$ is the most difficult since it has a general

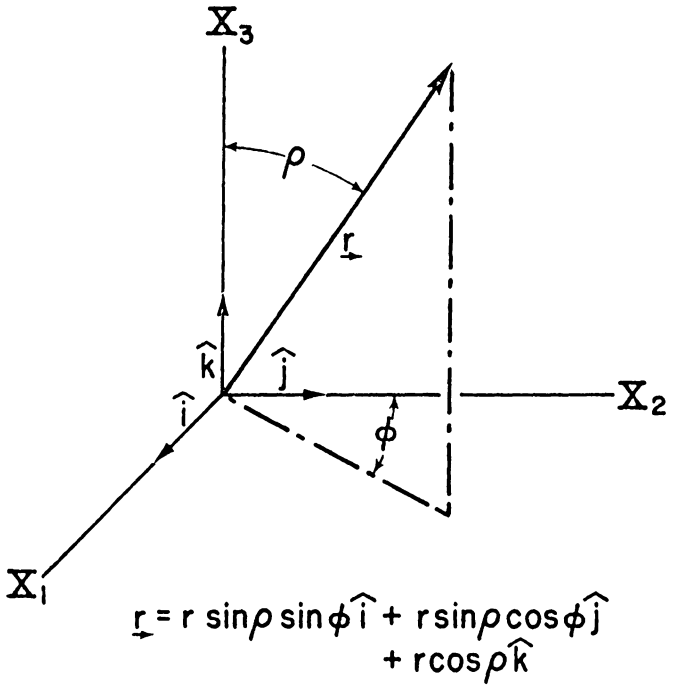

Figure 1-5: The spherical coordinate system used in crystallographic problems. Note that because of the definition of ϕ the crystallographic spherical coordinate system differs slightly from the system of spherical coordinates in general use.

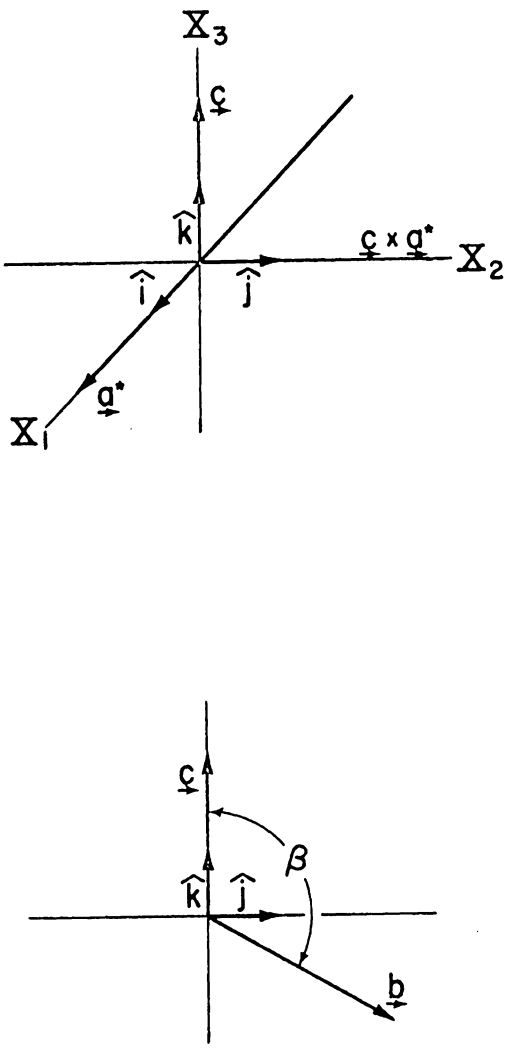

Figure 1-6: Relation between the crystal axial system and the orthogonal axial system. The relative orientation of the two systems is that suggested by the Institute of Radio Engineers (IRE). The bottom portion of the figure illustrates the orientation of the $\underset{\rightarrow}{b}$-axis of the crystal (Brown, 1967).

orientation. Obviously we have $\rho = \beta$ in this case. The value for ϕ may be determined using Figure (1-7). It is evident from the figure that we obtain $\phi = 180 - \gamma^*$. This results in

$$(1\text{-}86)\quad \underset{\rightarrow}{a} = a\sin\beta\sin(180 - \gamma^*)\hat{i} + a\sin\beta\cos(180 - \gamma^*)\hat{j} + a\cos\beta\hat{k}$$

We have

$$(1\text{-}87)\quad \sin(180 - \gamma^*) - \sin 180\cos\gamma^* - \sin\gamma^*\cos 180 = \sin\gamma^*$$

and

$$(1\text{-}88)\quad \cos(180 - \gamma^*) = \cos 180\cos\gamma^* + \sin 180\sin\gamma^* = -\cos\gamma^*$$

This yields

$$(1\text{-}89)\quad \underset{\rightarrow}{a} = a\sin\beta\sin\gamma^*\hat{i} - a\sin\beta\cos\gamma^*\hat{j} + a\cos\beta\hat{k}$$

We may therefore write

$$(1\text{-}90)\quad \begin{bmatrix} \underset{\rightarrow}{a} \\ \underset{\rightarrow}{b} \\ \underset{\rightarrow}{c} \end{bmatrix} = \begin{bmatrix} a\sin\beta\sin\gamma^* & -a\sin\beta\cos\gamma^* & a\cos\beta \\ 0 & b\sin\alpha & b\cos\alpha \\ 0 & 0 & c \end{bmatrix} \begin{bmatrix} \hat{i} \\ \hat{j} \\ \hat{k} \end{bmatrix}$$

The matrix

$$(1\text{-}91)\quad S = \begin{bmatrix} a\sin\beta\sin\gamma^* & -a\sin\beta\cos\gamma^* & a\cos\beta \\ 0 & b\sin\alpha & b\cos\alpha \\ 0 & 0 & c \end{bmatrix}$$

is referred to as the S-matrix (Bollmann, 1970). It takes the simplest form when expressed in terms of both reciprocal and direct cell parameters. It is for this reason that equation (1-91) is different in form from Ohashi's equation (A-4). Actually Ohashi's equation (A-4) and equation (1-91) are equivalent.

The position of a material point in space before the deformation may be denoted (in terms of the undeformed crystal axes a_o, b_o, and c_o)

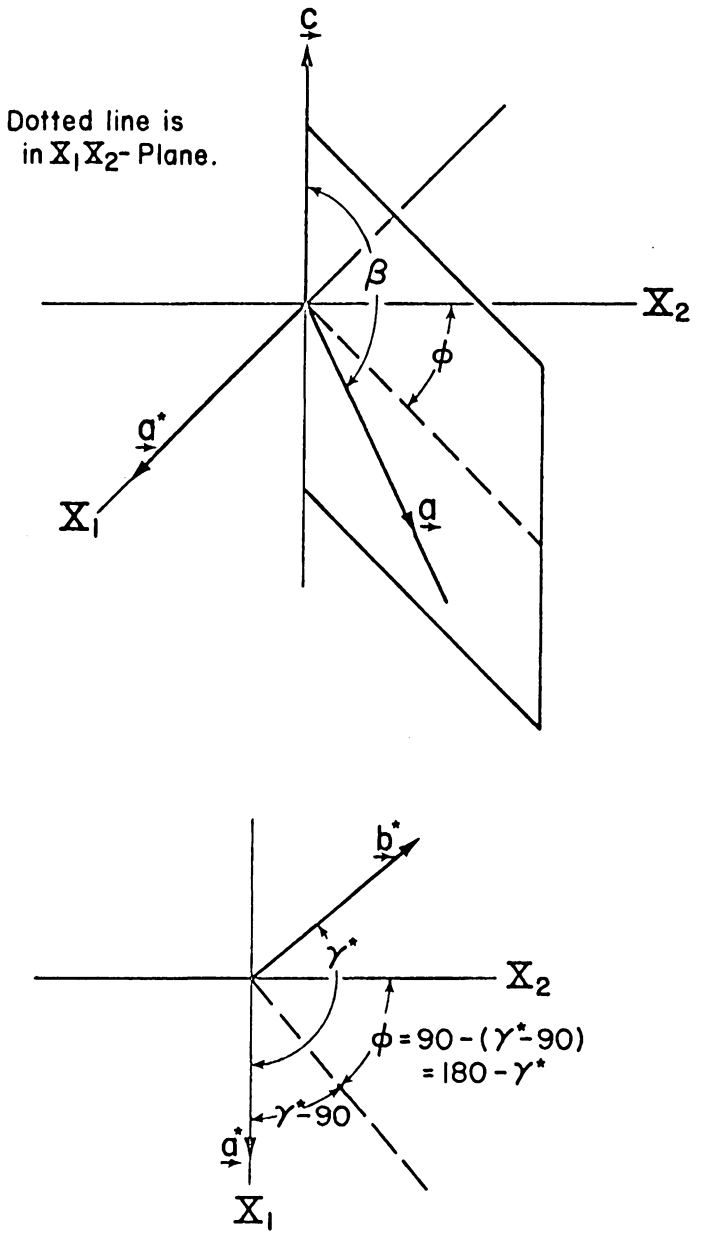

Figure 1-7: The resolution of the a-axis. The $\underset{\rightarrow}{a}$ axis of the crystal has a general orientation relative to $\hat{i}$, $\hat{j}$, and $\hat{k}$. It is evident from the figure that $\rho = \beta$ and $\phi = 180 - \gamma^*$ for this axis.

by

$$(1\text{-}92)\quad \underset{\rightarrow}{r}_o = X_1^c \underset{\rightarrow}{a}_o + X_2^c \underset{\rightarrow}{b}_o + X_3^c \underset{\rightarrow}{c}_o \ .$$

In the orthogonal coordinates previously described the same material particle will have coordinates

$$(1\text{-}93)\quad \underset{\rightarrow}{r}_o = X_1\hat{i} + X_2\hat{j} + X_3\hat{k} \ .$$

Therefore we obtain

$$(1\text{-}94)\quad \underset{\rightarrow}{r} = X_1\hat{i} + X_2\hat{j} + X_3\hat{k} = X_1^c \underset{\rightarrow}{a}_o + X_2^c \underset{\rightarrow}{b}_o + X_3^c \underset{\rightarrow}{c}_o$$

$$= X_1^c(a_o \sin\beta_o \sin\gamma_o^*\hat{i} - a_o \sin\beta_o \cos\gamma_o^*\hat{j} + a_o \cos\beta_o\hat{k})$$

$$+ X_2^c(0\hat{i} + b_o \sin\alpha_o\hat{j} + b_o \cos\alpha_o\hat{k}) + X_3^c(0\hat{i} + 0\hat{j} + c_o\hat{k})$$

$$= (a_o \sin\beta_o \sin\gamma_o^* X_1^c)\hat{i} + (-a_o \sin\beta_o \cos\gamma_o^* X_1^c + b_o \sin\alpha_o X_2^c)\hat{j}$$

$$+ (a_o \cos\beta_o X_1^c + b_o \cos\alpha_o X_2^c + c_o X_3^c)\hat{k}$$

or

$$(1\text{-}95)\quad \begin{bmatrix} X_1 \\ X_2 \\ X_3 \end{bmatrix} = \begin{bmatrix} a_o \sin\beta_o \sin\gamma_o^* & 0 & 0 \\ -a \sin\beta_o \cos\gamma_o^* & b_o \sin\alpha_o & 0 \\ a_o \cos\beta_o & b_o \cos\alpha_o & C \end{bmatrix} \begin{bmatrix} X_1^c \\ X_2^c \\ X_3^c \end{bmatrix}$$

On writing (1-95) in matrix form we obtain

$$(1\text{-}96)\quad X = S_o^T X^c$$

The coordinates of the same point after deformation will be

$$(1\text{-}97)\quad \underset{\rightarrow}{r}_i = x_1^c \underset{\rightarrow}{a}_1 + x_2^c \underset{\rightarrow}{b}_1 + x_3^c \underset{\rightarrow}{c}_1$$

or in cartesian coordinates

$$(1\text{-}98)\quad \begin{bmatrix} x_1 \\ x_2 \\ x_3 \end{bmatrix} = \begin{bmatrix} a_1\sin\beta_1\sin\gamma_1^* & 0 & 0 \\ -a_1\sin\beta_1\cos\gamma_1^* & b_1\sin\alpha_1 & 0 \\ a_1\cos\beta_1 & b_1\cos\alpha_1 & c_1 \end{bmatrix} \begin{bmatrix} x_1^c \\ x_2^c \\ x_3^c \end{bmatrix}$$

which may be written in matrix form as

$$(1\text{-}99)\quad x = S_1^T x^c \ .$$

We recall, from equation (1-41), that deformations of the type which occur during thermal expansion may be written in the form

$$(1\text{-}100)\quad x_i = X_i + u_i = X_i + I_{ij}X_j = (\delta_{ij} + I_{ij})X_j = R_{ij}X_j$$

which in matrix form becomes

$$(1\text{-}101)\quad \begin{bmatrix} x_1 \\ x_2 \\ x_3 \end{bmatrix} = \begin{bmatrix} 1 + I_{11} & I_{12} & I_{13} \\ I_{21} & 1 + I_{11} & I_{23} \\ I_{31} & I_{32} & 1 + I_{32} \end{bmatrix} \begin{bmatrix} X_1 \\ X_2 \\ X_3 \end{bmatrix}$$

$$= \begin{bmatrix} R_{11} & R_{12} & R_{13} \\ R_{21} & R_{22} & R_{23} \\ R_{31} & R_{32} & R_{33} \end{bmatrix} \begin{bmatrix} X_1 \\ X_2 \\ X_3 \end{bmatrix}$$

where

$$(1\text{-}102)\quad R = I + \mathit{I}$$

(I is the identity matrix). We will therefore write

$$(1\text{-}103)\quad x = (I + \mathit{I})X = RX$$

and since $X = S_o^T X^c$ this becomes

$$(1\text{-}104)\quad x = RS_o^T x^c \ .$$

We also know that $x = S_1^T x^c$ so that

$$(1\text{-}105)\quad S_1^T x^c = R S_o^T X^c \ .$$

However since it is obvious that (Born and Haung, 1968)

$$(1\text{-}106)\quad x^c = X^c$$

equation (1-105) becomes

$$(1\text{-}107)\quad S_1^T = R S_o^T \ .$$

We now solve for R by right multiplying both sides by S_o^{-T} to obtain

$$(1\text{-}108)\quad R = S_1^T S_o^{-T} \ .$$

We then use the definition of R to obtain

$$(1\text{-}109)\quad I = S_1^T S_o^{-T} - \mathit{I} \ .$$

We now recall that the linear Lagrangian strain tensor [ℓ] is given by

$$(1\text{-}110)\quad [\ell] = \frac{1}{2}[I + I^T]$$

so that

$$(1\text{-}111)\quad [\ell] = \frac{1}{2}[S_1^T S_o^{-T} + (S_1^T S_o^{-T})^T] - \mathit{I}$$

which on further simplification yields

$$(1\text{-}112)\quad [\ell] = \frac{1}{2}[S_o^{-1} S_1 + (S_o^{-1} S_1)^T] - \mathit{I} \ .$$

Equation (1-112) is the same as the Ohashi-Burnham result given in their equation (A-9). The matrix S_1 is given in equation (1-91) and S_o^{-1} has the form

$$(1\text{-}113)\quad S_o^{-1} = \begin{bmatrix} 1/(a_o \sin\beta_o \sin\gamma_o^*) & \cos\gamma_o^*/(b_o \sin\alpha_o \sin\gamma_o^*) & -(\cos\alpha_o \sin\beta_o \cos\gamma_o^* + \sin\alpha_o \cos\beta_o)/(c_o \sin\alpha_o \sin\beta_o \sin\gamma_o^*) \\ 0 & 1/(b_o \sin\alpha_o) & -\cos\alpha_o/(c_o \sin\alpha_o) \\ 0 & 0 & 1/c_o \end{bmatrix}$$

On carrying out the operations indicated in equation (1-112) we obtain:

$$(1\text{-}114)\quad \ell_{11} = \frac{a_1 \sin\beta_1 \sin\gamma_1^*}{a_o \sin\beta_o \sin\gamma_o^*} - 1 \ ,$$

$$(1\text{-}115)\quad \ell_{12} = \ell_{21} = \frac{1}{2}\left(\frac{b_1 \sin\alpha_1 \cos\gamma_o^*}{b_o \sin\alpha_o \sin\gamma_o^*} - \frac{a_1 \sin\beta_1 \cos\gamma_1^*}{a_o \sin\beta_o \sin\gamma_o^*}\right)$$

$$(1\text{-}116)\quad \ell_{13} = \ell_{31} = \frac{1}{2}\left(\frac{a_1 \cos\beta_1}{a_o \sin\beta_o \sin\gamma_o^*} + \frac{b_1 \cos\alpha_1}{b_o \sin\alpha_o} - \frac{c_1 \cos\alpha_o \cos\gamma_o^*}{c_o \sin\alpha_o \sin\gamma_o^*} - \frac{c_1 \cos\beta_o}{c_o \sin\beta_o \sin\gamma_o}\right),$$

$$(1\text{-}117)\quad \ell_{22} = \frac{b_1 \sin\alpha_1}{b_o \sin\alpha_o} - 1$$

$$(1\text{-}118)\quad \ell_{23} = \ell_{32} = \frac{1}{2}\left(\frac{b_1 \cos\alpha_1}{b_o \sin\alpha_o} - \frac{c_1 \cos\alpha_o}{c_i \sin\alpha_o}\right),$$

and

$$(1\text{-}119)\quad \ell_{33} = \frac{c_1}{c_o} - 1$$

Mean values of the thermal expansion coefficients may then be found from the expression

$$(1\text{-}120)\quad \langle\lambda_{ij}\rangle = \ell_{ij}/\Delta T$$

where $\Delta T = T - T_o$.

The previous results are valid for all crystal systems. These formulas do not appear to be in the literature at the present time. They are, however, implicitly given by Ohashi and Burnham (1973) in their equation (A-9). Since the appearance of these equations in 1973 they have been used rather extensively, for example, Willaime, Brown, and Perucaud (1974).

For the monoclinic case, where $\alpha = \gamma = 90$, these expressions become

$$(1\text{-}121) \quad \ell_{11} = \frac{a_1 \sin\beta_1}{a_o \sin\beta_o} - 1 ,$$

$$(1\text{-}122) \quad \ell_{12} = \ell_{21} = 0 ,$$

$$(1\text{-}123) \quad \ell_{13} = \ell_{31} = \frac{1}{2}\left(\frac{a_1 \cos\beta_1}{a_o \sin\beta_o} - \frac{c_1 \cos\beta_1}{c_o \sin\beta_o}\right) ,$$

$$(1\text{-}124) \quad \ell_{23} = \ell_{32} = 0 ,$$

and

$$(1\text{-}125) \quad \ell_{33} = \frac{c_1}{c_o} - 1 .$$

These latter expressions are given in the paper by Ohashi and Burnham (1973).

The Schlenker-Gibbs-Boisen Method (1975)

This method is an extension of the procedure introduced in the thirties and forties by Eucken and Dannohl (1939) (Connell and Martin, 1939), Owen and Roberts (1936), and Stokes and Wilson (1941) (See section entitled "Early Methods of Calculating the Thermal Expansion

Coefficients of Cubic, Tetragonal, Hexagonal, and Orthorhombic Crystals"). Here we extend this approach to the monoclinic and triclinic crystal systems. The thermal expansion coefficients are expressed in differential form as functions of the cell parameters. Two sets of expressions are developed. The first set of expressions is termed by us linear Lagrangian thermal expansion coefficients. These correspond in form to the "instantaneous linear thermal expansion coefficient[s]" of Kempter and Elliott (1959). The second set of expressions is called linear Eulerian thermal expansion coefficients and correspond in form to Kempter and Elliott's (1959) "true thermal expansion coefficient[s]." The relation of these equations to the previously discussed results of Ohashi and Burnham is also explained.

Let us allow $[\alpha_{ij}(T)]$ to stand for a general type of thermal expansion tensor without specifying the type. Symmetry considerations and Neumann's principle suffice to show that for a monoclinic crystal (second setting) the thermal expansion coefficient tensor has the form

$$(1\text{-}126)\quad \begin{bmatrix} \alpha_{11}(T) & 0 & \alpha_{13}(T) \\ 0 & \alpha_{22}(T) & 0 \\ \alpha_{13}(T) & 0 & \alpha_{33}(T) \end{bmatrix}$$

The form for a triclinic crystal is

$$(1\text{-}127)\quad \begin{bmatrix} \alpha_{11}(T) & \alpha_{12}(T) & \alpha_{13}(T) \\ \alpha_{12}(T) & \alpha_{22}(T) & \alpha_{23}(T) \\ \alpha_{13}(T) & \alpha_{23}(T) & \alpha_{33}(T) \end{bmatrix}$$

There are several approaches which may be used to obtain the $\lambda_{ij}(T)$. For the monoclinic case we may proceed by using equation (1-65). The

expansion along the a*-axis (which coincides $\hat{i}$) is

$\frac{1}{d_o(100)} d[d_{(100)}(T)]/dT$, and the direction cosines of a line normal to (100) are ($n_1 = 1$, $n_2 = 0$, $n_3 = 0$). Therefore equation (1-65) becomes

$$(1\text{-}128) \quad \lambda_{11}(T) = \frac{1}{d_o(010)} \frac{d[d_{(100)}(T)}{dT} = \frac{1}{a_o \sin_o} \frac{d[a(T)\sin\beta(T)]}{dT}$$

The $\underset{\sim}{b}$ and $\underset{\sim}{c}$ axes have direction cosines (0,1,0) and (0,0,1) respectively so that, on using equation (1-62) we obtain

$$(1\text{-}129) \quad \lambda_{22}(T) = \frac{1}{b_o} \frac{db(T)}{dT} \quad ,$$

and

$$(1\text{-}130) \quad \lambda_{33}(T) = \frac{1}{c_o} \frac{dc(T)}{dT} \quad .$$

The off diagonal element $\lambda_{13}(T)$ is more difficult to obtain. The thermal expansion along the a cell edge is given, in the Lagrangian formulation, by

$$(1\text{-}131) \quad \lambda_a(T) = \frac{1}{a_o} \frac{da(T)}{dT} \quad .$$

Since the initial direction cosines (n_1,n_2,n_3) of $\underset{\sim}{a}$ are $(\sin\beta_o,0,\cos\beta_o)$ we can use equation (1-62) to obtain

$$(1\text{-}132) \quad \frac{1}{a_o} \frac{da(T)}{dT} = \lambda_{11}(T)\sin^2\beta_o + \lambda_{13}(T)\sin 2\beta_o + \lambda_{33}(T)\cos^2\beta_o \quad .$$

On replacing $\lambda_{11}(T)$ and $\lambda_{33}(T)$ by equations (1-128) and (1-130) and solving for $\lambda_{13}(T)$ we obtain

$$(1\text{-}133) \quad \lambda_{13}(T) = \frac{1}{a_o \sin 2\beta_o} \frac{da(T)}{dT} - \frac{1}{2}\left(\frac{1}{a_o \cos\beta_o} \frac{d[a(T)\sin\beta(T)]}{dT} + \right.$$

$$\left. \frac{\cot\beta_o}{c_o} \frac{dc(T)}{dT} \right)$$

By means of equation (1-60) we can obtain a slightly different form for $\lambda_{13}(T)$. On differentiating (1-60) we obtain

$$(1\text{-}134) \quad \left(\bar{n}_i(T) n_i \frac{d\ell(T)}{dT} + n_i \ell(T) \frac{d\bar{n}_i(T)}{dT} \right) / \ell_o = \frac{d\ell_{ij}(T)}{dT} n_i n_j$$

$$= \lambda_{ij}(T) n_i n_j \ .$$

Since the initial direction cosines (n_1, n_2, n_3) of a are $(\sin\beta_o, 0, \cos\beta_o)$ and the final direction cosines $(\bar{n}_1, \bar{n}_2, \bar{n}_3)$ are $(\sin\beta(T), 0, \cos\beta(T))$.

We can expand (1-134) to obtain

$$(1\text{-}135) \quad \frac{1}{a_o}[\sin\beta_o \sin\beta(T) + \cos\beta_o \cos\beta(T)] \frac{da(T)}{dT} + \frac{a(T)}{a_o}$$

$$[\sin\beta_o \cos\beta(T) + 0 - \cos\beta_o \sin\ (T)] \frac{d\beta(T)}{dT}$$

$$= \lambda_{11}(T) \sin^2\beta_o + 2\sin\beta_o \cos\beta_o \lambda_{13}(T) + \lambda_{33}(T) \cos^2\beta_o \ .$$

On inserting the expressions previously obtained, equations (1-128) and (1-130), for $\lambda_{11}(T)$ and $\lambda_{33}(T)$ and solving for $\lambda_{13}(T)$ we obtain

$$(1\text{-}136) \quad \lambda_{13}(T) = \frac{1}{2} \left(\frac{1}{a_o \sin\ _o} \frac{d[a(T)\cos\ (T)]}{dT} - \frac{\cot\beta_o}{c_o} \frac{dc(T)}{dT} \right) .$$

The difference between the result given by (1-133) and (1-136) is due to the fact that (1-133) was developed from the usual result of finite Lagrangian strain theory, namely $(\ell - \ell_o)/\ell_o \simeq \ell_{ij} n_i n_j$ (see Mase (1970) and Frederick and Chang (1959)). This expression becomes exact only in the limit of an infinitesimal material displacement gradient, defined as $[I_{ij}] = [\partial u_i / \partial X_j]$. Values of $\lambda_{13}(T)$ for diopside were calculated using both equations. The results are shown in Figure 1-8.

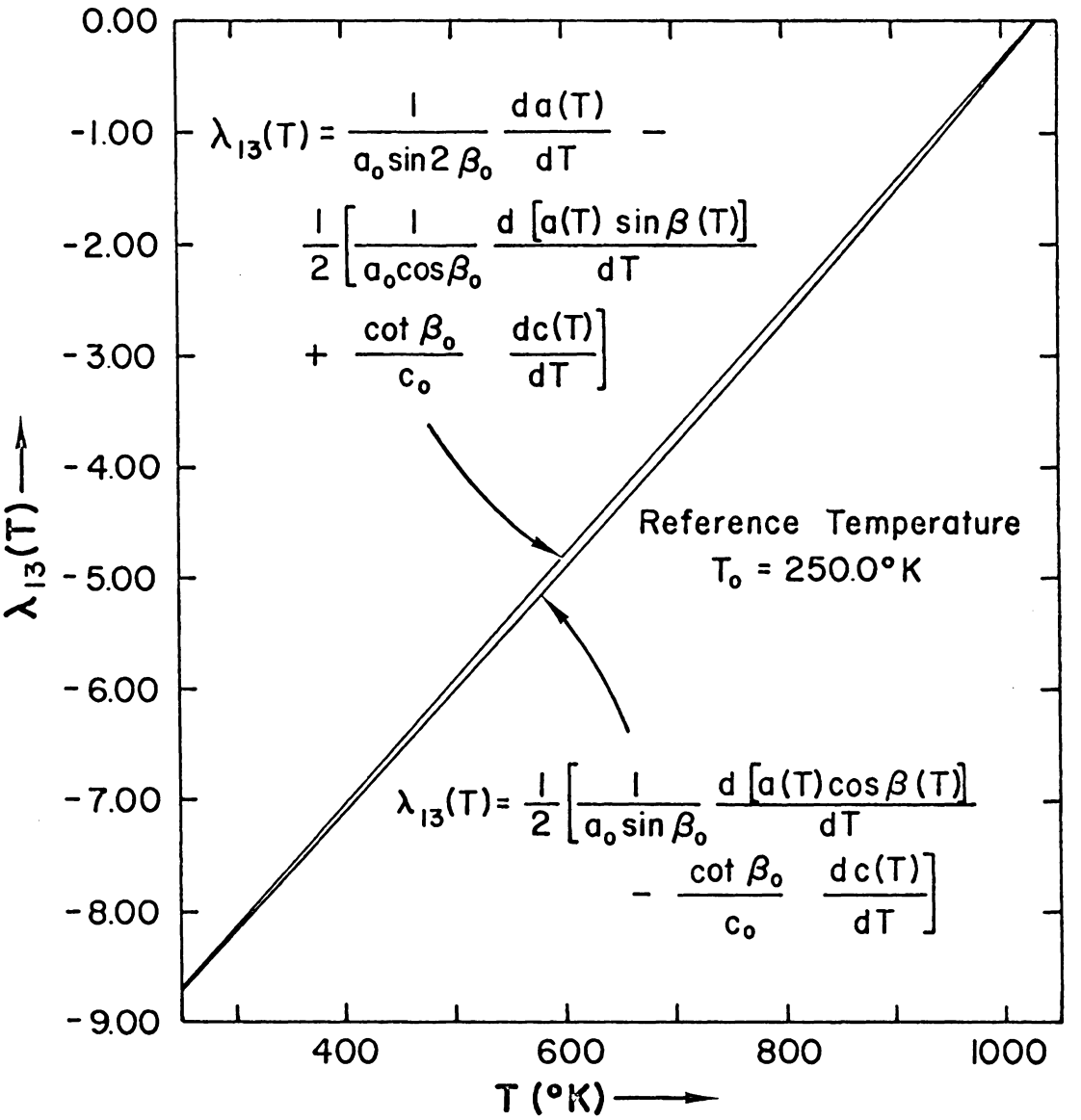

Figure 1-8: A comparison of two formulae for computing the off-diagonal element of the thermal expansion coefficient tensor, $\lambda_{13}(T)$, for a monoclinic crystal (see text for discussion). Although the results are very close the expression given in the lower right hand portion of the diagram is the more exact. The substance used for this calculation was diopside ($CaMgSi_2O_6$).

The similarity of the results is proof that the approximations inherent in equation (1-51) are well justified in this case.

The mean value of $\lambda_{ij}(T)$, between the temperature T_o and T, can be calculated using

$$(1\text{-}137) \quad \langle\alpha_{ij}\rangle = \frac{1}{T-T_o}\int_{T_o}^{T} \alpha_{ij}(T)dT \ .$$

When this is used to calculate the mean thermal expansion coefficients of $\lambda_{11}(T)$, $\lambda_{22}(T)$, $\lambda_{33}(T)$, and $\lambda_{13}(T)$ we obtain

$$(1\text{-}138) \quad \langle\lambda_{11}\rangle = \frac{1}{T-T_o}\left(\frac{a_1\sin\beta_1}{a_o\sin\beta_o} - 1\right) \ ,$$

$$(1\text{-}139) \quad \langle\lambda_{22}\rangle = \frac{1}{T-T_o}\left(\frac{b_1}{b_o} - 1\right) \ ,$$

$$(1\text{-}140) \quad \langle\lambda_{33}\rangle = \frac{1}{T-T_o}\left(\frac{c_1}{c_o} - 1\right) \ ,$$

and

$$(1\text{-}141) \quad \langle\lambda_{13}\rangle = \frac{1}{2(T-T_o)}\left(\frac{a_1\cos\beta_1}{a_o\sin\beta_o} - \frac{c_1\cos\beta_o}{c_o\sin\beta_o}\right) \ .$$

We see immediately that these expressions are identical with the Ohashi-Burnham results for the monoclinic case. This indicates that the Ohashi-Burnham equations give mean values for the λ_{ij} which are valid in the temperature interval between T_o and T. Equation (1-141) has obtained by integrating (1-136). The mean value of equation (1-133) is

$$(1\text{-}142)\quad \langle\lambda_{13}\rangle = \frac{1}{2(T-T_o)}\left(\frac{a_1\left(1-\sin\beta_1\sin\beta_o\right)}{a_o\ \sin\beta_o\cos\beta_o} - \frac{c_1\cos\beta_o}{c_o\sin\beta_o}\right)$$

which differs slightly from the Ohashi-Burnham result.

Equations for the triclinic case could be obtained in the same fashion. However it is simpler to proceed by simply taking the derivatives of those expressions given in equations (1-114) through (1-119). When this is done we obtain

$$(1\text{-}143)\quad \lambda_{11}(T) = \frac{1}{a_o\sin\beta_o\sin\gamma^*_o}\cdot\frac{d[a(T)\cos\beta(T)\sin\gamma^*(T)]}{dT}\ ,$$

$$(1\text{-}144)\quad \lambda_{12}(T) = \lambda_{21}(T) = \frac{\cos\gamma^*_o}{2b_o\sin\beta_o\sin\gamma^*_o}\cdot\frac{d[a(T)\sin\beta(T)\cos\gamma^*(T)]}{dT}$$
$$- \frac{1}{2a_o\sin\beta_o\sin\gamma^*_o}\cdot\frac{d[a(T)\cos\beta(T)\sin\gamma^*(T)]}{dT}$$

$$(1\text{-}145)\quad \lambda_{13}(T) = \lambda_{31}(T) = \frac{1}{2}\left(\frac{1}{a_o\sin\beta_o\sin\gamma^*_o}\cdot\frac{d[a(T)\cos\beta(T)\sin\gamma^*(T)]}{dT}\right.$$
$$+ \frac{\cos\gamma^*_o}{b_o\sin\alpha_o\sin\gamma^*_o}\frac{d[b(T)\sin\alpha(T)]}{dT}$$
$$- \frac{\cos\alpha_o\cos\gamma^*_o}{c_o\sin\alpha_o\sin\gamma^*_o}\frac{dc(T)}{dT}$$
$$\left. - \frac{\cos\beta_o}{c_o\sin\beta_o\sin\gamma^*_o}\frac{dc(T)}{dT}\right),$$

$$(1\text{-}146)\quad \lambda_{22}(T) = \frac{1}{b_o\sin\alpha_o}\frac{d[b(T)\sin\alpha(T)]}{dT}\ ,$$

$$(1\text{-}147)\quad \lambda_{23}(T) = \lambda_{32}(T) = \frac{1}{2}\left(\frac{1}{b_o\sin\alpha_o}\frac{d[b(T)\cos\alpha(T)]}{dT}\right.$$
$$\left. - \frac{\cos\alpha_o}{c_o\sin\alpha_o}\frac{dc(T)}{dT}\right),$$

and

$$(1\text{-}148)\quad \lambda_{33}(T) = \frac{1}{c_o}\frac{dc(T)}{dT} \quad .$$

These expressions are quite complex but note that they reduce correctly to the previously obtained monoclinic case. Equations (1-143) through (1-148) could also be obtained using equation (1-134) however this would be a very tedious undertaking.

An analogous set of expressions, termed linear Eulerian thermal expansion coefficients may be obtained from (1-64) and (1-66) on using equation (1-66) we obtain

$$(1\text{-}149)\quad \varepsilon_{11}(T) = \frac{1}{d_{(100)}(T)}\frac{d[d_{(100)}(T)]}{dT} = \frac{d[\ell n(a(T)\sin\beta(T))]}{dT}$$

$$= \frac{1}{a(T)}\frac{da(T)}{dT} + \cot\beta(T)\frac{d\beta(T)}{dT} \quad .$$

On using equation (1-64) we arrive at

$$(1\text{-}150)\quad \varepsilon_{22}(T) = \frac{1}{b(T)}\frac{db(T)}{dT} \quad ,$$

and

$$(1\text{-}151)\quad \varepsilon_{33}(T) = \frac{1}{c(T)}\frac{dc(T)}{dT} \quad .$$

An expression for $\varepsilon_{13}(T)$ may be obtained by expanding (1-64) and realizing that the instantaneous direction cosines $(\bar{n}_1,\bar{n}_2,\bar{n}_3)$ of $\underset{\rightarrow}{a}$ are $(\sin\beta(T),0,\cos\beta(T))$. On solving the expanded form of (1-64) for $\varepsilon_{13}(T)$ one obtains

$$(1\text{-}152)\quad \varepsilon_{13}(T) = \frac{\cot\beta(T)}{2}\left(\frac{1}{a(T)}\frac{da(T)}{dT} - \frac{1}{c(T)}\frac{dc(T)}{dT}\right) - \frac{1}{2}\frac{d\beta(T)}{dT} \quad .$$

It should be noted that these expressions differ from the corresponding Lagrangian forms in that there is no need to make an arbitrary choice

of initial reference temperature. This makes the $\varepsilon_{ij}(T)$ unique.

By means of (1-137) we obtain the following average values for the ε_{ij}

$$(1\text{-}153)\quad \langle\varepsilon_{11}\rangle = \frac{1}{T-T_o}\,\ell n\left(\frac{a_1 \sin\beta_1}{a_o \sin\beta_o}\right) \simeq \frac{1}{T-T_o}\left(\frac{a_1 \sin\beta_1}{a_o \sin\beta_o} - 1\right) ,$$

$$(1\text{-}154)\quad \langle\varepsilon_{22}\rangle = \frac{1}{T-T_o}\,\ell n\left(\frac{b_1}{b_o}\right) \simeq \frac{1}{T-T_o}\left(\frac{b_1}{b_o} - 1\right) ,$$

$$(1\text{-}155)\quad \langle\varepsilon_{33}\rangle = \frac{1}{T-T_o}\,\ell n\left(\frac{c_1}{c_o}\right) \simeq \frac{1}{T-T_o}\left(\frac{c_1}{c_o} - 1\right)$$

The expression for $\varepsilon_{13}(T)$ cannot be integrated exactly (because of the assumptions inherent in the theory of linear strain it is not an exact differential). A numerical approximation to the integral using, for example, the trapezoidal rule, is easily made.

In equations (1-153) through (1-155) we have used the first term of the expansion

$$(1\text{-}156)\quad \ell nx = (x - 1) - \frac{1}{2}(x - 1)^2 + \frac{1}{3}(x - 1)^3 - \cdots$$

Error Evaluation: Formulas for Computing the Variances of the Linear Eulerian Thermal Expansion Coefficients (Monoclinic Case)

We will assume that $\underset{\rightarrow}{a}$, $\underset{\rightarrow}{b}$, $\underset{\rightarrow}{c}$ and β have been expressed in power series expansions of the form

$$(1\text{-}157)\quad a(T) = [a_o + a_1 T + a_2 T^2 + \cdots]\ \text{Å},$$

$$(1\text{-}158)\quad b(T) = [b_o + b_1 T + b_2 T^2 + \cdots]\ \text{Å},$$

$$(1\text{-}159)\quad c(T) = [c_o + c_1 T + c_2 T^2 + \cdots]\ \text{Å},$$

and

$$\beta(T) = [\beta_o + \beta_1 T + \beta_2 T^2 + \ldots] \text{ degrees.} \quad (1\text{-}160)$$

The variances of $\varepsilon_{22}(T)$ and $\varepsilon_{33}(T)$ are simplest to obtain. For $\varepsilon_{22}(T)$ we have

$$\text{Var}[\varepsilon_{22}(T)] = \sum_{n=0}^{\infty} \sum_{m=0}^{\infty} \left(\frac{\partial \varepsilon_{22}(T)}{b_n}\right)\left(\frac{\partial \varepsilon_{22}(T)}{b_m}\right) V^b_{nm} \quad (1\text{-}161)$$

where V^b_{nm} are the elements of the variance-covariance matrix for the regression coefficients given in the expression for b(T) (equation 1-158)).

This matrix has the form

$$\begin{bmatrix} V^b_{00} & V^b_{01} & V^b_{02} \cdots \\ V^b_{10} & V^b_{11} & V^b_{22} \cdots \\ \cdots\cdots\cdots\cdots\cdots \\ \cdots\cdots\cdots\cdots\cdots \end{bmatrix} \quad (1\text{-}162)$$

It is easy to show from equations (1-150) and (1-158) that

$$\frac{\partial \varepsilon_{22}(T)}{\partial bn} = [nT^{n-1} - T^n \varepsilon_{22}(T)]/b(T) \quad (1\text{-}163)$$

For $\varepsilon_{33}(T)$ the equation for the variance is of the form

$$\text{Var}[\varepsilon_{33}(T)] = \sum_{n=0}^{\infty} \sum_{m=0}^{\infty} \left(\frac{\partial \varepsilon_{33}(T)}{\partial c_n}\right)\left(\frac{\partial \varepsilon_{33}(T)}{\partial c_m}\right) V^c_{nm} \quad (1\text{-}164)$$

where

$$\frac{\partial \varepsilon_{33}(T)}{\partial c_n} = [nT^{n-1} - T^n \varepsilon_{33}(T)]/c(T) \; . \quad (1\text{-}165)$$

The expression for the variance of $\varepsilon_{11}(T)$ is more complex because the angle $\beta(T)$ is involved.

β is usually given in degrees but must be expressed in radians in these calculations. This means that equation (1-149) becomes

$$(1\text{-}166)\quad \varepsilon_{11}(T) = \frac{1}{a(T)}\frac{da(T)}{dT} + \frac{\pi}{180}\cot\beta(T)\frac{d\beta(T)}{dT}$$

if β is given in degrees.

We can write (1-166) as

$$(1\text{-}167)\quad \varepsilon_{11}(T) = \frac{a_1 + 2a_2T + 3a_3T^2 + \ldots}{a_o + a_1T + a_2T^2 + \ldots} + \cot[\beta_o + \beta_1T + \beta_2T^2 + \ldots][\tfrac{\pi}{180}(\beta_1 + 2\beta_2T^2 + \ldots)]$$

and the variance will be

$$(1\text{-}168)\quad \mathrm{Var}[\varepsilon_{11}(T)] = \sum_{n=0}^{\infty}\sum_{m=0}^{\infty}\left(\frac{\partial\varepsilon_{11}(T)}{\partial a_n}\right)\left(\frac{\partial\varepsilon_{11}(T)}{\partial a_m}\right)V^a_{nm} + \left(\frac{\partial\varepsilon_{11}(T)}{\partial(\frac{\pi\beta_n}{180})}\right)\left(\frac{\partial\varepsilon_{11}(T)}{\partial(\frac{\pi\beta_m}{180})}\right)(\tfrac{\pi}{180})^2V^\beta_{nm}\ .$$

It is easily shown that

$$(1\text{-}169)\quad \frac{\partial\varepsilon_{11}(T)}{\partial a_n} = nT^{n-1} - \frac{1}{a(T)}\frac{da(T)}{dT}$$

and that

$$(1\text{-}170)\quad \frac{\partial\varepsilon_{11}(T)}{\partial(\frac{\pi\beta_r}{180})} = nT^{n-1}\cos\beta(T) - \frac{\pi T^n}{180}[\csc^2\beta(T)]\frac{d\beta(T)}{dT}$$

where the $\frac{d\beta(T)}{dT}$ in the last term is given in degrees.

The expression for the variance of $\varepsilon_{13}(T)$ is still more complex because the expression for $\varepsilon_{13}(T)$ involves $a(T)$, $c(T)$, and $\beta(T)$. We

have

$$\text{(1-171)}\quad \mathrm{Var}[\varepsilon_{13}(T)] = \sum_{n=0}^{\infty}\sum_{m=0}^{\infty}\left(\frac{\partial\varepsilon_{13}(T)}{\partial a_n}\right)\left(\frac{\partial\varepsilon_{13}(T)}{\partial a_m}\right)V^{a}_{nm} + \left(\frac{\partial\varepsilon_{13}(T)}{\partial c_n}\right)\left(\frac{\partial\varepsilon_{13}(T)}{\partial c_m}\right)V^{c}_{nm} + \left(\frac{\partial\varepsilon_{13}(T)}{\partial c_n}\right)\left(\frac{\partial\varepsilon_{13}(T)}{\partial c_m}\right)V^{c}_{nm} + \left(\frac{\partial\varepsilon_{13}(T)}{\partial\left(\frac{\pi\beta_n}{180}\right)}\right)\left(\frac{\partial\varepsilon_{13}(T)}{\partial\left(\frac{\pi\beta_m}{180}\right)}\right)\frac{\pi}{180}^{2}V^{\beta}_{nm}$$

It is easy to show that if $a(T)$, $c(T)$, and $\beta(T)$ have the form given in equations (1-157), (1-159), and (1-160) that

$$\text{(1-172)}\quad \frac{\partial\alpha_{13}(T)}{\partial a_n} = \frac{\cot\beta(T)}{2a(T)}\left(nT^{n-1} - \frac{T^n}{a(T)}\frac{da(T)}{dT}\right),$$

$$\text{(1-173)}\quad \frac{\partial\alpha_{13}(T)}{c_n} = \frac{-\cot\beta(T)}{2c(T)}\left(nT^{n-1} - \frac{T^n}{c(T)}\frac{dc(T)}{dT}\right),$$

and

$$\text{(1-174)}\quad \frac{\partial\alpha_{13}(T)}{\partial\left(\frac{\pi\beta_n}{180}\right)} = -\frac{1}{2}\left[T^n\csc^2\beta(T)\left(\frac{1}{a(T)}\frac{da(T)}{dT} - \frac{1}{c(T)}\frac{dc(T)}{dT} + nT^{n-1}\right)\right].$$

The tensor, $[\varepsilon]$, must now be diagonalized. This may be done as follows (Ohashi and Burnham, 1973)

$$\text{(1-175)}\quad \varepsilon_1(T) = \tfrac{1}{2}[\varepsilon_{11}(T) + \varepsilon_{33}(T) + \sqrt{D}\ ]\ ,$$

$$\text{(1-176)}\quad \varepsilon_2(T) = \varepsilon_{22}(T)\ ,$$

and

$$\text{(1-177)}\quad \varepsilon_3(T) = \tfrac{1}{2}[\varepsilon_{11}(T) + \varepsilon_{33}(T) - \sqrt{D}\ ]$$

where

$$(1\text{-}178)\quad D = [(\varepsilon_{11}(T) + \varepsilon_{33}(T))^2 + 4(\varepsilon_{13}(T)\cdot\varepsilon_{13}(T) + \varepsilon_{11}(T)\cdot\varepsilon_{33}(T))]$$

We have the following expressions for the variances of $\varepsilon_1(T)$, $\varepsilon_2(T)$, and $\varepsilon_3(T)$:

$$(1\text{-}179)\quad \mathrm{Var}[\varepsilon_1(T)] = \sum_{n=0}^{\infty}\sum_{m=0}^{\infty}\left(\frac{\partial\varepsilon_1(T)}{\partial a_n}\right)\left(\frac{\partial\varepsilon_1(T)}{\partial a_m}\right) V^a_{nm} + \left(\frac{\partial\varepsilon_1(T)}{\partial c_n}\right)\left(\frac{\partial\varepsilon_1(T)}{\partial c_m}\right) V^c_{nm} + \left(\frac{\partial\varepsilon_1(T)}{\partial(\frac{\pi\beta_n}{180})}\right)\left(\frac{\partial\varepsilon_1(T)}{\partial(\frac{\pi\beta_m}{180})}\right) (\tfrac{\pi}{180})^2 V^\beta_{nm} ,$$

$$(1\text{-}180)\quad \mathrm{Var}[\varepsilon_2(T)] = \mathrm{Var}[\varepsilon_{22}(T)] ,$$

and

$$(1\text{-}181)\quad \mathrm{Var}[\varepsilon_3(T)] = \sum_{n=0}^{\infty}\sum_{m=0}^{\infty}\left(\frac{\partial\varepsilon_3(T)}{\partial a_n}\right)\left(\frac{\partial\varepsilon_3(T)}{\partial a_m}\right) V^a_{nm} + \left(\frac{\partial\varepsilon_3(T)}{\partial c_n}\right)\left(\frac{\partial\varepsilon_3(T)}{\partial c_m}\right) V^c_{nm} + \left(\frac{\partial\varepsilon_3(T)}{\partial(\frac{\pi\beta_n}{180})}\right)\left(\frac{\partial\varepsilon_3(T)}{\partial(\frac{\pi\beta_n}{180})}\right) (\tfrac{\pi}{180})^2 V^\beta_{nm}$$

It is easy to show that

$$(1\text{-}182)\quad \frac{\partial\varepsilon_1(T)}{\partial a_n} = \frac{1}{2}\left[1 + \frac{(\varepsilon_{11} - \varepsilon_{33})}{\sqrt{D}}\right]\left(\frac{\partial\varepsilon_{11}(T)}{\partial a_n}\right) + \frac{2\varepsilon_{13}}{\sqrt{D}}\left(\frac{\partial\varepsilon_{13}}{\partial a_n}\right),$$

$$(1\text{-}183)\quad \frac{\partial\varepsilon_1(T)}{\partial c_n} = \frac{1}{2}\left[1 - \frac{(\varepsilon_{11} - \varepsilon_{33})}{\sqrt{D}}\right]\left(\frac{\partial\varepsilon_{33}(T)}{\partial c_n}\right) + \frac{2\varepsilon_{13}}{\sqrt{D}}\left(\frac{\partial\varepsilon_{13}}{\partial c_n}\right)$$

and

$$(1\text{-}184)\qquad \frac{\partial \varepsilon_1(T)}{\partial\left(\frac{\pi\beta_n}{180}\right)} = \frac{1}{2}\left(1 + \frac{(\varepsilon_{11} - \varepsilon_{33})}{\sqrt{D}}\right)\left(\frac{\partial \varepsilon_{11}}{\partial\left(\frac{\pi\beta_n}{180}\right)}\right) + \frac{2\varepsilon_{13}}{\sqrt{D}}\left(\frac{\partial \varepsilon_{13}}{\partial\left(\frac{\pi\beta_n}{180}\right)}\right).$$

Note that the necessary derivatives have already been obtained. We now take the derivatives of $\varepsilon_3(T)$ with respect to a_n, c_n, and $(\pi\beta_n/180)$. These are

$$(1\text{-}185)\qquad \frac{\partial \varepsilon_3(T)}{\partial a_n} = \frac{1}{2}\left(1 - \frac{(\varepsilon_{11} - \varepsilon_{33})}{\sqrt{D}}\right)\left(\frac{\partial \varepsilon_{11}}{\partial a_n}\right) + \frac{2\varepsilon_{13}}{\sqrt{D}}\left(\frac{\partial \varepsilon_{13}}{\partial a_n}\right),$$

$$(1\text{-}186)\qquad \frac{\partial \varepsilon_3(T)}{\partial c_n} = \frac{1}{2}\left(1 + \frac{(\varepsilon_{11} - \varepsilon_{33})}{\sqrt{D}}\right)\left(\frac{\partial \varepsilon_{33}}{\partial c_n}\right) - \frac{2\varepsilon_{13}}{\sqrt{D}}\left(\frac{\partial \varepsilon_{13}}{\partial c_n}\right),$$

and

$$(1\text{-}187)\qquad \frac{\partial \varepsilon_3}{\partial\left(\frac{\pi\beta_n}{180}\right)} = \frac{1}{2}\left(1 - \frac{(\varepsilon_{33} - \varepsilon_{11})}{\sqrt{D}}\right)\left(\frac{\partial \varepsilon_{11}}{\partial\left(\frac{\pi\beta_n}{180}\right)}\right) + \frac{2\varepsilon_{13}}{\sqrt{D}}\left(\frac{\partial \varepsilon_{13}}{\partial\left(\frac{\pi\beta_n}{180}\right)}\right)$$

We must also determine $\theta(T)$, the angle $\varepsilon_1(T)$ makes with the positive end of the *c*-axis. According to Ohashi and Burnham (1973) this is given by

$$(1\text{-}188)\qquad \theta(T) = \tan^{-1}\left[\frac{\varepsilon_{13}}{\varepsilon_1 - \varepsilon_{11}}\right].$$

We see that

$$(1\text{-}189)\qquad \frac{\partial \theta(T)}{\partial a_n} = \left[\frac{1}{(\varepsilon_1 - \varepsilon_{11})^2 + \varepsilon_{13}^2}\right]\left[(\varepsilon_1 - \varepsilon_{11})\left(\frac{\partial \varepsilon_{13}}{\partial a_n}\right) - \varepsilon_{13}\left(\frac{\partial \varepsilon_1}{\partial a_n}\right) - \left(\frac{\partial \varepsilon_{11}}{\partial a_n}\right)\right],$$

$$(1\text{-}190)\qquad \frac{\partial \theta(T)}{\partial c_n} = \left[\frac{1}{(\varepsilon_1 - \varepsilon_{11})^2 + \varepsilon_{13}^2}\right]\left[(\varepsilon_1 - \varepsilon_{11})\left(\frac{\partial \varepsilon_{13}}{\partial c_n}\right) - \varepsilon_{13}\left(\frac{\partial \varepsilon_1}{\partial c_n}\right)\right],$$

and

$$(1\text{-}191)\quad \frac{\partial\theta(T)}{\partial\left(\frac{\pi\beta_n}{180}\right)} = \left[\frac{1}{(\varepsilon_1 - \varepsilon_{11})^2 + \varepsilon_{13}^2}\right]\left[(\varepsilon_1 - \varepsilon_{11})\left(\frac{\partial\varepsilon_{13}}{\partial\left(\frac{\pi\beta_n}{180}\right)}\right) - \varepsilon_{13}\left(\frac{\partial\varepsilon_1}{\partial\left(\frac{\pi\beta_n}{180}\right)}\right) - \left(\frac{\partial\varepsilon_3}{\partial\left(\frac{\pi\beta_n}{180}\right)}\right)\right]$$

The expression for the variance is

$$(1\text{-}192)\quad \mathrm{Var}[\theta(T)] = \sum_{n=0}^{\infty}\sum_{m=0}^{\infty}\left(\frac{\partial\theta(T)}{\partial a_n}\right)\left(\frac{\partial\theta(T)}{\partial a_m}\right) V^a_{nm} + \left(\frac{\partial\theta(T)}{\partial c_n}\right)\left(\frac{\partial\theta(T)}{\partial c_m}\right) V^c_{nm} + \left(\frac{\partial\theta(T)}{\partial\left(\frac{\pi\beta_n}{180}\right)}\right)\left(\frac{\partial\theta(T)}{\partial\left(\frac{\pi\beta_n}{180}\right)}\right) V^c_{nm}$$

The Eulerian Thermal Expansion Coefficients for the Triclinic Case

It is possible to treat the triclinic case as follows. We recall that according to equation (1-42) that for a homogeneous deformation $u_i = J_{ij}x_j$ so that (see equation (1-1))

$$(1\text{-}193)\quad X_i = (\delta_{ij} - J_{ij})x_j \ .$$

We write this in matrix form as

$$(1\text{-}194)\quad X = (I - J)_x$$

and on substituting (1-96) and (1-99) for x and X we obtain

$$(1\text{-}195)\quad (I - J)X_1^T x^c = S_o^T X^c$$

as (since $x^c = X^c$)

$$(1\text{-}196)\quad (I - J)S_1^T = S_o^T \ .$$

On rearranging this gives

$$(1\text{-}197)\quad J = I - S_o^T S^{-T} \ .$$

Since the form of the spacial displacement gradient tensor is now known in terms of the initial and final crystallographic axes we can obtain the elements of the linear Eulerian strain tensor from the expression:

$$(1\text{-}198)\quad [e] = \frac{1}{2}(J + J^T)$$

This immediately gives

$$(1\text{-}199)\quad [e] = I - \frac{1}{2}[S_1^{-1}S_o + (S_1^{-1}S_o)^T]$$

This is the Eulerian equivalent of equation (A-9) of Ohashi and Burnham. Since S_1 and S_o are known (equations (1-95) and (1-98)) it is easy to find the elements of [e]. The results are

$$(1\text{-}200)\quad e_{11} = \frac{a_1\sin\beta_1\sin\gamma_1^* - a_o\sin\beta_o\sin\gamma_o^*}{a_1\sin\beta_1\sin\gamma_1^*}$$

$$(1\text{-}201)\quad e_{22} = \frac{b_1\sin\alpha_1 - b_o\sin\alpha_o}{b_1\sin\alpha_1}$$

$$(1\text{-}202)\quad e_{33} = \frac{c_1 - c_o}{c_1} \ ,$$

$$(1\text{-}203)\quad e_{12} = e_{21} = \frac{1}{2}\left(\frac{a_o\sin\beta_o\cos\gamma_o^*}{a_1\sin\beta_1\sin\gamma_1^*} - \frac{b_o\sin\alpha_o\cos\gamma_1^*}{b_1\sin\alpha_1\sin\gamma_1^*}\right),$$

$$(1\text{-}204)\quad e_{13} = e_{31} = \frac{1}{2}\left(\frac{c_o\cos\beta_1}{c_1\sin\beta_1\sin\gamma_1^*} + \frac{c_o\cos\alpha_1\cos\gamma_1^*}{c_1\sin\alpha_1\sin\gamma_1^*} - \frac{b_o\cos\alpha_o\cos\gamma_1^*}{b_1\sin\alpha_1\sin\gamma_1^*} - \frac{a_o\cos\beta_o}{a_1\sin\beta_1\sin\gamma_1^*}\right).$$

$$(1\text{-}205)\quad e_{23} = e_{32} = \frac{1}{2}\left(\frac{c_o\cos\alpha_1}{c_1\sin\alpha_1} - \frac{b_o\cos\alpha_o}{b_1\sin\alpha_1}\right)$$

Naturally the linear Eulerian thermal expansion coefficients for the triclinic case may be obtained by differentiating these expressions with respect to T. However, the results are somewhat complex. In the monoclinic case equations (1-200) through (1-205) reduce to

$$(1\text{-}206)\quad e_{11} = \frac{a_1\sin\beta_1 - a_o\sin\beta_o}{a_1\sin\beta_1} = 1 - \frac{a_o\sin\beta_o}{a_1\sin\beta_1} \quad ,$$

$$(1\text{-}207)\quad e_{22} = \frac{b_1 - b_o}{b_1} = 1 - \frac{b_o}{b_1} \quad ,$$

$$(1\text{-}208)\quad e_{33} = \frac{c_1 - c_o}{c_o} = 1 - \frac{c_o}{c_1} \quad ,$$

$$(1\text{-}209)\quad e_{12} = e_{21} = 0,$$

$$(1\text{-}210)\quad e_{13} = e_{31} = \frac{1}{2}\left(\frac{c_o\cos\beta_1}{c_1\sin\beta_1} - \frac{a_o\cos\beta_o}{a_1\sin\beta_1}\right)$$

and

$$(1\text{-}211)\quad e_{23} = e_{32} = 0 \ .$$

On differentiating with respect to temperature we obtain

$$(1\text{-}212)\quad \varepsilon_{11} = \frac{de_{11}}{dT} = \frac{a_o\sin\beta_o}{a^2_{(T)}\sin^2\beta(T)} \ \frac{d[a(T)\sin\beta(T)]}{dT} \quad ,$$

$$(1\text{-}213)\quad \varepsilon_{22} = \frac{b_o}{b^2_{(T)}} \ \frac{db(T)}{dT} \quad ,$$

$$(1\text{-}214)\quad \varepsilon_{33} = \frac{c_o}{c^2_{(T)}} \ \frac{dc(T)}{dT} \quad ,$$

and

$$(1\text{-}215)\quad \varepsilon_{13} = \varepsilon_{31} = \frac{1}{2}\left(\frac{a_o\cos\beta_o}{a^2(T)\sin\beta(T)}\frac{da(T)}{dT} - \frac{c_o\cos\beta(T)}{c^2(T)\sin\beta(T)}\frac{dc(T)}{dT}\right) + \left(\frac{1}{2}\frac{a_o\cos\beta_o\cos\beta(T)}{a(T)\sin^2\beta(T)} - \frac{c_o}{c(T)} - \frac{c_o\cos^2\beta(T)}{c(T)\sin^2\beta(T)}\frac{d\beta(T)}{dT}\right)$$

Note that these results are not independent of temperature nor do they agree with the results obtained using equation (1-64) (equations (1-212) through (1-215) should be compared with the results given by equations (1-149) through (1-152)), however the relationship between the two sets of results is easily seen. We know that the cell parameters of the crystal change only by a very small amount on heating. This means that very little error is introduced in equations (1-212) through (1-215) if we make the substitutions

$$(1\text{-}216\text{-}a)\quad a(T) = a_o\ ,$$

$$(1\text{-}216\text{-}b)\quad b(T) = b_o\ ,$$

$$(1\text{-}216\text{-}c)\quad c(T) = c_o\ ,$$

and

$$(1\text{-}217)\quad \beta(T) = \beta_o\ .$$

The ε_{ij} then obtained here then become identical to equations (1-149) through (1-152).

Although no formulation of the elements of the finite Lagrangian and Eulerian strain tensor in terms of the cell parameters has yet been made (this includes the Ohashi-Burnham treatment which is a linear Lagrangian formulation) this can now be accomplished. We note that according to equations (1-3) and (1-42) the elements of the finite

Eulerian strain tensor are

$$(1\text{-}218) \quad E_{ij} = \frac{1}{2}(J_{ij} + J_{ji} + J_{ik}J_{kj})$$

Since the elements of [J], the spacial displacement gradient tensor, are known from equation (1-197) the E_{ij} can be evaluated. The results, naturally, are quite complex and are not given here. Although such a formulation is not necessary to describe the small deformations which occur during thermal expansion they might be useful when larger deformations (such as those involved in chemical substitution) occur.

THERMAL EXPANSION: RELATION TO OTHER PHYSICAL PROPERTIES

Let us consider a cubic crystal subject only to hydrostatic pressure, that is, subject only to a stress of the type

$$(1\text{-}219)\qquad \begin{bmatrix} \sigma_{11} & \sigma_{12} & \sigma_{13} \\ \sigma_{21} & \sigma_{22} & \sigma_{23} \\ \sigma_{31} & \sigma_{32} & \sigma_{33} \end{bmatrix} = \begin{bmatrix} -P & 0 & 0 \\ 0 & -P & 0 \\ 0 & 0 & -P \end{bmatrix} .$$

In such a case equation (1-11) takes the form

$$(1\text{-}220)\qquad V = V(P,T)$$

As was shown previously the thermal expansion coefficient tensor for a cubic crystal has the form

$$(1\text{-}221)\qquad \begin{bmatrix} \varepsilon_{11} & \varepsilon_{12} & \varepsilon_{13} \\ \varepsilon_{21} & \varepsilon_{22} & \varepsilon_{23} \\ \varepsilon_{31} & \varepsilon_{32} & \varepsilon_{33} \end{bmatrix} = \begin{bmatrix} \varepsilon_1 & 0 & 0 \\ 0 & \varepsilon_2 & 0 \\ 0 & 0 & \varepsilon_3 \end{bmatrix}$$

where

$$(1\text{-}222)\qquad \varepsilon_1 = \varepsilon_2 = \varepsilon_3 \simeq \frac{1}{a(T)} \frac{da(T)}{dT} .$$

The coefficient of volume expansion is

$$(1\text{-}223)\qquad \beta = \frac{1}{V(T)} \frac{dV(T)}{dT} = \varepsilon_{11} + \varepsilon_{22} + \varepsilon_{33} = 3\varepsilon_1 .$$

The isothermal compressibility of such a crystal is

$$(1\text{-}224)\qquad \chi^T = -\frac{1}{V}\left(\frac{\partial V}{\partial P}\right)_T$$

and the isothermal bulk modulus (the reciprocal of the compressibility is

$$(1\text{-}225)\qquad B_T = \frac{1}{\chi^T} = -V\left(\frac{\partial P}{\partial V}\right)_T .$$

We therefore see that

$$(1\text{-}226)\quad \beta B_T = \frac{\beta}{\chi_T} = -\frac{1}{V}\left(\frac{\partial V}{\partial T}\right)_P \cdot V\left(\frac{\partial P}{\partial V}\right)_T$$

or

$$(1\text{-}227)\quad \beta B_T = \frac{\beta}{\chi_T} = -\left(\frac{\partial V}{\partial T}\right)_P \cdot \left(\frac{\partial P}{\partial V}\right)_T = \left(\frac{\partial P}{\partial T}\right)_V$$

where the identity

$$(1\text{-}228)\quad \left(\frac{\partial x}{\partial y}\right)_z = -\left(\frac{\partial x}{\partial z}\right)_y \cdot \left(\frac{\partial z}{\partial y}\right)_x$$

has been used. We now use the Maxwell relation

$$(1\text{-}229)\quad \left(\frac{\partial P}{\partial T}\right)_V = \left(\frac{\partial S}{\partial V}\right)_T$$

to obtain

$$(1\text{-}230)\quad \beta B_T = \frac{\beta}{\chi_T} = \left(\frac{\partial S}{\partial V}\right)_T$$

The Grüneisen parameter for a crystal may be introduced, ad hoc, via the definition

$$(1\text{-}231)\quad \gamma = \frac{V}{C_v}\left(\frac{\partial S}{\partial V}\right)_T$$

where C_v is the heat capacity of the crystal at constant volume. We therefore obtain

$$(1\text{-}232)\quad \gamma = \frac{V\beta B_T}{C_v} = \frac{V\beta}{\chi_T C_v} \quad .$$

This is the Grüneisen relation for a cubic crystal. For many cubic substances at room temperature $\gamma \simeq 2$. The Grüneisen parameter is dimensionless.

For noncubic crystals the situation is more complex. According to Wallace (1972) the stress which a crystal exerts on its surroundings

has the implicit form

$$(1\text{-}233)\quad \sigma_{ij} = \sigma_{ij}(\eta_{11},\eta_{12},\eta_{13},\eta_{21},\eta_{22},\eta_{23},\eta_{31},\eta_{32},\eta_{33},T)$$

so that

$$(1\text{-}234)\quad \partial\sigma_{ij} = \left(\frac{\partial\sigma_{ij}}{\partial\eta_{k\ell}}\right)_{\eta',T} d\eta_{k\ell} + \left(\frac{\partial\sigma_{ij}}{\partial T}\right)_{\eta',T} dT = C_{ijk\ell}d\eta_{k\ell} + b_{ij}dT$$

where the b_{ij} are the crystal's thermal stress coefficients. On differentiating equation (3-234) with respect to stress at constant strain we obtain

$$(1\text{-}235)\quad 0 = C_{ijk\ell}\left(\frac{\partial\eta_{k\ell}}{\partial T}\right)_{\sigma} + b_{ij} = C_{ijk\ell}\alpha_{k\ell} + b_{ij}$$

We now use

$$(1\text{-}236)\quad \left(\frac{\partial\sigma_{ij}}{\partial T}\right)_{\eta} = -\frac{1}{V}\left(\frac{\partial S}{\partial\eta_{ij}}\right)_{\eta',T} = b_{ij}$$

which is the generalized form of one of the Maxwell relations. Therefore equation (1-235) becomes

$$(1\text{-}237)\quad C_{ijk\ell}\alpha_{k\ell} = \frac{1}{V}\left(\frac{\partial S}{\partial\eta_{k\ell}}\right)_{\eta',T}$$

which, on solving for the thermal expansion takes the form

$$(1\text{-}238)\quad \alpha_{ij} = \frac{S_{ijk\ell}}{V}\left(\frac{\partial S}{\partial\eta_{k\ell}}\right)_{\eta',T}$$

where the $S_{ijk\ell}$ are the elastic compliance coefficients for the crystal. Barron (1970) writes this equation, using the reduced subscript notation, as

$$(1\text{-}239)\quad \alpha_i = \sum_{j=1}^{6} \frac{S_{ij}}{V}\left(\frac{\partial S}{\partial\eta_j}\right)_{\eta',T} .$$

In order to obtain the equation in this form it is necessary to

assume

$$(1\text{-}240)\quad \begin{bmatrix} \alpha_{11} & \alpha_{12} & \alpha_{13} \\ \alpha_{21} & \alpha_{22} & \alpha_{23} \\ \alpha_{31} & \alpha_{32} & \alpha_{33} \end{bmatrix} = \begin{bmatrix} \alpha_1 & \frac{\alpha_6}{2} & \frac{\alpha_5}{2} \\ \frac{\alpha_6}{2} & \alpha_2 & \frac{\alpha_4}{2} \\ \frac{\alpha_5}{2} & \frac{\alpha_4}{2} & \alpha_3 \end{bmatrix},$$

and

$$(1\text{-}241)\quad \begin{bmatrix} \left(\frac{\partial S}{\partial \eta_{11}}\right)_{\eta',T} & \left(\frac{\partial S}{\partial \eta_{12}}\right)_{\eta',T} & \left(\frac{\partial S}{\partial \eta_{13}}\right)_{\eta',T} \\ \left(\frac{\partial S}{\partial \eta_{21}}\right)_{\eta',T} & \left(\frac{\partial S}{\partial \eta_{22}}\right)_{\eta',T} & \left(\frac{\partial S}{\partial \eta_{23}}\right)_{\eta',T} \\ \left(\frac{\partial S}{\partial \eta_{31}}\right)_{\eta',T} & \left(\frac{\partial S}{\partial \eta_{32}}\right)_{\eta',T} & \left(\frac{\partial S}{\partial \eta_{33}}\right)_{\eta',T} \end{bmatrix}$$

$$= \begin{bmatrix} \left(\frac{\partial S}{\partial \eta_1}\right)_{\eta',T} & 2\left(\frac{\partial S}{\partial \eta_6}\right)_{\eta',T} & 2\left(\frac{\partial S}{\partial \eta_5}\right)_{\eta',T} \\ 2\left(\frac{\partial S}{\partial \eta_6}\right)_{\eta',T} & \left(\frac{\partial S}{\partial \eta_2}\right)_{\eta',T} & 2\left(\frac{\partial S}{\partial \eta_4}\right)_{\eta',T} \\ 2\left(\frac{\partial S}{\partial \eta_5}\right)_{\eta',T} & 2\left(\frac{\partial S}{\partial \eta_4}\right)_{\eta',T} & \left(\frac{\partial S}{\partial \eta_3}\right)_{\eta',T} \end{bmatrix},$$

and

$$(1\text{-}242)\quad S_{IJ} = S_{ijk\ell} \times \begin{Bmatrix} 1 \text{ if I and J = 1, 2, or 3} \\ 2 \text{ if I or J = 4, 5, or 6} \\ 4 \text{ if I and J = 4, 5, or 6} \end{Bmatrix}.$$

On solving equation (1-239) for the $(\partial S/\partial \eta_j)_{\eta',T}$ we obtain

$$(1\text{-}243)\quad \left(\frac{\partial S}{\partial \eta_j}\right)_{\eta',T} = V \sum_{j=1}^{6} C_{ij}\alpha_j$$

Since the α_j and C_{ij} can be measured experimentally it is possible to use equation (1-343) to calculate the strain dependence of the entropy function of the crystal as a function of temperature.

For noncubic crystals the single macroscopic Grüneisen parameter becomes a symmetric second rank tensor, denoted γ_{ij}, with nine components. In terms of purely classical thermodynamic theory these may be introduced via the simple definition

$$(1\text{-}244) \quad \gamma_{ij} = \frac{1}{C_\eta}\left(\frac{\partial S}{\partial \eta_{ij}}\right)_{\eta',T}$$

Where C_η is the heat capacity at constant strain. In the reduced subscript notation we have

$$(1\text{-}245) \quad \begin{bmatrix} \gamma_{11} & \gamma_{12} & \gamma_{13} \\ \gamma_{21} & \gamma_{22} & \gamma_{23} \\ \gamma_{31} & \gamma_{32} & \gamma_{33} \end{bmatrix} = \begin{bmatrix} \gamma_1 & \gamma_6 & \gamma_5 \\ \gamma_6 & \gamma_2 & \gamma_4 \\ \gamma_5 & \gamma_4 & \gamma_3 \end{bmatrix}$$

Therefore the Grüneisen relations for a noncubic crystal are

$$(1\text{-}246) \quad \alpha_{ij} = VS_{ijk\ell}\gamma_{k\ell}/C_\eta$$

or

$$(1\text{-}247) \quad \gamma_{ij} = VS_{ijk\ell}\alpha_{k\ell}/C_\eta$$

in the tensor notation and

$$(1\text{-}248) \quad \alpha_i = \frac{C_\eta}{V}\sum_{j=1}^{6} S_{ij}\gamma_j$$

or

$$(1\text{-}249) \quad \gamma_i = \frac{V}{C_\eta}\sum_{j=1}^{6} C_{ij}\alpha_j$$

in the reduced subscript notation. The significance of these γ_i will

be discussed in the following sections.

Atomic Models for Thermal Expansion

Up to this point the discussion of thermal expansion has been essentially phenomenological in nature and no account has been taken of the crystal's atomistic nature. Due to the lack of an adequate theory very little can be said about the fundamental cause of thermal expansion in complex crystals which is not entirely superficial in nature. However, as a result of Barron's (1970) generalization of the Grüneisen parameter (a second rank tensor in Barron's treatment) some slight progress is possible.

It should be said at the outset that any treatment of thermal expansion in crystals which even pretends at rigor must have as its starting point the determination of the frequencies of the lattice modes of the crystal and their strain dependence. It is only in this way that a quantitative theory can be constructed. It is very doubtful that simply carrying out structure refinements at high temperatures will ever lead to any insight into this problem which is not essentially qualitative in nature.

The Quasiharmonic Approximation

It is well known that the expansion which occurs in solids on heating is a result of the anharmonic nature of the forces acting between atoms (Levy, 1968). Consider, for example, two atoms interacting via a potential

$$(1\text{-}250) \quad V(x) = ax^2 - gx^3 - fx^4 - \cdots .$$

Suppose the equilibrium internuclear separation of these atoms at $T = 0$ is r_o (r_o corresponds to the minimum in the potential energy curve). Let r denote the instantaneous internuclear separation. We see that

$$(1\text{-}251) \quad x = r - r_o$$

Since, according to Amoros and Canut-Amoros (1968), the kinetic energy of the thermal motion is always negligible compared to the potential energy of the system, the Boltzmann distribution function for this oscillator becomes

$$(1\text{-}252) \quad P(x) = Ne^{-V/k_BT}$$

where

$$N = 1/\int_{-\infty}^{+\infty} e^{-V(x)/k_BT}\, dx$$

Therefore the mean value of x is

$$(1\text{-}253) \quad \langle x(T)\rangle = N\int_{-\infty}^{+\infty} xe^{-V(x)/k_BT}\, dx$$

$$(1\text{-}254) \quad \langle x(T)\rangle = N\int_{-\infty}^{+\infty} xe^{-(ax^2 - gx^3 - fx^4)/k_BT}\, dx$$

$$= N\int_{-\infty}^{+\infty} xe^{-ax^2/k_BT}\, e^{(gx^3 + fx^4 + \cdots)/k_BT}\, dx$$

$$\simeq N\int_{-\infty}^{+\infty} e^{-ax^2/k_BT}\, (x + gx^4 + fx^5)/k_BT\, dx$$

$$= N\left[\left(\frac{3g}{4k_BT}\right)\left(\frac{\pi k_B^5 T^5}{a^5}\right) + \cdots\right]\left(\frac{3g}{4k_BT}\right)\left(\frac{\pi k_B^5 T^5 + \cdots}{a^5}\right)^{1/2}$$

$$\left(\frac{a}{\pi k_B T}\right)^{1/2}$$

$$= \frac{3gk_BT}{4a^2} + \cdots$$

(note that g,f << a) since

$$(1\text{-}255)\quad 1/N = \int_{-\infty}^{+\infty} e^{-(ax^2 - gx^3 - fx^4/k_BT)}\, dx \simeq 2\int_0^{+\infty} e^{-ax^2/k_BT}\, dx$$

$$= \left(\frac{\pi k_B T}{a}\right)^{1/2}$$

The mean equilibrium separation of the two atoms at temperature T is therefore

$$(1\text{-}256)\quad \langle r(T)\rangle = r_o + \frac{3gk_BT}{4a^2} + \cdots .$$

On defining the logarithmic strain (Mase, 1970) as

$$(1\text{-}257)\quad e(T) = \ln \frac{\langle r(T)\rangle}{\langle r(T_o)\rangle} ,$$

where $\langle r(T_o)\rangle$ is the bond length at some reference temperature T_o we can calculate the thermal expansion coefficient of the bond as

$$(1\text{-}258)\quad \varepsilon = \frac{de(T)}{dT} = \frac{1}{\langle r(T)\rangle}\frac{d\langle r(T)\rangle}{dT} = \frac{1}{r_o + \frac{3gk_BT}{4a^2} + \cdots}\left(\frac{3gk_B}{4a^2} + \cdots\right)$$

$$\simeq \frac{3gk_B}{4a^2 r_o}$$

(Zhdanov, 1965) indicating that the change in the bond length with temperature is solely due to the higher (anharmonic) terms in the potential energy curve.

Although the anharmonic model can be extended to crystals the result is very complex. Because of this thermal expansion in crystals is usually discussed in terms of a slight modification of the harmonic model called the quasiharmonic approximation.

The essential nature of the harmonic model can be illustrated most easily for a molecule consisting of N atoms. The potential energy of this molecule can be written as a Taylor series expansion in the atomic displacements:

$$(1\text{-}259)\quad V = V_o + \sum_{\kappa=1}^{N}\sum_{\alpha=1}^{3}\left(\frac{\partial V}{\partial u_\alpha(\kappa)}\right)_0 u_\alpha(\kappa) + \frac{1}{2}\sum_{\kappa=1}^{N}\sum_{\alpha=1}^{3}\sum_{\kappa=1}^{N}\sum_{\alpha=1}^{3}\left(\frac{\partial^2 V}{\partial u_\alpha(\kappa)\partial u_{\alpha'}(\kappa')}\right)_0 u_{\alpha(\kappa)}u_{\alpha'}(\kappa') + \cdots$$

where $u_\alpha(\kappa)$ represents the αth component of the displacement of the κth atom from its equilibrium position. Since the energy is a minimum when the atoms are in their equilibrium positions we must have

$$(1\text{-}260)\quad \left(\frac{\partial V}{\partial u_\alpha(\kappa)}\right)_0 = 0$$

for $\kappa = 1, \cdots, N$; $\alpha = 1, 2, 3$. In the harmonic model all terms in the expansion higher than the second are neglected so that (1-259) becomes

$$(3\text{-}261)\quad V = V_o + \frac{1}{2}\sum_{\kappa=1}^{N}\sum_{\alpha=1}^{3}\sum_{\kappa'=1}^{N}\sum_{\alpha'=1}^{3}\left(\frac{\partial^2 V}{\partial u_\alpha(\kappa)\partial u_{\alpha'}(\kappa')}\right)_0 u_\alpha(\kappa)u_{\alpha'}(\kappa')$$

It is conventional to set V_o equal to zero.

For molecules we introduce the symbol

$$(1\text{-}262)\quad \phi_{\alpha\alpha'}(\kappa\kappa') = \left(\frac{\partial^2 V}{\partial u_\alpha(\kappa)\partial u_{\alpha'}(\kappa')}\right)_0$$

and write (1-257) as

$$(1\text{-}263)\quad V = V_o + \frac{1}{2}\sum_{\kappa=1}^{N}\sum_{\alpha=1}^{3}\sum_{\kappa'=1}^{N}\sum_{\alpha'=1}^{3}\phi_{\alpha\alpha'}(\kappa\kappa')u_\alpha(\kappa)u_\alpha(\kappa')$$

The quantity $[\phi_{\alpha\alpha'}(\kappa\kappa')]$ may be thought of as a 3 x 3 force constant matrix describing the interaction (in the harmonic approximation) of the κ and κ' atoms of the molecule. For a crystal which is N_1 unit cells long in the $\underset{\rightarrow}{a}$ direction, N_2 unit cells long in the $\underset{\rightarrow}{b}$ direction, N_3 unit cells long in the $\underset{\rightarrow}{c}$ direction, and which contains n atoms per unit cell the potential energy (again in the harmonic approximation) is given by

$$(1\text{-}264)\quad V = V_o + \frac{1}{2}\sum_{\ell_3=1}^{N_3}\sum_{\ell_2=1}^{N_2}\sum_{\ell_1=1}^{N_1}\sum_{\kappa=1}^{n}\sum_{\alpha=1}^{3}\sum_{\ell_3'=1}^{N_3}\sum_{\ell_2'=1}^{N_2}\sum_{\ell_1'=1}^{N_1}\sum_{\kappa'=1}^{n}\sum_{\alpha'=1}^{3}$$

$$\phi_{\alpha\alpha'}\begin{vmatrix}\kappa & \kappa'\\ \ell_1 & \ell_1'\\ \ell_2 & \ell_2'\\ \ell_3 & \ell_3'\end{vmatrix} u_\alpha\begin{vmatrix}\ell_1\\ \kappa\ \ell_2\\ \ell_3\end{vmatrix} u_{\alpha'}\begin{vmatrix}\ell_1'\\ \kappa'\ \ell_2'\\ \ell_3'\end{vmatrix}$$

where $u_\alpha\begin{vmatrix}\ell_1\\ \kappa\ \ell_2\\ \ell_3\end{vmatrix}$ represents the αth component of the displacement of the κth atom in the unit cell designated by the triple (ℓ_1,ℓ_2,ℓ_3) from its equilibrium position in that cell.

Equation (1-264) is the starting point for a Born-von Kármén analysis of the crystal. Much of the apparent complexity of this

formula is notational. This theory has now been applied to a large number of cubic substances. Simple noncubic substances, such as quartz and rutile, are also within the reach of this approach. The difficulty with this approach with regard to physical properties is that harmonic theory (strictly applied) predicts that many well known physical properties of crystals should not exist. A crystal whose interatomic forces were truly harmonic would exhibit no thermal expansion, no temperature dependence of the elastic constants and would lack many other properties which real crystals have (Willis and Pryor, 1975).

Fortunately thermal expansion can be introduced into the harmonic model without going beyond the quadratic term in the crystal potential by allowing the frequencies of the normal modes of the crystal to be strain dependent. When this is done the model is said to be "quasi-harmonic" in nature.

The Nature of the Normal Modes of a Crystal

A three dimensional crystal with N primitive cells and n atoms per primitive cell will have 3Nn lattice (normal) modes. Lattice modes are modes of vibration of the entire crystal. Consider a crystal with the dimensions $N_1\underset{\rightarrow}{a}$, $N_2\underset{\rightarrow}{b}$, and $N_3\underset{\rightarrow}{c}$. The total number of unit cells (assumed primitive) will be $N = N_1N_2N_3$. At any temperature above absolute zero thermal waves (called phonons in the quantum theory) will be propagating through the crystal in all directions. It is these propagating thermal waves interacting with x-rays that cause the TDS (temperature diffuse scattering) seen on many x-ray photographs. The

displacement of the κth atom in the ℓth cell (ℓ denotes a triple of numbers (ℓ_1,ℓ_2,ℓ_3)) due to the normal mode with frequency $\omega(\underset{\rightarrow}{k})$ and wave vector $\underset{\rightarrow}{k}$ is the real part of

$$(1\text{-}265)\quad \underset{\rightarrow}{u}(\kappa\ell,t) = \underset{\rightarrow}{u}(\kappa|\underset{\rightarrow}{k})\exp[i\underset{\rightarrow}{k}\cdot\underset{\rightarrow}{r}(\kappa\ell) - \omega(\underset{\rightarrow}{k})t] \ .$$

The total displacement of this atom is the sum of its displacements due to each excited normal mode. Note that the direction of displacement and the maximum amplitude of that displacement is independent of the unit cell.

The frequency of a given mode $\omega(\underset{\rightarrow}{k})$ depends on the value of $\underset{\rightarrow}{k}$ and the dependence of ω on $\underset{\rightarrow}{k}$ in a given direction specifies the dispersion relation for that particular direction of the crystal. In reality the permitted values of $\omega(\underset{\rightarrow}{k})$ are not continuous, however, they are so close together that continuity is assumed. Associated with each value of $\underset{\rightarrow}{k}$ are 3n frequencies. Each of these 3n frequencies belongs to a different branch of the crystal's dispersion relation. The wave-vector dependence of $\omega(\underset{\rightarrow}{k})$ is generally different in each branch and in each direction of the crystal. The branches are of two kinds - accoustical and optical. A crystal always has 3 accoustical and 3n-3 optic branches. The accoustical branches may be distinguished from the optical branches because $\omega(\underset{\rightarrow}{k}) \to 0$ as $\underset{\rightarrow}{k} \to 0$ for an accoustical branch (see Figure 1-9). Note that a crystal with only one atom per primitive cell will have no optic branches in its dispersion relation. The total number of values of $\underset{\rightarrow}{k}$ is equal to the number of primitive cells in the sample while the number of branches is equal to the number of atoms per primitive cell.

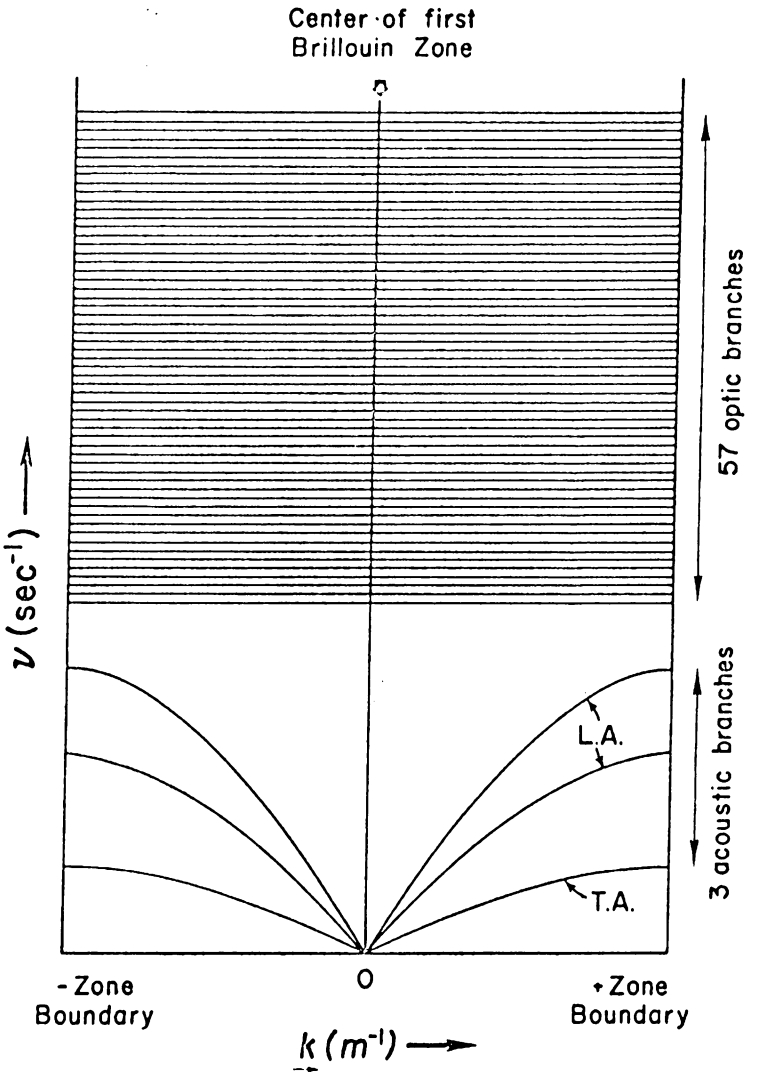

Figure 1-9: Schematic illustration of the acoustic and optic branches of the dispersion relation for diopside along an arbitrary direction in reciprocal space. Since the formula for diopside is $CaMgSi_2O_6$ and there are two molecules per primitive cell we have a total of 20 atoms in each cell. There is therefore a total of $3 \cdot 20 - 3 = 57$ optic branches in the dispersion relation.

The permissible values of $\underset{\rightarrow}{k}$ are entirely confined to the first Brillouin zone of the crystal and the end points of these vectors form a uniformly distributed mesh in this zone (see Figure 1-10). The first Brillouin zone is always identical with the Wigner-Seitz cell which may be found as follows. Choose a point of the reciprocal lattice as an origin and draw lines to all nearby lattice points. Pass planes through the midpoints of each of these lines perpendicular to the line involved. These planes will completely enclose a small region of reciprocal lattice space. This small region of space is the Wigner-Seitz cell. This cell has a volume $(2\pi)^3/V_a$ where V_a is the volume of the primitive cell in direct space (the $(2\pi)^3$ is a scale factor used by physicists which is generally ignored by crystallographers). The possible values of $\underset{\rightarrow}{k}$ are given by

$$(1\text{-}266) \quad k = \frac{2\pi j_1 \underset{\rightarrow}{a}^*}{N_1} + \frac{2\pi j_2 \underset{\rightarrow}{b}^*}{N_2} + \frac{2\pi j_3 \underset{\rightarrow}{c}^*}{N_3} = k_1 \underset{\rightarrow}{a}_1^* + k_2 \underset{\rightarrow}{b}_1^* + k_3 \underset{\rightarrow}{c}_1^*$$

where j_1, j_2 and j_3 are integers such that

$$(1\text{-}267) \quad -\frac{N_1}{2} \leq j_1 \leq \frac{N_1}{2} \quad ,$$

$$(1\text{-}268) \quad -\frac{N_2}{2} \leq j_2 \leq \frac{N_2}{2} \quad ,$$

and

$$(1\text{-}269) \quad -\frac{N_3}{2} \leq j_3 \leq \frac{N_3}{2} \quad ;$$

$$(1\text{-}270) \quad \underset{\rightarrow}{a}^* = \frac{\underset{\rightarrow}{b} \times \underset{\rightarrow}{c}}{V} \quad ,$$

$$(1\text{-}271) \quad \underset{\rightarrow}{b}^* = \frac{\underset{\rightarrow}{c} \times \underset{\rightarrow}{a}}{V} \quad ,$$

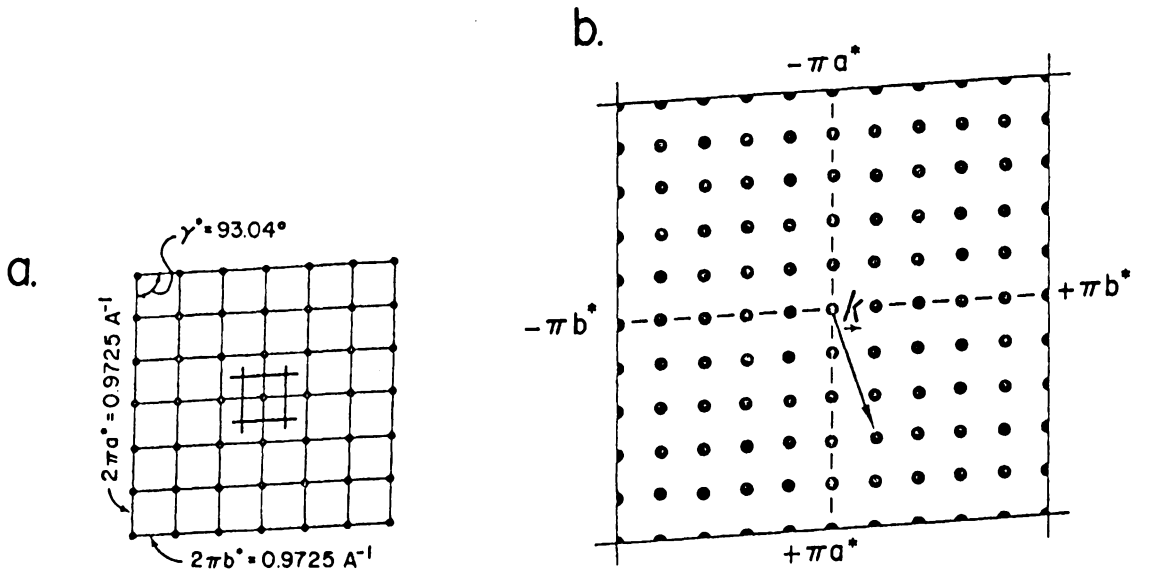

Figure 1-10: The first Brillouin zone of diopside. The first Brillouin zone is identical with the Wigner-Seitz cell. All vibrational modes of the crystal must have wave vectors ($\vec{k}$) which lie within this zone. The permissible values of $\vec{k}$ for a crystal 10 unit cells long in the a' direction and 10 unit cells long in the b' direction are shown on the right hand side of the diagram. The technique for constructing the zone is shown on the left. There are 60 frequencies associated with each value of $\vec{k}$. In order to calculate the thermal expansion coefficients it is necessary to know not only the magnitude of each frequency but also its strain dependence. The direct cell parameters (primitive cell) used in the construction of this figure are: a' = 6.599 Å, b' = 6.599 Å, c' = 5.251 Å, α' = 101.48°, β' = 101.48°, and γ' = 84.798°.

$$(1\text{-}272)\quad \underset{\rightarrow}{c}^* = \frac{\underset{\rightarrow}{a} \times \underset{\rightarrow}{b}}{V} \quad ,$$

and

$$(1\text{-}273)\quad V = \underset{\rightarrow}{a} \cdot (\underset{\rightarrow}{b} \times \underset{\rightarrow}{c}) \quad ;$$

and

$$(1\text{-}274)\quad \underset{\rightarrow}{a}_1^* = \underset{\rightarrow}{a}^* / |\underset{\rightarrow}{a}^*| \quad ,$$

$$(1\text{-}275)\quad \underset{\rightarrow}{b}_1^* = \underset{\rightarrow}{b}^* / |\underset{\rightarrow}{b}^*| \quad ,$$

and

$$(1\text{-}276)\quad \underset{\rightarrow}{c}_1^* = \underset{\rightarrow}{c}^* / |\underset{\rightarrow}{c}^*|$$

(Chatak and Kothari, 1972).

The Relation Between the Thermal Expansion Coefficients of a Crystal and the Normal Modes

In the quasiharmonic approximation the oscillations of the lattice are still assumed to appear as independent normal modes but the true anharmonic nature of the atomic forces manifests itself by causing the frequencies of these modes to be strain dependent. At any temperature above absolute zero the various modes will be excited to different levels. The level of excitation of any particular mode will depend on statistical considerations. The energy of the mode with wave vector $\underset{\rightarrow}{k}$ in the rth branch of the dispersion relation will be

$$(1\text{-}277)\quad E_r^n(\underset{\rightarrow}{k}) = (n + \tfrac{1}{2})h\omega_r(\underset{\rightarrow}{k})$$

when that mode is excited to the nth level. Each mode may be regarded as an independent system which is in thermodynamic equilibrium with its surroundings. The partition function (Zustand Summe) for the mode

with circular frequency $\omega_r(\vec{k})$ is

$$(1\text{-}278)\quad Z = \sum_{n=0}^{\infty} e^{-[\hbar\omega_r(\vec{k})(n+\frac{1}{2})/k_BT]} = \frac{e^{-\hbar\omega_r(\vec{k})/2k_BT}}{1 - e^{-\hbar\omega_r(\vec{k})/k_BT}}$$

Since according to statistical mechanics

$$(1\text{-}279)\quad A = -k_BT\ell nZ$$

we obtain

$$(1\text{-}280)\quad A_r(\vec{k}) = \frac{1}{2}\hbar\omega_r(\vec{k}) + k_BT\ell n[1 - e^{-\hbar\omega_r(\vec{k})/k_BT}]$$

and, since

$$(1\text{-}281)\quad S = -\left(\frac{\partial A}{\partial T}\right)_V ,$$

$$(1\text{-}282)\quad S_r(\vec{k}) = k_B\left[\frac{\hbar\omega_r(\vec{k})/k_BT}{(e^{\hbar\omega_r(\vec{k})/k_BT}-1} - \ell n[1 - e^{-\hbar\omega_r(\vec{k})/k_BT}]\right]$$

Since the internal energy is

$$(1\text{-}283)\quad U = A + TS$$

we also obtain

$$(1\text{-}284)\quad U_r(\vec{k}) = \frac{1}{2}\hbar\omega_r(\vec{k}) + \frac{k_BT(\hbar\omega_r(\vec{k})/k_BT)}{e^{\hbar\omega_r(\vec{k})/k_BT}-1}$$

and

$$(1\text{-}285)\quad C_v^r(\vec{k}) = \left(\frac{\partial U_r(\vec{k})}{\partial T}\right)_V = \frac{k_B(\hbar\omega_r(\vec{k})/k_BT)^2 \cdot e^{\hbar\omega_r(\vec{k})/k_BT}}{(e^{\hbar\omega_r(\vec{k})/k_BT} - 1)^2}$$

From equation (1-282) we see that the vibrational entropy of the entire crystal is

$$(1\text{-}286)\quad S_{vib} = \sum_{r\vec{k}} S_r(\vec{k}) = \sum_{r\vec{k}} k_B\left[\frac{\hbar\omega_r(\vec{k})/k_BT}{e^{\hbar\omega_r(\vec{k})/k_BT} - 1} - \ell n[1 - e^{-\hbar\omega_r(\vec{k})/k_BT}]\right].$$

Therefore we obtain

$$(1\text{-}287)\quad \left(\frac{\partial S_{vib}}{\partial \eta_{ij}}\right)_{\eta',T} = \sum_{r\vec{k}} k_B \Bigg[\frac{\hbar/k_BT}{(e^{\hbar\omega_r(\vec{k})/k_BT} - 1)} \left(\frac{\partial \omega_r(\vec{k})}{\partial \eta_{ij}}\right)_{\eta',T}$$

$$- \frac{\hbar^2\omega_r(\vec{k})/k_B^2T^2 \ell^{\hbar\omega_r(\vec{k})/k_BT}}{(\ell^{\hbar\omega_r/k_BT} - 1)^2} \left(\frac{\partial \omega_r(\vec{k})}{\partial \eta_{ij}}\right)_{\eta',T}$$

$$- \frac{\hbar k_B/T \cdot e^{-\hbar\omega_r(\vec{k})/k_BT}}{(1 - e^{-\hbar\omega_r(\vec{k})/k_BT}} \left(\frac{\partial \omega_r(\vec{k})}{\partial \eta_{ij}}\right)_{\eta',T} \Bigg]$$

$$= \sum_{r\vec{k}} k_B \Bigg[\frac{\hbar/k_BT}{(\ell^{\hbar\omega_r(\vec{k})/k_BT} - 1)} \left(\frac{\partial \omega_r(\vec{k})}{\partial \eta_{ij}}\right)_{\eta',T}$$

$$- \frac{(\hbar/k_BT)}{(\ell^{\hbar\omega_r/k_BT} - 1)} \left(\frac{\partial \omega_r(\vec{k})}{\partial \eta_{ij}}\right)_{\eta',T}$$

$$- \frac{(\hbar\omega_r(\vec{k})/k_BT)^2 \ell^{\hbar\omega_r(\vec{k})/k_BT}}{(\ell^{\hbar\omega_r(\vec{k})/k_BT} - 1)^2} \cdot \frac{1}{\omega_r(\vec{k})} \left(\frac{\partial \omega_r(\vec{k})}{\partial \eta_{ij}}\right)_{\eta',T} \Bigg]$$

$$= - \sum_{r\vec{k}} \frac{C_v^r(\vec{k})}{\omega_r(\vec{k})} \left(\frac{\partial \omega_r(\vec{k})}{\partial \eta_{ij}}\right)_{\eta',T} ,$$

that is

$$(1\text{-}288)\quad \left(\frac{\partial S_{vib}}{\partial \eta_{ij}}\right)_{\eta',T} = - \sum_{r\vec{k}} \frac{C_v^r(\vec{k})}{\omega_r(\vec{k})} \left(\frac{\partial \omega_r(\vec{k})}{\partial \eta_{ij}}\right)_{\eta',T}$$

Let us now define a set of parameters, $\gamma_{ij}^r(\vec{k})$, which will be referred to as mode Grüneisen parameters, as

$$(1\text{-}289)\quad \gamma_{ij}^r(\vec{k}) = - \frac{1}{\omega_r(\vec{k})} \left(\frac{\partial \omega_r(\vec{k})}{\partial \eta_{ij}}\right)_{\eta',T} = - \left(\frac{\partial \ell n \omega_r(\vec{k})}{\partial \eta_{ij}}\right)_{\eta',T}$$

We then obtain

$$(1\text{-}290)\quad \left(\frac{\partial S_{vib}}{\partial \eta_{ij}}\right)_{\eta',T} = \sum_{r\vec{k}} C_v^r(\vec{k})\gamma_{ij}^r(\vec{k})$$

The total entropy of the crystal is the sum of the entropies from various sources. Barron (1970) writes the entropy as

$$(1\text{-}291)\quad S = S_{vib} + S_e$$

where S_{vib} and S_e are the crystal vibrational and electronic (due to the conduction electrons) entropies respectively. Since most minerals are insulators, configurational entropy is far more important than electronic entropy in mineralogy and we write

$$(1\text{-}292)\quad S = S_{vib} + S_{config}$$

where S_{config} is the configurational entropy of the crystal. This means that (see equation (1-244))

$$(1\text{-}293)\quad \gamma_{ij} = \frac{1}{C_\eta}\left[\left(\frac{\partial S_{vib}}{\partial \eta_{ij}}\right)_{\eta',T} + \left(\frac{\partial S_{config}}{\partial \eta_{ij}}\right)_{\eta',T}\right] = \gamma_{ij}(vib) + \gamma_{ij}(config)$$

The second term is probably unimportant in most cases, however, it may be significant in minerals like β-eucryptite (Pillars and Peacor, 1973) where unusual thermal expansion behavior appears to be associated with a change in ordering.

The relationship between the normal modes and the thermal expansion is now clear. Using equations (1-238) and (1-290) we obtain

$$(1\text{-}294)\quad \alpha_{ij} = \frac{S_{ijk\ell}}{V}\left(\frac{\partial S_{vib}}{\partial \eta_{k\ell}}\right)_{\eta',T} = \frac{\partial S_{ijk\ell}}{V}\sum_{r\vec{k}} C_v^r(\vec{k})\gamma_k^r(\vec{k}) \ .$$

Thus we see that being able to calculate the thermal expansion

coefficients hinges on knowing $\omega_r(\underset{\rightarrow}{k})$ and $(\partial\omega_r(\underset{\rightarrow}{k})/\partial\eta_{k\ell})_{\eta',T}$ for each of the crystal's 3Nn modes.

If we define

$$(1\text{-}295)\quad \gamma_{ij} = \sum_{r\underset{\rightarrow}{k}} C_\eta^r(\underset{\rightarrow}{k})\gamma_{ij}^r(\underset{\rightarrow}{k}) \; / C_\eta(\text{vib})$$

then we can write

$$(1\text{-}296)\quad \alpha_{ij} = \frac{C_\eta S_{ijk\ell}\gamma_{k\ell}}{V} \quad .$$

Therefore we have recovered equation (1-246). Equation (1-295) gives the relation between the crystal's microscopic and macroscopic Grüneisen parameters. It is unfortunate, but true, that although a crystal's macroscopic Grüneisen parameters can be calculated from a knowledge of the microscopic parameters the reverse is not true.

On the Relation between Negative Thermal Expansion, Strain Dependence of Entropy, and Elasticity in Indialite, Emerald, and Beryl

In this section thermal expansion coefficients have been calculated for indialite (high cordierite), and for emerald and beryl using the x-ray data of Fischer (1974) and Morosin (1972) respectively. This data is given in Table 1-1. Since all these materials are hexagonal their thermal expansion behavior is characterized by two thermal expansion coefficients ε_1 and ε_3. In all cases it was found that ε_1 and ε_3 are small and that ε_3 is negative near room temperature. Since this unusual behavior leads to low volume coefficients of thermal expansion ($\beta = 2\varepsilon_1 + \varepsilon_3$) these materials are suitable for use as low expansion catalysis supports.

Morosin (1972) noted that the temperature at which the length of the c-axis of beryl is a minimum is strongly influenced by the presence of small amounts of impurities. The Grüneisen equation has been used to examine this effect which appears to result because the values of at least some mode Grüneisen parameters are strongly affected by the presence of impurities while the value of ratio $2|S_{13}|/S_{33}$ is not.

Calculation of the Thermal Expansion Coefficients

The thermal expansion coefficient tensor for hexagonal crystals has the form (Nye, 1957)

$$\begin{bmatrix} \varepsilon_1(T) & 0 & 0 \\ 0 & \varepsilon_1(T) & 0 \\ 0 & 0 & \varepsilon_3(T) \end{bmatrix} \quad (1\text{-}296)$$

. The cell parameters

Table 1-1

Lattice Parameters of Cordierite at Elevated Temperatures (Fischer, 1974)

Temperature (°C)	Temperature (°K)	$a(\sigma_a)$ Å	$c(\sigma_a)$ Å
0022	0295.16	9.7666(30)	9.3417(25)
0200	0473.16	9.7717(30)	9.3322(25)
0400	1673.16	9.7773(30)	9.3275(25)
0600	1873.16	9.7830(30)	9.3290(25)
0800	1073.16	9.7889(30)	9.3305(25)
1000	1273.16	9.7948(30)	9.3320(25)
1200	1473.16	9.8004(30)	9.3335(25)

Lattice Parameters of Emerald at Reduced and Elevated Temperatures (Morosin, 1972)

-150	0123.16	9.2120(9)	9.1950(9)
-100	0173.16	9.2130(9)	9.1940(9)
-050	0223.16	9.2140(9)	9.1930(10)
0023	0296.16	9.2153(5)	9.1924(7)
0169	0442.16	9.2176(6)	9.1931(10)
0300	0573.16	9.2190(7)	9.1939(10)
0400	0673.16	9.2196(8)	9.1943(9)
0500	0773.16	9.2222(8)	9.1952(9)
0600	0873.16	9.2243(9)	9.1970(10)
0800	1073.16	9.2276(8)	9.2001(9)

Lattice Parameters of Beryl at Elevated Temperatures (Morosin, 1972)

0023	0296.16	9.2088(5)	9.1896(7)
0024	0297.16	9.2094(8)	9.1898(7)
0050	323.16	9.2099(8)	9.1884(7)
0100	0373.16	9.2109(8)	9.1875(8)
0145	0418.16	9.2115(8)	9.1869(8)
0150	0423.16	9.2120(8)	9.1865(9)
0200	0473.16	9.2131(9)	9.1849(9)
0250	0523.16	9.2140(10)	9.1840(9)
0300	0573.16	9.2153(9)	9.1839(9)
0350	0623.16	9.2167(8)	9.1841(8)
0400	0673.16	9.2187(9)	9.1843(9)
0400	0673.16	9.2181(8)	9.1845(8)
0425	0698.16	9.2197(8)	9.1850(8)
0545	0818.16	9.2219(0)	9.1860(9)
0700	0973.16	9.2254(9)	9.1885(9)
0800	1073.16	9.2265(10)	9.1905(10)

were expressed as functions of temperature by means of power series of the form

$$(1\text{-}297)\quad a(T) = a_o + a_1T + a_2T^2 + \cdots \quad \text{and}$$

$$(1\text{-}298)\quad c(T) = c_o + c_1T + c_2T^2 + \cdots \quad .$$

The regression coefficients and variance-covariance matrices used in these calculations were obtained by weighted host squares using the Statistical Analysis System of Barr and Goodnight (1972). Regression models were fitted using various degree polynomials. Tests of significance were performed on the coefficients using the probability tables of the normal distributions. Error variances were assumed to be known and were taken from the esds obtained by refinement of the cell parameters. These results are given in Table 1-2. The Z-value associated with each individual regression coefficient is included in this table. The results are plotted in Figures 1-11-a, 1-12-a, and 1-13-a. The variation of a with T is linear in every case. The variation of c with temperature is best expressed by a quadratic expression in the case of beryl and emerald and by a cubic equation in the case of indialite.

$$(1\text{-}299)\quad \varepsilon_1 = \varepsilon_2 = \left(\frac{\partial e_1}{\partial T}\right)_\sigma = \left(\frac{\partial e_2}{\partial T}\right)_\sigma = \frac{1}{a(T)}\frac{da(T)}{dT} = \frac{a_1 + 2a_2T + \cdots}{a_o + a_1T + a_2T^2 + \cdots} \quad , \text{ and}$$

Table 1-2

Regression Coefficients, Z-Values for Regression Coefficients, and Variance-Covariance Matrices for Indialite, Beryl, and Emerald

Regression Coefficients and Z-Values

	Regression Coefficient	Z-Value	Regression Coefficient	Z-Value	Regression Coefficient	Z-Value
			a-axis			
	Indialite		Beryl		Emerald	
a_o	9.758(3)	3539.6	9.2019(5)	17579.3	9.2104(5)	19246.9
a_1	$2.88(29) \times 10^{-5}$	10.0	$2.40(9) \times 10^{-5}$	26.4	$1.553(83) \times 10^{-5}$	18.6
			c-axis			
c_o	9.7318(114)	850.3	9.2014(14)	6426.5	9.1956(10)	9380.3
c_1	$-1.405(488) \times 10^{-4}$	2.9	$-5.239(499) \times 10^{-5}$	11.6	$-1.339(418) \times 10^{-5}$	3.2
c_2	$1.415(605) \times 10^{-7}$	2.3	$3.991(492) \times 10^{-8}$	10.2	$1.661(113) \times 10^{-8}$	4.6
c_3	$-4.337(2264) \times 10^{-11}$	1.9	.....		.....	

Table 1-2 (continued)

Variance-Covariance Matrices

a-axis

V^a_{00}	07.60×10^{-06}	02.74×10^{-07}	02.29×10^{-07}
V^a_{01}	-7.21×10^{-09}	-4.40×10^{-10}	-3.49×10^{-09}
V^a_{11}	08.23×10^{-12}	08.28×10^{-13}	06.96×10^{-13}

c-axis

V^c_{00}	01.31×10^{-04}	02.05×10^{-06}	09.61×10^{-07}
V^c_{01}	-5.44×10^{-07}	-6.96×10^{-09}	-3.74×10^{-09}
V^c_{02}	06.50×10^{-07}	05.18×10^{-12}	2.90×10^{-12}
V^c_{03}	-2.33×10^{-07}	.....	.....
V^c_{11}	02.38×10^{-09}	02.05×10^{-11}	01.75×10^{-11}
V^c_{12}	-2.92×10^{-09}	-1.92×10^{-14}	-1.46×10^{-14}
V^c_{13}	1.07×10^{-09}	.....	.....
V^c_{22}	03.66×10^{-15}	01.54×10^{-17}	01.28×10^{-17}

Table 1-2 (continued)

V^c_{23}	-1.361×10^{-09}	.....	.....
V^c_{33}	5.125×10^{-22}	.....	.....

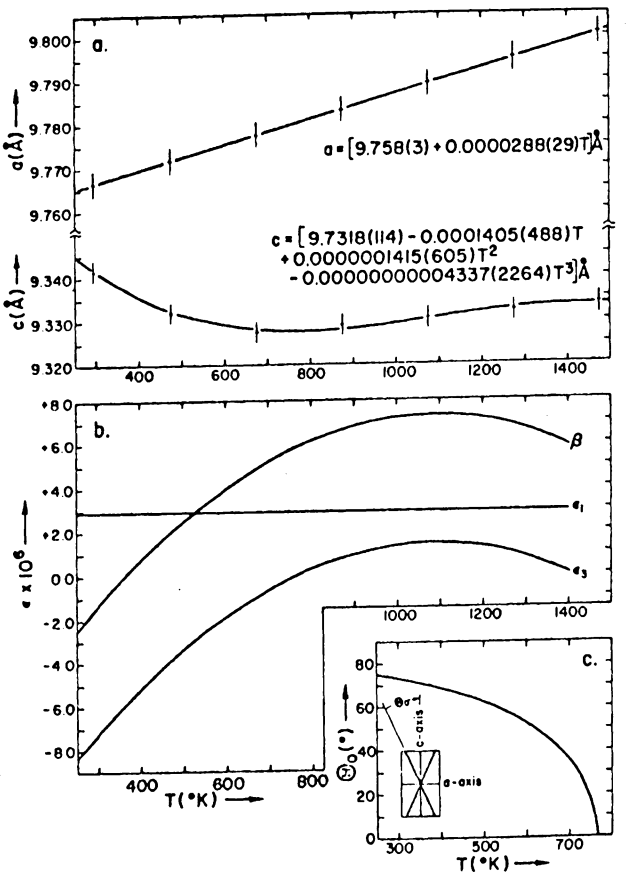

Figure 1-11-a: Cell parameters of indialite as a function of temperature. Plotted points represent the measurements of Fischer (1974). The regression equations are also given.

Figure 1-11-b: Thermal expansion coefficients of indialite along the a-axis (ε_1) and the c-axis (ε_3). The coefficient of volume expansion (β) is also given.

Figure 1-11-c: The semiopening angle of the cone of zero expansion for indialite plotted as a function of temperature.

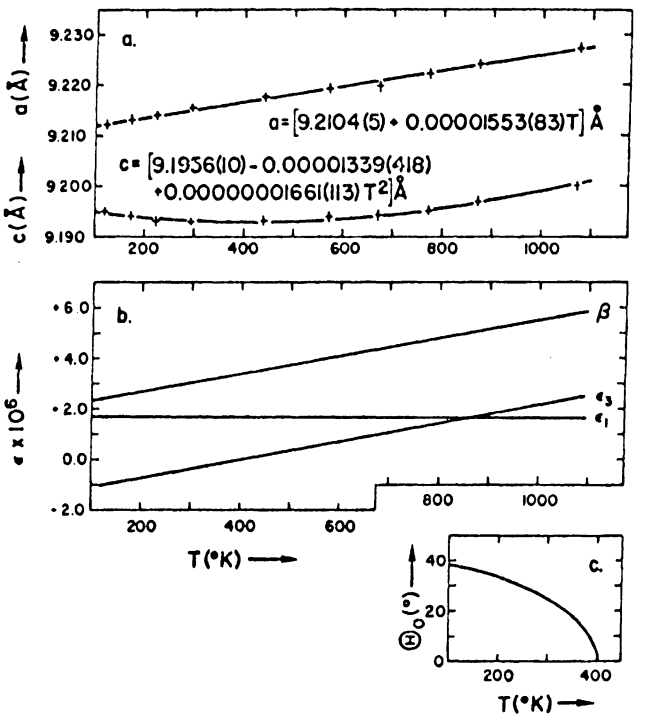

Figure 1-12-a: Cell parameters of beryl as a function of temperature. Plotted points represent the measurements of Morosin (1972). The regression equations are also given.

Figure 1-12-b: Thermal expansion coefficients of beryl along the a-axis (ε_1) and the c-axis (ε_3). The coefficient of volume expansion (β) is also given.

Figure 1-12-c: The semiopening angle of the cone of zero expansion for beryl plotted as a function of temperature.

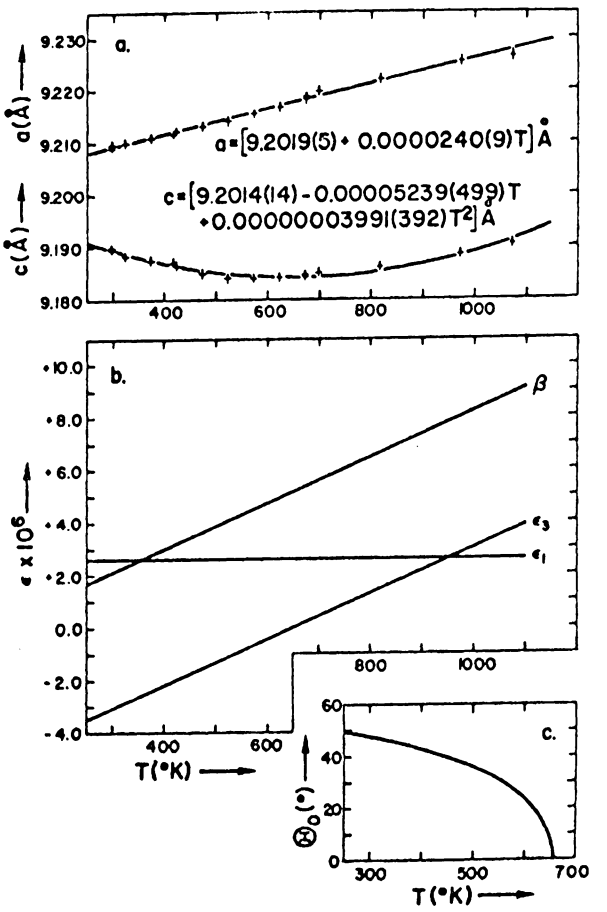

Figure 1-13-a: Cell parameters of emerald as a function of temperature. Plotted points represent the measurements of Morosin (1972). The regression equations are also given.

Figure 1-13-b: Thermal expansion coefficients of emerald along the a-axis (ε_1) and the c-axis (ε_3). The coefficient of volume expansion (β) is also given.

Figure 1-13-c: The semiopening angle of the cone of zero expansion for emerald plotted as a function of temperature.

$$(1\text{-}300)\quad \varepsilon_3 = \left(\frac{\partial e_3}{dT}\right)_\sigma = \frac{1}{c(T)}\,\frac{dc(T)}{dT} = \frac{c_1 + 2e_2T + \ldots}{c_o + c_1T + c_2T^2 + \ldots}\,.$$

These expressions are identical in form to those used by Pathak and Vasavada (1970) to calculate the thermal expansion coefficients of NaCl, KCl, and CsBr.

The variance formulae given previously reduce to

$$(1\text{-}301)\quad \mathrm{Var}[\varepsilon_1(T)] = \sum_{n=0}^{\infty}\sum_{m=0}^{\infty} \left(\frac{\partial \varepsilon_3(T)}{\partial c_n}\right)\left(\frac{\partial \varepsilon_3(T)}{\partial c_m}\right) V^c_{nm}$$

where

$$(1\text{-}303)\quad \frac{\partial \varepsilon_1(T)}{\partial a_n} = \left[\, nT^{n-1} - T^n \varepsilon_1(T) \,\right] / a(T) \quad \text{and}$$

$$\frac{\partial \varepsilon_3(T)}{\partial c_n} = \left[\, nT^{n-1} - T^n\, \varepsilon_3(T)\right] / c(T).$$

When dealing with polycrystalline specimens and in industrial applications the bulk expansion (volume coefficient of thermal expansion) is generally more useful that ε_1 or ε_3. This parameter is defined as

(1-304) $\beta(T) = 2\varepsilon_1(T) + \varepsilon_3(T)$ in this case. The variance is

$$(1\text{-}305)\quad \mathrm{var}[\beta(T)] = 2\mathrm{var}[\varepsilon_1(T)] + \mathrm{var}[\varepsilon_3(T)]$$

Another interesting parameter which may be computed for hexagonal and tetragonal crystals which are contracting along one axis while simultaneously expanding along the other is the semiopening angle of the cone of zero expansion (Wooster, 1973). The magnitude of this angle is given by

$$(1\text{-}306)\quad \theta_o(T) = \cos^{-1}\left[\left(\frac{\varepsilon_1(T)}{\varepsilon_1(T) - \varepsilon_3(T)}\right)^{\frac{1}{2}}\right]$$

The variance is

$$(1\text{-}307)\quad \mathrm{Var}[\theta_o(T)] = [\sin^4\theta_o\ \mathrm{var}[\varepsilon_1(T)] + \cos^4\theta_o\ \mathrm{var}[\varepsilon_3(T)]]/ \sin^2\theta_o\cos^2\theta_o(\varepsilon_1(T) - \varepsilon_3(T))^2 .$$

A single crystal section cut so that its normal coincides with this semi-opening angle will not change in thickness as the crystal is heated.

Computed values of $\varepsilon_1(T)$, $\varepsilon_3(T)$, $\beta(T)$, and $\beta_o(T)$ for all three compounds are given in Table 1-3. Standard deviations of these parameters are also included. The results are presented graphically in Figures 1-11-b, 1-11-c, 1-12-b, 1-12-c, 1-13-b, and 1-13-c. The values obtained are compared with values previously given by Fischer and Morosin in Table 1-4. The magnitude of ε_1 is independent of temperature in all cases. Thermal expansion along the c-axis, however, differs drastically from that which occurs along *a*. Near room temperature the length of the c-axis of all these materials decreases with increasing temperature. At the temperatures 766.8°K (indialite), 656.4 (beryl) and 403.3 (emerald) the sign of the thermal expansion reverses and the length of *c* begins to increase with increasing temperature. The similar behavior of indialite and emerald and beryl is expected because these materials are homeotypic. The magnitude of ε_3 in indialite, however, is not, as in the case with beryl and emerald, a linear function of temperature.

Although the thermal expansion of emerald and beryl is similar there are several differences in detail. In emerald ε_1 is smaller and

Table 1-3

Tabulation of the Thermal Expansion Coefficients of Indialite

Temperature (°K)	Temperature (°C)	$\varepsilon_1(\sigma_{\varepsilon_1}) \times 10^6$	$\varepsilon_3(\sigma_{\varepsilon_3}) \times 10^6$	$\beta(\sigma_\beta) \times 10^6$	$\Theta_o(\sigma_{\Theta_o})$ degrees
250	-023.16	2.9(.3)	-8.0(2.3)	-2.1(2.4)	58.8(8.0)
300	026.84	2.9(.3)	-6.9(1.9)	-1.0(2.0)	56.9(7.9)
350	076.84	2.9(.3)	-5.9(1.6)	0.0(1.6)	54.8(7.8)
400	126.84	2.9(.3)	-5.0(1.3)	0.9(1.3)	52.4(7.6)
450	176.84	2.9(.3)	-4.1(1.0)	1.8(1.0)	49.6(7.3)
500	226.84	2.9(.3)	-3.3(0.7)	2.6(0.8)	46.4(7.1)
550	276.84	2.9(.3)	-2.5(0.6)	3.3(0.7)	42.6(7.0)
600	326.84	2.9(.3)	-1.8(0.5)	4.1(0.6)	38.1(7.7)
650	376.84	2.9(.3)	-1.2(0.5)	4.7(0.6)	32.4(10.5)
700	426.84	2.9(.3)	-0.6(0.5)	5.2(0.7)	24.9(17.9)
750	476.84	2.9(.3)	-0.1(0.6)	5.7(0.7)	12.6(47.3)
800	526.84	2.9(.3)	+0.3(0.6)	6.2(0.7)	-
850	576.84	2.9(.3)	+0.6(0.6)	6.5(0.8)	-
900	626.84	2.9(.3)	+0.9(0.7)	6.8(0.8)	-
950	676.84	2.9(.3)	+1.1(0.6)	7.0(0.7)	-
1000	726.84	2.9(.3)	+1.3(0.6)	7.2(0.7)	-
1050	776.84	2.9(.3)	+1.4(0.5)	7.2(0.7)	-
1100	826.84	2.9(.3)	+1.4(0.4)	7.3(0.6)	-
1150	876.84	2.9(.3)	+1.3(0.4)	7.2(0.6)	-
1200	926.84	2.9(.3)	+1.2(0.5)	7.1(0.6)	-
1250	976.84	2.9(.3)	+1.0(0.6)	6.9(0.7)	-
1300	1026.84	2.9(.3)	+0.8(0.8)	6.7(0.9)	-
1350	1076.84	2.9(.3)	+0.5(1.1)	6.3(1.2)	-
1400	1126.84	2.9(.3)	+0.1(1.4)	6.0(1.5)	-

Tabulation of the Thermal Expansion Coefficients of Beryl

300	026.84	2.6(.1)	-3.1(0.3)	2.1(0.3)	47.5(2.9)
350	076.84	2.6(.1)	-2.7(0.3)	2.6(0.3)	45.3(3.0)
400	126.84	2.6(.1)	-2.2(0.2)	3.0(0.3)	42.8(3.0)
450	176.84	2.6(.1)	-1.8(0.2)	3.4(0.2)	39.7(3.0)
500	226.84	2.6(.1)	-1.4(0.2)	3.8(0.2)	35.8(3.1)
550	276.84	2.6(.1)	-0.9(0.1)	4.3(0.2)	30.8(3.4)
600	326.84	2.6(.1)	-0.5(0.1)	4.7(0.2)	23.4(4.5)
650	376.84	2.6(.1)	-0.1(0.1)	5.2(0.2)	8.3(15.4)
700	426.84	2.6(.1)	+0.4(0.1)	5.6(0.2)	-
750	476.84	2.6(.1)	+0.8(0.1)	6.0(0.2)	-
800	526.84	2.6(.1)	+1.2(0.2)	6.4(0.2)	-
850	576.84	2.6(.1)	+1.7(0.2)	6.9(0.3)	-
900	626.84	2.6(.1)	+2.1(0.3)	7.3(0.3)	-
950	676.84	2.6(.1)	+2.6(0.3)	7.8(0.3)	-
1000	726.84	2.6(.1)	+3.0(0.3)	8.2(0.4)	-
1050	776.84	2.6(.1)	+3.4(0.4)	8.6(0.4)	-
1100	826.84	2.6(.1)	+3.9(0.4)	9.0(0.4)	-
1150	876.84	2.6(.1)	+4.3(0.5)	9.5(0.5)	-

Table 1-3, continued

Temperature (°K)	Temperature (°C)	$\varepsilon_1(\sigma_{\varepsilon_1}) \times 10^6$	$\varepsilon_3(\sigma_{\varepsilon_3}) \times 10^6$	$\beta(\sigma_\beta) \times 10^6$	$\Theta_o(\sigma_{\Theta_o})$ degrees
Tabulation of the Thermal Expansion Coefficients of Emerald					
100	-173.16	1.69(.09)	-1.1(0.4)	2.3(0.4)	38.9(9.8)
150	-123.16	1.69(.09)	-0.9(0.3)	2.5(0.4)	36.4(10.3)
200	-073.16	1.69(.09)	-0.7(0.3)	2.6(0.3)	33.4(11.0)
250	-023.16	1.69(.09)	-0.6(0.3)	2.8(0.3)	29.8(12.1)
300	26.84	1.69(.09)	-0.4(0.2)	3.0(0.3)	25.2(13.9)
350	76.84	1.69(.09)	-0.2(0.2)	3.1(0.2)	18.6(18.0)
400	126.84	1.69(.09)	-0.1(0.2)	3.4(0.2)	4.6(69.3)
450	176.84	1.69(.09)	+0.2(0.1)	3.5(0.2)	-
500	226.84	1.69(.09)	+0.4(0.1)	3.7(0.2)	-
550	276.84	1.69(.09)	+0.5(0.1)	3.9(0.2)	-
600	326.84	1.69(.09)	+0.7(0.1)	4.1(0.2)	-
650	376.84	1.69(.09)	+0.9(0.1)	4.3(0.1)	-
700	426.84	1.69(.09)	+1.1(0.1)	4.4(0.2)	-
750	476.84	1.69(.09)	+1.3(0.2)	4.6(0.2)	-
800	526.84	1.69(.09)	+1.4(0.2)	4.8(0.2)	-
850	576.84	1.69(.09)	+1.6(0.2)	5.0(0.3)	-
900	626.84	1.69(.09)	+1.8(0.3)	5.2(0.3)	-
950	676.84	1.69(.09)	+2.0(0.3)	5.3(0.3)	-
1000	726.84	1.69(.09)	+2.2(0.3)	5.5(0.4)	-
1050	776.84	1.69(.09)	+2.3(0.4)	5.7(0.4)	-
1100	826.84	1.69(.09)	+2.5(0.4)	5.8(0.4)	-

the rate of increase of ε_3 with temperature is lower. This causes the volume coefficient of thermal expansion of emerald to be considerably less than that of beryl at high temperatures. In addition the sign reversal of ε_3 in emerald occurs at a temperature which is about 250°K below that of the similar reversal in beryl. This appears quite remarkable when we consider that emerald differs from beryl only through the presence of a small amount of chromium impurity (about 0.3 wt.%. Cr and 0.05 wt.% Fe in this case).

The Theory of Thermal Expansion in Hexagonal Crystals.

The basic principles governing the thermal expansion of solids may be considered from several points of view. One approach is essentially geometric in nature and is concerned with the sizes of atoms and ions, with their arrangements in the crystal structure and with changes in the lengths of the bonds and the magnitudes of the angles which join them (Austin, 1952). Morosin used this approach in his discussion of the expansion of emerald and beryl. The second, or thermodynamic approach, outlined in the previous sections, makes use of the Grüneisen relation to examine the thermal dilation behavior of a substance.

It is easily seen by integrating equations (1-299) and (1-300) between T_o and T that

(1-308) $e_1(T) = e_2(T) = \ell n\, a(T) - \ell n\, a_o$ and

(1-309) $e_3(T) = \ell n\, c(T) - \ell n\, c_o$ so that

(1-310) $de_1 = de_2 = d\, \ell n\, a$ and

(1-111) $de_3 = d\, \ell n\, c$

On writing (1-248) in matrix form we obtain (for a hexagonal crystal)

$$(1\text{-}312)\quad \begin{bmatrix} \varepsilon_1 \\ \varepsilon_2 \\ \varepsilon_3 \\ 0 \\ 0 \\ 0 \end{bmatrix} = \frac{1}{V} \begin{bmatrix} S_{11} & S_{12} & S_{13} & 0 & 0 & 0 \\ S_{12} & S_{11} & S_{13} & 0 & 0 & 0 \\ S_{13} & S_{13} & S_{33} & 0 & 0 & 0 \\ 0 & 0 & 0 & S_{44} & 0 & 0 \\ 0 & 0 & 0 & 0 & S_{44} & 0 \\ 0 & 0 & 0 & 0 & 0 & S_{66} \end{bmatrix}$$

$$\begin{bmatrix} \tfrac{1}{2}(\partial S/\partial \ \ell n\ a)_{c,T} \\ \tfrac{1}{2}(\partial S/\partial \ \ell n\ a)_{c,T} \\ (\partial S/\partial \ \ell n\ c)_{a,T} \\ 0 \\ 0 \\ 0 \end{bmatrix} \qquad \text{or}$$

$$(1\text{-}313)\quad \varepsilon_1 = \varepsilon_2 = \frac{1}{2V}\left[(S_{11} + S_{12}) \left(\frac{\partial S}{\partial \ \ell n\ a}\right)_{c,T} + 2S_{13} \left(\frac{\partial S}{\partial \ \ell n\ c}\right)_{a,T}\right] = \frac{C_v}{V} \left[(S_{11} + S_{12})\ \gamma_1 + S_{13}\gamma_3\right] \text{ and}$$

$$(1\text{-}314)\quad \varepsilon_3 = \frac{1}{v}\left[S_{13} \left(\frac{\partial S}{\partial \ \ell n\ a}\right)_{c,T} + S_{33} \left(\frac{\partial S}{\partial \ \ell n\ c}\right)_{a,T}\right] =$$

$$\frac{C_v}{V} \left[2S_{13}\gamma_1 + S_{33}\gamma_3\right].$$

Table 1-4

Comparison with Previous Results

Cordierite	Fischer (200°C)	This work (200°C)
ε_1	2.93×10^{-6}	$2.9(.3) \times 10^{-6}$
Beryl	**Morosin (25°C)**	**This work (25°C)**
ε_1	$2.6(.1) \times 10^{-6}$	$2.6(.1) \times 10^{-6}$
ε_3	$-2.9(.4) \times 10^{-6}$	$-3.1(.3) \times 10^{-6}$
Emerald	**Morosin (25°C)**	**This work (25°C)**
ε_1	$1.7(.1) \times 10^{-6}$	$1.69(.09) \times 10^{-6}$
ε_3	$\sim[-0.16(.6) \times 10^{-6}]$	$-0.4(.2) \times 10^{-6}$

These two expressions are the specific form taken by the extended Grüneisen equation in the case of a hexagonal crystal. They give the relation between the magnitude of the thermal expansion coefficients, the elasticity, and the strain dependence of entropy in such a crystal In accordance with the usual interpretation relating physical properties the Grüneisen parameters γ_1 and γ_3 may be regarded as a measure of the thermodynamic driving force producing the expansion. The elastic constants then determine (characterize) the response of the solid and the thermal expansion coefficients ε_1 and ε_3 describe the solids resultant behavior (Munn, 1970).

It is shown by Auld (1973) that if the strain energy is to be a positive definite quadratic function we must have

(1-315) $S_{11} + S_{12} > 0$ and

(1-316) $S_{33} > 0$. Unfortunately no such rigorous restriction can be placed on the sign of S_{13}. In practice, however, S_{13} is always negative (Simmons and Wang, 1971). We therefore see that (assuming $\gamma_1 > 0$ and $\gamma_3 > 0$) the conditions for positive expansion along a and c are

(1-317) $$\frac{S_{11} + S_{12}}{|S_{13}|} > \frac{\gamma_3}{\gamma_1} > \frac{2|S_{13}|}{S_{33}}$$. It is only when the ratio of γ_3/γ_1 lies with these limits that the expansion along a and c is positive. The variation of γ_3/γ_1 with temperature for emerald and beryl (obtained by solving for the ratio γ_3/γ_1 in equations (1-313) and (1-314)) is given in Figure 1 - 14 . Because $\gamma_3/\gamma_1 < 2|S_{13}|/S_{33}$ for

emerald (below 403.3°K) and for beryl (below 656.4°K) the inequality given in eq. (1-317) is not satisfied and the thermal expansion along the c-axis is negative. With increasing temperature the ratio γ_3/γ_1 increases for both emerald and beryl. As the temperature rises, however, the rate of increase slows and both curves appear to approach a common limit at high temperature. For ε_1 to become negative it would be necessary for the ratio γ_3/γ_1 to exceed the value of $(S_{11} + S_{12})/|S_{13}|$. This never occurs for either substance.

The ratios $(S_{11} + S_{12})/|S_{13}|$ and $2|S_{13}|/S_{33}$ do not appear to be highly sensitive to composition. A comparison of these ratios for a pale blue aquamarine and a colorless goshenite (Yoon and Newnham, 1973) and for a structure consisting of only hexagonally close packed atoms is given in Table 1-5. The compositions of these specimens (including the composition of the beryl and emerald specimens used by Morosin) is given in Table 1-6. The difference in composition of the aquamarine and goshenite is much larger than the difference in composition of beryl and emerald. It therefore appears that the difference in the thermal expansion behavior of beryl and emerald can to a large extent, be attributed to the effect impurity atoms have on the ratio γ_3/γ_1. Since it is evident from equation (1-289) and (1-290) that the ultimate cause of thermal expansion in crystals is the strain dependence of the frequencies of the normal modes, it appears that the small amount of chromium impurity strongly influences the strain dependence of the frequencies of at least some of the normal modes. This, of course, assumes that the strain dependence of the configurational entropy is unimportant. If this is not the case then an expres-

Table 1-5

Magnitude of Critical Ratios for the Grüneisen Equation

Ratio	Pale blue aquamarine	Colorless goshenite	HCP atoms (theoretical value)
$2S_{13}/S_{33} = 2C_{13}/(C_{11} + C_{12})$	2.39	2.42	4.00
$(S_{11} + S_{12})/S_{13} = C_{33}/C_{13}$	0.54	0.54	0.40

Table 1-6

Chemical Analyses of the Brazilian Beryls
(after Yoon and Newnham, 1973)

	Ideal Beryl	Pale blue Aquamarine [+]	Colorless Goshenite [†]
BeO	13.96 wt %	13.60 wt %	12.66 wt %
Al_2O_3	18.97	18.20	18.24
SiO_2	67.07	65.92	65.18
Fe_2O_3		0.167	0.006
FeO		0.11	0.08
TiO_2		0.020	0.011
Li_2O		0.03	0.69
Na_2O		0.13	0.79
K_2O		0.013	0.05
Pb_2O		0.001	0.021
$C_{52}O$		0.675	0.16
H_2O^+		1.36	1.68
H_2O^-		0.02	0.02

Composition Emerald and Beryl used by Morosin (After Morosin, 1972)

Emerald	Beryl
0.3 wt % Cr (0.44 wt % Cr_2O_3)	0.1 wt % Fe (.14 wt % Fe_2O_3)
0.05 wt % Fe (0.07 wt % Fe_2O_3)	Trace ($\leq$0.001%) K and Ca
Trace amount of Mg, Ca, and Ti	

[+]Total amount of oxides other than BeO, Al_2O_3, and SiO_2 present is 2.28%.

† " is 3.92%.

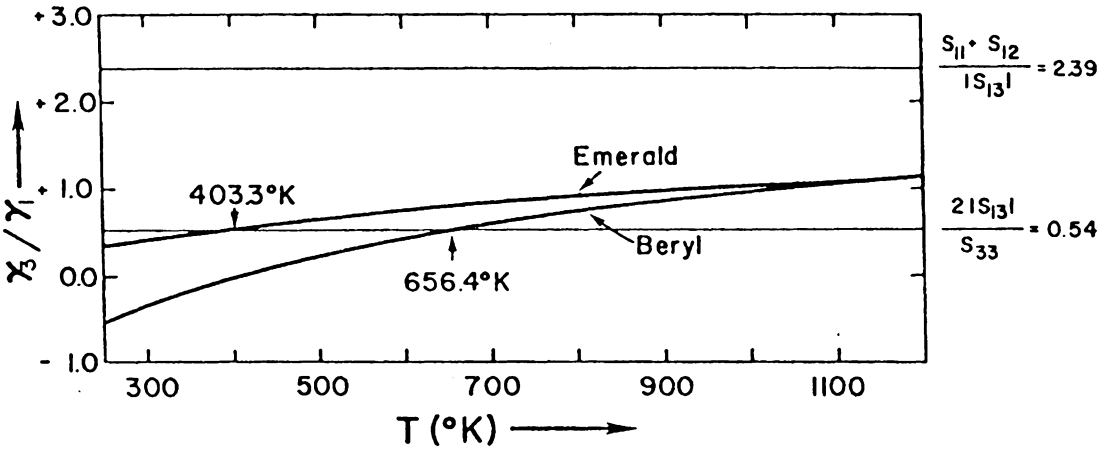

Figure 1-14: Variation of the Grüneisen parameter ratio γ_3/γ_1 with temperature for beryl and emerald. Expansion along c is negative when $\gamma_3/\gamma_1 < 2|S_{13}|/S_{33}$ while expansion along a is negative if

$$\gamma_3/\gamma_1 > \frac{S_{11} + S_{12}}{|S_{13}|}$$

(this never occurs for either substance). A crystal where the width of the band

$$\frac{S_{11} + S_{12}}{|S_{13}|} - \frac{2|S_{13}|}{S_{33}}$$

was very narrow could conceivably have negative expansion along both a and c (not simultaneously). However, such a crystal would tend to be unstable since it is required that $(S_{11} + S_{12})S_{33} > 2S_{13}^2$. Note that the ratio γ_3/γ_1 appears to approach a common limit for beryl and emerald at high temperatures.

sion of the form given by (1-293) applies. There is not sufficient information to permit one to determine the relative important of the strain dependence of the thermal and configurational entropy in this case.

It should also be pointed out that the sign of γ_3 for beryl is negative at low temperatures. The exact reason for this is unknown, however, Barron (1970) has pointed out that this is an effect which frequently occurs in somewhat open structures. A quick inspection of equations (1-313) and (1-314) will suffice to show that when $\gamma_3 < 0$ and $\gamma_1 > 0$ the thermal expansion along c must be negative while expansion along a must be positive.

Throughout this discussion we have assumed that the crystals elastic constants are independent of temperature.

Conclusion

In this section we have used the previously presented theory to compute accurate thermal expansion coefficients for indialite, beryl, and emerald and have made a careful estimate of the errors present in these calculations. Since these materials are of some significance industrially a tabulation of the results has been given (Table 1-3) It has been pointed out that from a thermodynamic point of view beryl and emerald contract at low temperatures because $\gamma_3/\gamma_1 < 2|S_{13}|/S_{33}$. It has been suggested that the differences in the thermal expansion behavior of beryl and emerald are due to the chromium impurity exerting a strong influence on the strain dependence of the frequencies of the normal modes of the crystal while the ratio $2|S_{13}|/S_{33}$ is affected to only a limited extent. It would be possible to verify this hypothesis by inelastic neutron scattering but a specialized apparatus would

be required since one needs not merely the frequencies of the noraml modes but also their strain dependence (Daniels, 1973).

At the present time it is not possible to calculate the magnitudes of the individual γ_1 and γ_3 for beryl and emerald because no specific heat data is available for these minerals. No measurements of the elastic constants of cordierite appear to have been made.

The Thermal Expansion of the Clinopyroxenes: Spodumene, Jadeite, Acmite, Ureyite, Hedenbergite, and Diopside

In this section the thermal expansion coefficients of spodumene, jadeite, acmite, ureyite, hedenbergite, and diopside are calculated using the expressions for the linear Eulerian thermal expansion coefficients developed earlier. The results are then compared with those obtained using the Ohashi-Burnham equations.

The data used were obtained from Cameron, Sueno, Prewitt, and Papike (1973) (spodumene, jadeite, acmite, ureyite, hedenbergite, and diopside), Nolan and Edgar (acmite and diopside), and Clark, Appleman, and Papike (1969) (diopside). These data are tabulated in Table 1-7. The necessary regression equations were obtained using the Statistical Analysis System (SAS) developed by Barr and Goodnight (1972). The resulting regression coefficients and variance-covariance matrices are given in Table 1-8. The results are plotted and compared with measured values in Figures 1-15, 1-16-a, 1-16-b, 1-17, and 1-18.

The principal coefficients of thermal expansion were then computed using a program written for this purpose. The orientation of the representation quadric was also computed. The results are tabulated in Table 1-9 and plotted in Figures 1-19 and 1-20. The angle θ given in Figure 1-22 is the angle the direction of principal expansion ε_1 makes with the positive end of the c-axis. This angle is positive when measured in a counterclockwise direction.

Table 1-7

Unit Cell Parameters of the Clinopyroxenes: Spodumene, Jadeite, Acmite, Ureyite, Hedenbergite, and Diopside.

	Temperature °K	Temperature °C	a(A)	b(A)	c(A)	(°)
Spodumene	297.16	24	9.463(1)	8.392(1)	5.218(1)	110.15(1)
	573.16	300	9.468(1)	8.412(1)	5.224(1)	110.05(1)
	733.16	460	9.473(2)	8.430(1)	5.229(1)	109.99(1)
	1033.16	760	9.489(1)	8.460(1)	5.236(1)	109.88(1)
Jadeite	297.16	24	9.423(1)	8.564(1)	5.223(1)	107.56(1)
	673.16	400	9.450(2)	8.594(1)	5.233(1)	107.57(1)
	873.16	600	9.469(2)	8.614(1)	5.240(1)	107.57(1)
	1073.16	800	9.483(1)	8.630(1)	5.2490(4)	107.59(1)
Acmite	297.16	24	9.658(2)	8.795(2)	5.294(1)	107.42(2)
	673.16	400	9.677(1)	8.829(1)	5.298(1)	107.33(1)
	873.16	600	9.699(1)	8.855(1)	5.307(1)	107.32(1)
	1073.16	800	9.711(1)	8.876(1)	5.312(1)	107.29(1)
Ureyite	297.16	24	9.579(2)	8.722(1)	5.267(1)	107.37(1)
	673.16	400	9.597(1)	8.751(1)	5.274(1)	107.29(1)
	873.16	600	9.612(1)	8.770(1)	5.279(1)	107.25(1)
Hedenbergite	297.16	24	9.845(1)	9.024(1)	5.245(1)	104.74(1)
	673.16	400	9.870(1)	9.077(1)	5.258(1)	105.01(1)
	873.16	600	9.884(1)	9.110(1)	5.264(1)	105.11(1)
	1073.16	800	9.897(1)	9.138(1)	5.269(1)	105.17(1)
	1173.16	900	9.906(1)	9.164(1)	5.273(1)	105.22(1)
	1273.16	1000	9.916(1)	9.179(1)	5.276(1)	105.28(1)

Table 1-7 (continued)

	Temperature °K	Temperature °C	a(A)	b(A)	c(A)	(°)
Diopside	297.16	24[a]	9.746(4)	8.899(5)	5.251(6)	105.63(6)
	297.16	24[b]	9.748(5)	8.924(5)	5.251(5)	105.79(5)
	297.16	24[c]	9.753(4)	8.922(3)	5.249(2)	105.95(3)
	297.16	24[g]	9.7506(8)	8.9294(7)	5.2518(4)	105.898(7)
	297.16	24[h]	9.752(2)	8.926(2)	5.248(2)	105.83(5)
	373.16	100[c]	9.756(4)	8.936(3)	5.252(1)	105.99(2)
	473.16	200[c]	9.758(7)	8.949(7)	5.253(3)	105.88(5)
	573.16	300[c]	9.770(7)	8.954(7)	5.258(3)	105.94(5)
	598.16	325[d]	9.771(10)	8.970(10)	5.262(10)	105.87(3)
	673.16	400[c]	9.774(5)	8.979(4)	5.264(1)	105.89(3)
	673.16	400[f]	9.776(1)	8.979(1)	5.267(1)	105.94(1)
	773.16	500[c]	9.784(3)	8.997(2)	5.267(1)	105.94(2)
	873.16	600[c]	9.795(3)	9.015(2)	5.272(1)	105.96(2)
	898.16	625[d]	9.794(4)	9.018(4)	5.274(1)	106.00(3)
	973.16	700[f]	9.799(1)	9.029(1)	5.274(1)	106.00(1)
	973.16	700[c]	9.804(5)	9.030(3)	5.275(2)	105.98(3)
	1073.16	800[c]	9.810(6)	9.054(6)	5.277(3)	106.02(5)
	1098.16	825[d]	9.807(2)	9.056(1)	5.286(10)	106.00(1)
	1123.16	850[f]	9.806(1)	9.050(1)	5.280(1)	106.00(1)
	1273.16	1000[f]	9.822(4)	9.081(1)	5.285(3)	105.98(3)

[a]Clark *et al* (1969); [b]Nolan and Edgar (1963); [c]Finger and Ohashi (1976); [d]Deganello (1973); [f]Cameron *et al* (1973); [g]Warner and Luth (1974), [h]Rutstein and Yund (1969)

Table 1-8

Regression Coefficients and Variance-Covariance Matrices for the Clinopyroxenes: Spodumene, Jadeite, Acmite, Ureyite, Hedenbergite, and Diopside

Spodumene

a-axis Regression Coefficient	b-axis Regression Coefficient	c-axis Regression Coefficient	β Regression Coefficient
9.4502(13)	8.4063(148)	5.2104(13)	110.260(13)
$3.61(19) \times 10^{-5}$	$-1.382(840) \times 10^{-4}$	$2.48(19) \times 10^{-5}$	$-3.67(19) \times 10^{-4}$
.....	$3.51(140) \times 10^{-7}$	.....	.....
.....	$1.617(702) \times 10^{-10}$	.....	.....

Variance-Covariance Matrices

$V^a_{00} = 1.79 \times 10^{-6}$	$V^b_{00} = 9.19 \times 10^{-4}$	$V^c_{00} = 1.78 \times 10^{-6}$	$V^\beta_{00} = 1.78 \times 10^{-4}$
$V^a_{01} = -2.30 \times 10^{-9}$	$V^b_{01} = -1.24 \times 10^{-6}$	$V^c_{01} = -2.32 \times 10^{-9}$	$V^\beta_{01} = -2.32 \times 10^{-7}$
$V^a_{02} =$	$V^b_{02} = 2.04 \times 10^{-9}$	$V^c_{02} =$	$V^\beta_{02} =$ .....
$V^a_{03} =$	$V^b_{03} = -1.01 \times 10^{-12}$	$V^c_{03} =$	$V^\beta_{03} =$ .....
$V^a_{11} = 3.59 \times 10^{-12}$	$V^b_{11} = 7.06 \times 10^{-9}$	$V^c_{11} = 3.52 \times 10^{-12}$	$V^\beta_{11} = 3.52 \times 10^{-10}$
$V^a_{12} =$	$V^b_{12} = -1.17 \times 10^{-11}$	$V^c_{12} =$	$V^\beta_{12} =$ .....
$V^a_{13} =$	$V^b_{I3} = 5.85 \times 10^{-15}$	$V^c_{13} =$	$V^\beta_{13} =$ .....

Table 1-8 (continued)

V^a_{22} = ...	V^b_{22} = 1.95×10^{-11}	V^c_{22} = ...	V^β_{22} = ...
V^a_{23} = ...	V^b_{23} = -9.80×10^{-18}	V^c_{23} = ...	V^β_{23} = ...
V^a_{33} = ...	V^b_{33} = 4.93×10^{-21}	V^c_{33} = ...	V^β_{33} = ...

Jadeite

a-axis Regression Coefficient	b-axis Regression Coefficient	c-axis Regression Coefficient	β Regression Coefficient
9.3998(14)	8.5665(139)	5.2189(29)	107.584(14)
$7.76(18) \times 10^{-5}$	$-6.91(768) \times 10^{-5}$	$8.4(92) \times 10^{-6}$	$3.4(17) \times 10^{-5}$
.....	$2.37(121) \times 10^{-7}$	$1.83(63) \times 10^{-8}$	.....
.....	$1.096(573) \times 10^{-10}$	.....	.....

Variance-Covariance Matrices

V^a_{00} = 2.00×10^{-6}	V^b_{00} = 1.94×10^{-4}	V^c_{00} = 8.41×10^{-6}	V^β_{00} = 1.87×10^{-4}
V^a_{01} = -2.27×10^{-9}	V^b_{01} = -1.07×10^{-6}	V^c_{01} = -2.55×10^{-8}	V^β_{01} = -2.22×10^{-7}
V^a_{02} = ...	V^b_{02} = 1.66×10^{-9}	V^c_{02} = 1.66×10^{-11}	V^β_{02} = ...
V^a_{03} = ...	V^b_{03} = -7.80×10^{-13}	V^c_{03} = ...	V^β_{03} = ...
V^a_{11} = 3.23×10^{-12}	V^b_{11} = 5.90×10^{-9}	V^c_{11} = 8.48×10^{-11}	V^β_{11} = 3.04×10^{-10}

Table 1-8 (continued)

V^a_{12} = ...	V^b_{12} = -9.25×10^{-12}	V^c_{12} = -5.76×10^{-14}	V^β_{12} = ...
V^a_{13} = ...	V^b_{13} = 4.36×10^{-15}	V^c_{13} = ...	V^β_{13} = ...
V^a_{22} = ...	V^b_{22} = 1.46×10^{-14}	V^c_{22} = 3.99×10^{-17}	V^β_{22} = ...
V^a_{23} = ...	V^b_{23} = -6.90×10^{-18}	V^c_{23} = ...	V^β_{23} = ...
V^a_{33} = ...	V^b_{33} = 3.28×10^{-21}	V^c_{33} = ...	V^β_{33} = ...

Acmite

a-axis Regression Coefficient	b-axis Regression Coefficient	c-axis Regression Coefficient	β Regression Coefficient
9.7150(154)	8.811(15)	5.237(14)	107.439(22)
$-3.577(802) \times 10^{-4}$	$-1.53(80) \times 10^{-4}$	$-1.59(77) \times 10^{-4}$	$-1.42(25) \times 10^{-4}$
$6.45(124) \times 10^{-7}$	$3.8(12) \times 10^{-7}$	$3.2(12) \times 10^{-7}$	.....
$-2.941(582) \times 10^{-10}$	$-1.69(\ \ ) \times 10^{-10}$	$-1.41(57) \times 10^{-10}$	.....

Variance-Covariance Matrices

V^a_{00} = 2.37×10^{-4}	V^b_{00} = 2.37×10^{-4}	V^c_{00} = 9.94×10^{-4}	V^β_{00} = 4.70×10^{-4}
V^a_{01} = -1.22×10^{-6}	V^b_{01} = -1.22×10^{-6}	V^c_{01} = -1.07×10^{-6}	V^β_{01} = -5.29×10^{-7}
V^a_{02} = 1.83×10^{-9}	V^b_{02} = 1.83×10^{-9}	V^c_{02} = 1.66×10^{-9}	V^β_{02} = ...

Table 1-8 (continued)

$V^a_{03} = -8.47 \times 10^{-10}$	$V^b_{03} = -8.47 \times 10^{-13}$	$V^c_{03} = 7.80 \times 10^{-13}$	$V^\beta_{03} =$ .....
$V^a_{11} = 6.44 \times 10^{-9}$	$V^b_{11} = 6.44 \times 10^{-9}$	$V^c_{11} = 5.90 \times 10^{-9}$	$V^\beta_{11} = 6.39 \times 10^{-10}$
$V^a_{12} = -9.87 \times 10^{-12}$	$V^b_{12} = -9.87 \times 10^{-12}$	$V^c_{12} = -9.25 \times 10^{-12}$	$V^\beta_{12} =$ .....
$V^a_{13} = 4.60 \times 10^{-15}$	$V^b_{13} = 4.60 \times 10^{-15}$	$V^c_{13} = 4.36 \times 10^{-15}$	$V^\beta_{13} =$ .....
$V^a_{22} = 1.53 \times 10^{-12}$	$V^b_{22} = -1.53 \times 10^{-14}$	$V^c_{22} = 1.46 \times 10^{-14}$	$V^\beta_{22} =$ .....
$V^a_{23} = -7.18 \times 10^{-18}$	$V^b_{23} = -7.18 \times 10^{-18}$	$V^c_{23} = -6.90 \times 10^{-18}$	$V^\beta_{23} =$ .....
$V^a_{33} = 3.39 \times 10^{-21}$	$V^b_{33} = 3.39 \times 10^{-21}$	$V^c_{33} = 3.28 \times 10^{-21}$	$V^\beta_{33} =$ .....

Ureyite

a-axis Regression Coefficient	b-axis Regression Coefficient	c-axis Regression Coefficient	β Regression Coefficient
9.5742(67)	8.7053(47)	5.2607(16)	107.432(16)
$0.2(23) \times 10^{-5}$	$4.7(19) \times 10^{-5}$	$2.06(24) \times 10^{-5}$	$-2.09(24) \times 10^{-4}$
$4.7(18) \times 10^{-8}$	$3.1(16) \times 10^{-8}$	.....	.....
.....	.....	.....	.....

Variance-Covariance Matrices

$V^a_{00} = 4.44 \times 10^{-5}$	$V^b_{00} = 2.23 \times 10^{-5}$	$V^c_{00} = 2.54 \times 10^{-6}$	$V^\beta_{00} = 2.54 \times 10^{-4}$

Table 1-8 (continued)

$V_{01}^{a} = -1.46 \times 10^{-7}$	$V_{01}^{b} = -8.77 \times 10^{-8}$	$V_{01}^{c} = -3.59 \times 10^{-9}$	$V_{01}^{\beta} = -3.59 \times 10^{-7}$
$V_{02}^{a} = 1.11 \times 10^{-10}$	$V_{02}^{b} = 7.35 \times 10^{-11}$	$V_{02}^{c} =$	$V_{02}^{\beta} =$ .....
$V_{03}^{a} =$	$V_{03}^{b} =$	$V_{03}^{c} = 5.84 \times 10^{-12}$	$V_{03}^{\beta} = 5.85 \times 10^{-10}$
$V_{11}^{a} = 1.17 \times 10^{-10}$	$V_{11}^{b} = 3.64 \times 10^{-10}$	$V_{11}^{c} =$	$V_{11}^{\beta} =$ .....
$V_{12}^{a} = -4.12 \times 10^{-13}$	$V_{12}^{b} = -3.13 \times 10^{-13}$	$V_{12}^{c} =$	$V_{12}^{\beta} =$ .....
$V_{13}^{a} =$	$V_{13}^{b} =$	$V_{13}^{c} =$	$V_{13}^{\beta} =$ .....
$V_{22}^{a} = 3.37 \times 10^{-16}$	$V_{22}^{b} = 2.74 \times 10^{-16}$	$V_{22}^{c} =$	$V_{22}^{\beta} =$ .....
$V_{23}^{a} =$	$V_{23}^{b} =$	$V_{23}^{c} =$	$V_{23}^{\beta} =$ .....
$V_{33}^{a} =$	$V_{33}^{b} =$	$V_{33}^{c} =$	$V_{33}^{\beta} =$ .....

Hedenbergite

a-axis Regression Coefficient	b-axis Regression Coefficient	c-axis Regression Coefficient	β Regression Coefficient
9.8163(68)	8.9891(24)	5.2362(12)	104.304(68)
$1.17(34) \times 10^{-4}$	$1.087(69) \times 10^{-4}$	$3.13(12) \times 10^{-5}$	$1.91(34) \times 10^{-3}$
$-8.1(47) \times 10^{-8}$	$3.20(43) \times 10^{-8}$	.....	$-1.68(47) \times 10^{-6}$
$4.0(20) \times 10^{-11}$	.....	.....	$6.1(20) \times 10^{-10}$

Table 1-8 (continued)

Variance-Covariance Matrices

$V^a_{00} = 4.64 \times 10^{-5}$	$V^b_{00} = 5.94 \times 10^{-6}$	$V^c_{00} = 1.38 \times 10^{-6}$	$V^\beta_{00} = 4.64 \times 10^{-3}$
$V^a_{01} = -2.26 \times 10^{-7}$	$V^b_{01} = -1.58 \times 10^{-8}$	$V^c_{01} = -1.36 \times 10^{-9}$	$V^\beta_{01} = -2.26 \times 10^{-5}$
$V^a_{02} = 3.09 \times 10^{-10}$	$V^b_{02} = 9.16 \times 10^{-12}$	$V^c_{02} = ...$	$V^\beta_{02} = 3.09 \times 10^{-8}$
$V^a_{03} = -1.27 \times 10^{-13}$	$V^b_{03} = ...$	$V^c_{03} = ...$	$V^\beta_{03} = -1.27 \times 10^{-11}$
$V^a_{11} = 1.14 \times 10^{-9}$	$V^b_{11} = 4.71 \times 10^{-11}$	$V^c_{11} = 1.52 \times 10^{-12}$	$V^\beta_{11} = 1.14 \times 10^{-7}$
$V^a_{12} = -1.58 \times 10^{-12}$	$V^b_{12} = -2.90 \times 10^{-14}$	$V^c_{12} = ...$	$V^\beta_{12} = -1.58 \times 10^{-10}$
$V^a_{13} = 6.59 \times 10^{-16}$	$V^b_{13} = ...$	$V^c_{13} = ...$	$V^\beta_{13} = 6.59 \times 10^{-14}$
$V^a_{22} = 2.24 \times 10^{-15}$	$V^b_{22} = 1.84 \times 10^{-17}$	$V^c_{22} = ...$	$V^\beta_{22} = 2.24 \times 10^{-13}$
$V^a_{23} = -9.39 \times 10^{-19}$	$V^b_{23} = ...$	$V^c_{23} = ...$	$V^\beta_{23} = -9.39 \times 10^{-17}$
$V^a_{33} = 3.98 \times 10^{-22}$	$V^b_{33} = ...$	$V^c_{33} = ...$	$V^\beta_{33} = 3.98 \times 10^{-20}$

Table 1-8 (continued)

Diopside

a-axis	b-axis	c-axis	β
Regression Coefficient	Regression Coefficient	Regression Coefficient	Regression Coefficient
9.730(1)	8.8914(18)	5.2409(6)	105.861(9)
$6.95(12 \times 10^{-5}$	$1.145(58) \times 10^{-4}$	$3.51(8) \times 10^{-5}$	$1.26(10) \times 10^{-4}$
.....	$2.75(39) \times 10^{-8}$	.....	

Variance-Covariance Matrices

$V^a_{00} = 9.33 \times 10^{-7}$	$V^b_{00} = 3.21 \times 10^{-6}$	$V^c_{00} = 3.05 \times 10^{-7}$	$V^\beta_{00} = 7.47 \times 10^{-5}$
$V^a_{01} = -1.08 \times 10^{-9}$	$V^b_{01} \quad -9.86 \times 10^{-9}$	$V^c_{01} \quad -4.14 \times 10^{-10}$	$V^\beta_{01} = -8.44 \times 10^{-8}$
$V^a_{02} =$	$V^b_{02} = 6.20 \times 10^{-12}$	V^c_{02}	$V^\beta_{02} = 1.15 \times 10^{-10}$
$V^a_{03} =$	$V^b_{03} =$	$V^c_{03} =$	$V^\beta_{03} =$ .....
$V^a_{11} = 1.52 \times 10^{-12}$	$V^b_{11} = 3.39 \times 10^{-11}$	$V^c_{11} = 7.13 \times 10^{-13}$	V^β_{11}
$V^a_{12} =$	$V^b_{12} = -2.23 \times 10^{-14}$	$V^c_{12} =$	$V^\beta_{12} =$
$V^a_{13} =$	V^b_{13}	$V^c_{13} =$	$V^\beta_{13} =$ .....
$V^a_{22} =$	$V^b_{22} = 1.51 \times 10^{-17}$	$V^c_{22} =$	$V^\beta_{22} =$
$V^a_{23} =$	$V^b_{23} =$	$V^c_{23} =$	$V^\beta_{23} =$ .....
$V^a_{33} =$	$V^b_{33} =$	$V^c_{33} =$	$V^\beta_{33} =$ .....

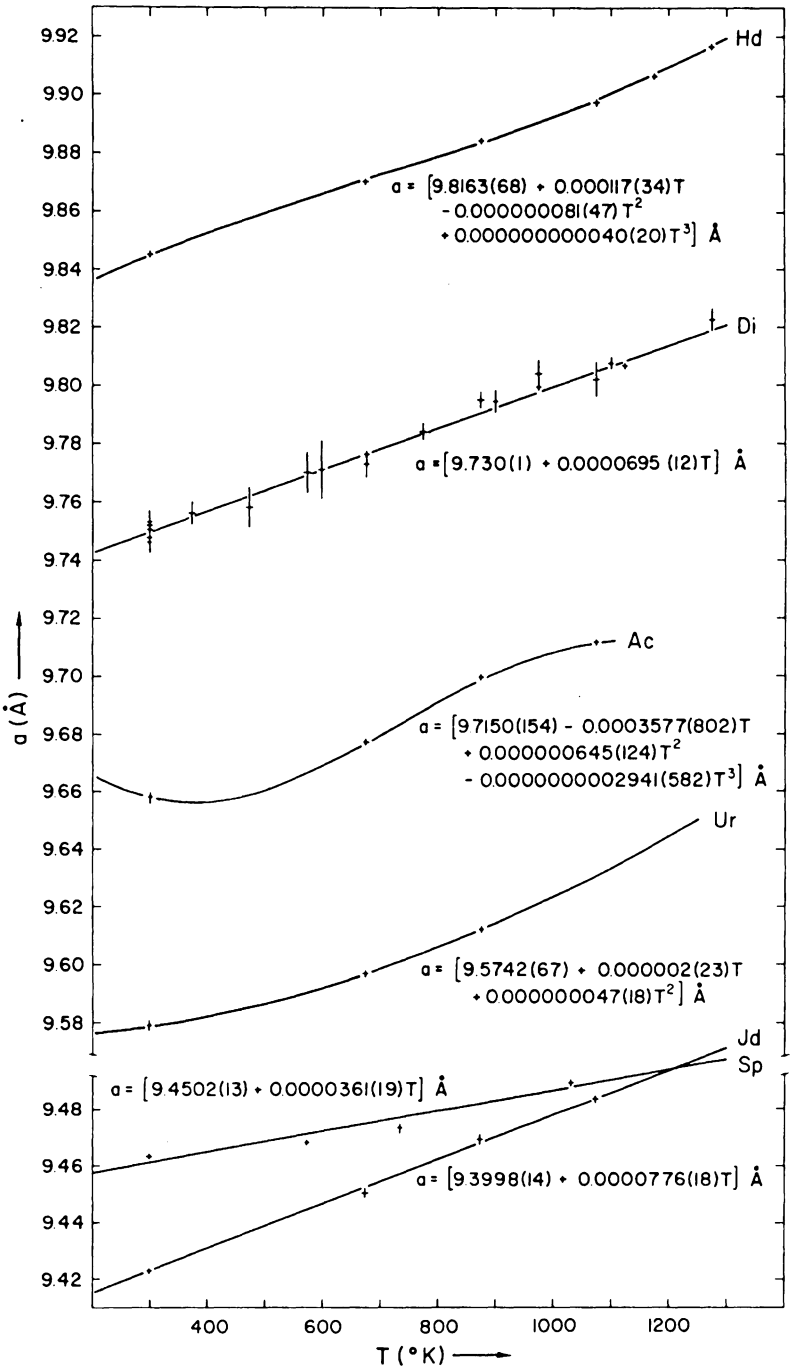

Figure 1-15: Length of the a-cell edge of the clinopyroxenes spodumene, jadeite, acmite, ureyite, hedenbergite, and diopside as a function of temperature. Plotted points represent measured values with their standard deviations. Regression equations are also given.

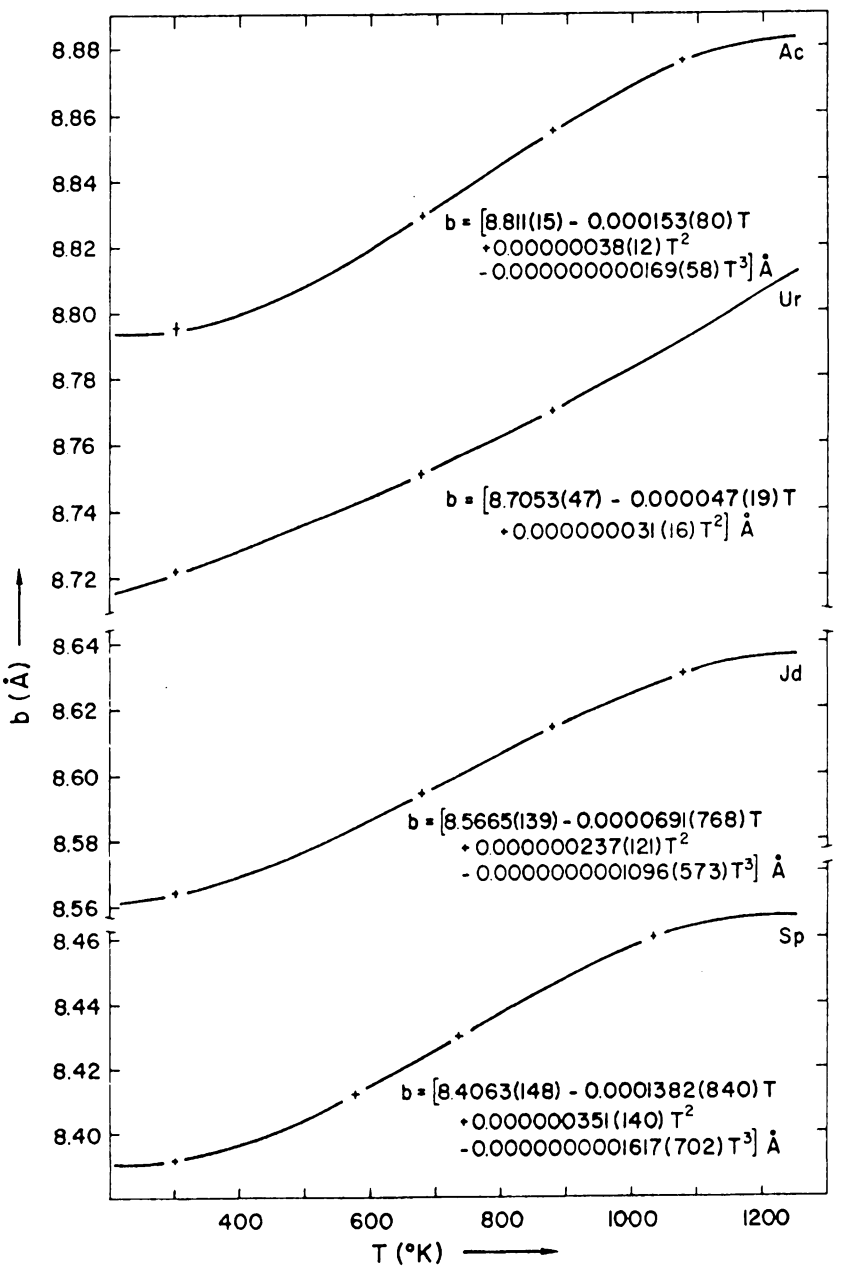

Figure 1-16-a: Length of the b-cell edge of the clinopyroxenes spodumene, jadeite, acmite, and ureyite as a function of temperature. Plotted points represent measured values with their standard deviations. Regression equations are also given.

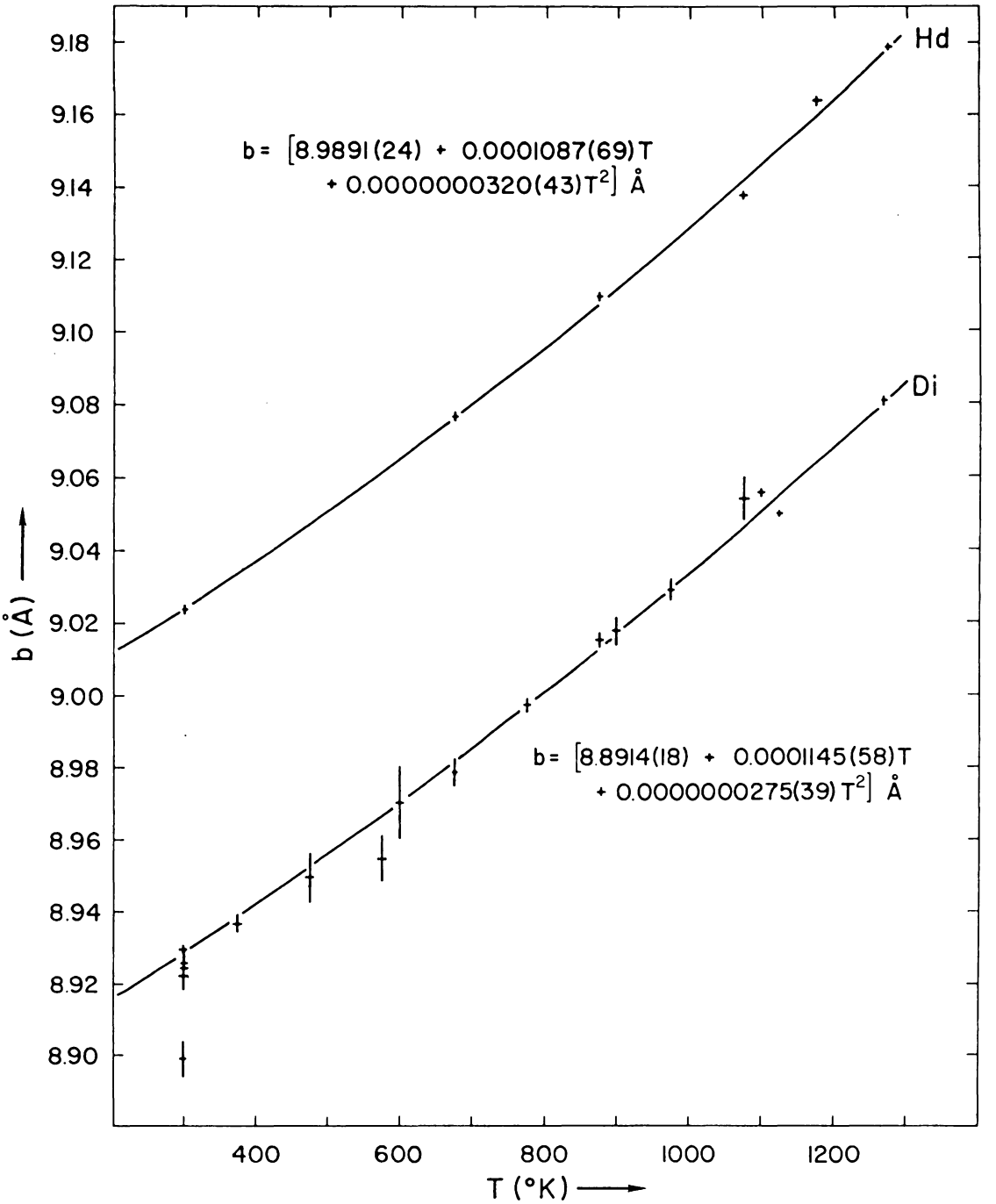

Figure 1-16-b: Length of the b-cell edge of the clinopyroxenes hedenbergite and diopside as a function of temperature. Plotted points represent measured values with their standard deviations. Regression equations are also given.

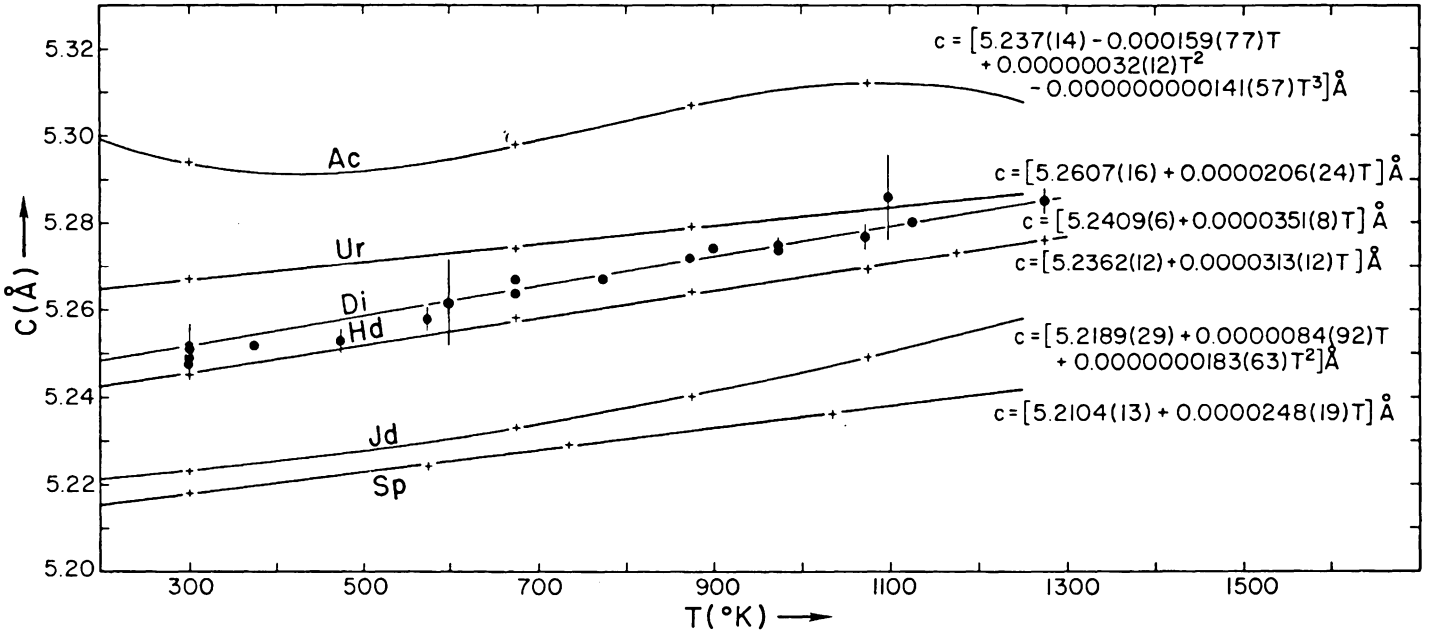

Figure 1-17: Length of the c-cell edge of the clinopyroxenes spodumene, jadeite, acmite, ureyite, hedenbergite, and diopside as a function of temperature. Plotted points represent measured values with their standard deviations. Regression equations are also given.

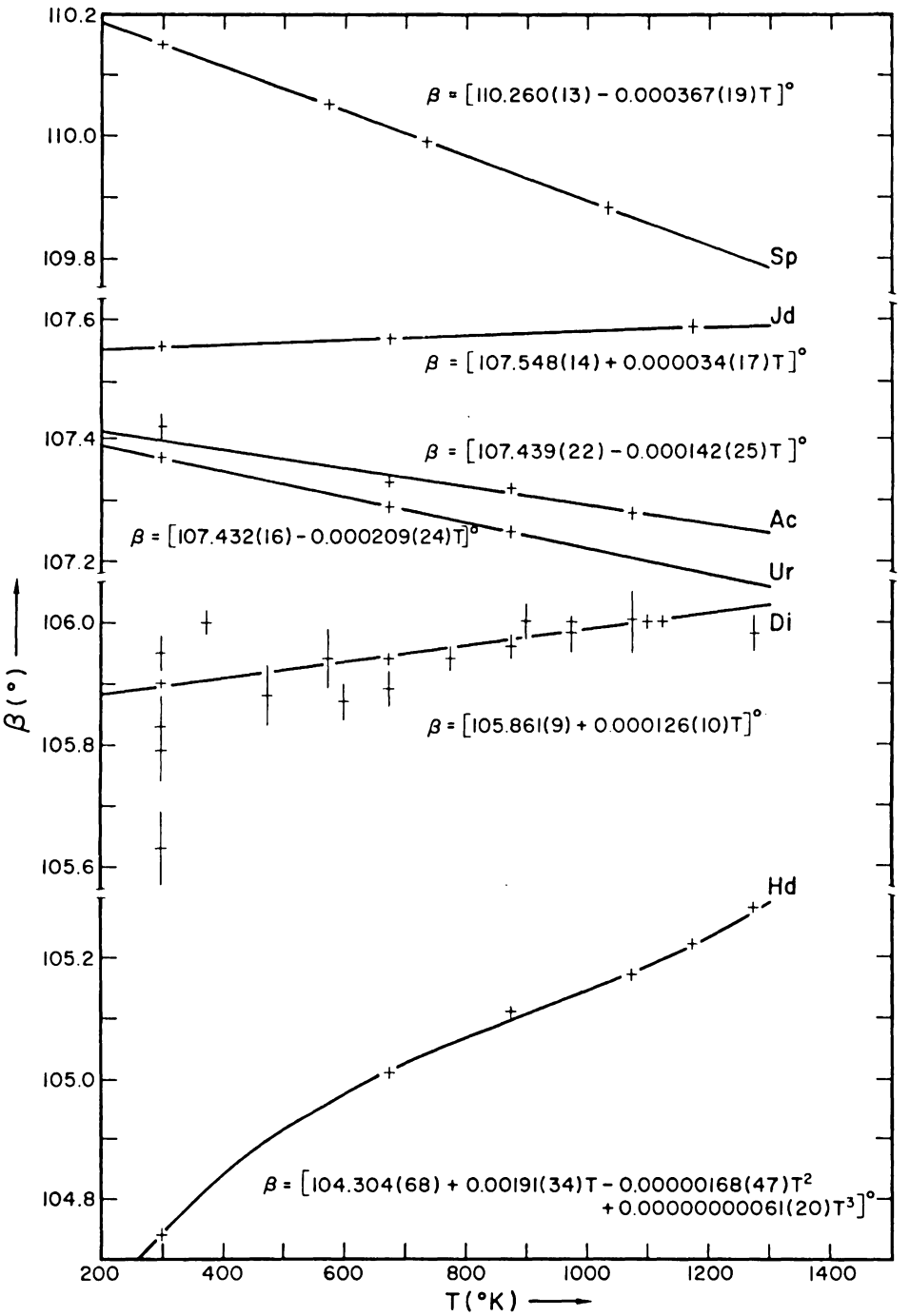

Figure 1-18: Magnitude of the β angle of the clinopyroxenes spodumene, jadeite, acmite, ureyite, hedenbergite, and diopside as a function of temperature. Plotted points represent measured values with their standard deviations. Regression equations are also given.

Table 1-9

Tabulation of the Thermal Expansion Coefficients of Spodumene, Jadeite, Acmite, Ureyite, Hedenbergite, and Diopside

Spodumene

Temperature (°K)	$\varepsilon_1(\sigma_{\varepsilon_1})$	$\varepsilon_2(\sigma_{\varepsilon_2})$	$\varepsilon_3(\sigma_{\varepsilon_3})$	$\Theta(°)$	β
250	8.9(.2)	0.8(3.3)	2.0(.3)	50.9(.2)	11.8(3.3)
300	8.9(.2)	3.4(2.3)	2.0(.3)	50.9(.2)	14.3(2.4)
400	8.9(.2)	7.7(.8)	2.0(.3)	50.9(.2)	18.6(.9)
500	8.9(.2)	10.9(.6)	2.0(.3)	50.9(.2)	21.8(.7)
600	8.9(.2)	12.9(1.0)	2.0(.3)	50.9(.2)	23.8(1.1)
700	8.9(.2)	13.7(1.1)	2.0(.3)	50.9(.2)	24.6(1.2)
800	8.9(.2)	13.4(.7)	2.0(.3)	50.9(.2)	24.3(0.8)
900	8.9(.2)	11.9(.6)	2.0(.3)	50.9(.2)	22.7(.7)
1000	8.9(.2)	9.3(1.9)	2.0(.3)	50.9(.2)	20.2(1.9)
1050	8.9(.2)	7.6(2.8)	2.0(.3)	50.9(.2)	18.4(2.8)

Jadeite

250	8.2(.3)	3.4(3.2)	3.1(1.1)	-77.8(1.1)	14.8(3.4)
300	8.2(.3)	5.8(1.9)	3.5(1.1)	-77.3(1.0)	16.8(2.5)
400	8.2(3)	7.9(1.0)	4.2(.8)	-76.8(.9)	20.4(1.3)
500	8.2(.3)	9.9(.3)	4.9(.6)	-75.8(.8)	23.1(.7)
600	8.2(.3)	11.3(.8)	5.6(.4)	-74.3(.6)	25.1(.9)
700	8.2(.3)	11.8(1.0)	6.3(.3)	-71.6(.5)	26.3(1.0)
800	8.2(.3)	11.6(.8)	7.0(.3)	-66.0(.8)	26.8(.9)
900	8.3(.3)	10.5(.5)	7.6(.4)	-49.9(3.0)	26.5(.7)
1000	8.7(.2)	8.8(1.0)	7.9(.2)	-19.5(.3)	25.4(1.2)
1050	9.0(7)	7.7(1.6)	7.8(.2)	-10.6(.2)	24.6(1.8)

Acmite

250	-8.3(2.7)	0.6(3.4)	-11.8(4.4)	74.8(5.6)	22.9(1.7)
300	-4.2(2.1)	3.3(2.5)	-7.9(3.4)	76.7(4.4)	23.3(1.3)
400	2.6(1.0)	7.9(1.2)	-1.4(1.5)	79.1(2.1)	24.1(.8)
500	7.8(.5)	11.4(.6)	3.5(.6)	80.1(0.5)	25.0(.5)
600	11.1(.7)	13.6(.8)	6.8(1.2)	80.1(1.7)	26.0(.4)
700	12.5(.8)	14.8(.9)	8.5(1.4)	79.1(2.0)	27.0(.5)
800	12.3(.7)	14.7(.8)	8.5(1.1)	76.8(1.5)	28.2(.5)
900	9.9(.4)	13.5(.5)	6.9(.6)	72.4(.8)	29.3(.5)
1000	6.4(.8)	11.2(1.0)	3.6(1.2)	64.7(1.6)	30.6(.4)
1100	(2.2)	7.8(2.3)	-1.5(2.1)	52.3(4.8)	32.0(.6)

Ureyite

250	7.2(1.2)	1.8(1.0)	5.9(.6)	44.2(6.9)	14.9(2.0)
300	7.5(1.1)	2.2(.8)	6.1(.6)	47.8(1.8)	15.7(1.7)
400	8.2(.7)	2.7(.5)	6.5(.5)	55.4(.5)	17.4(1.2)
500	8.9(.4)	3.1(.4)	7.1(.4)	62.8(.3)	19.1(.8)
600	9.6(.3)	3.3(.4)	7.8(.3)	69.1(.3)	20.8(.7)
700	10.3(.6)	3.5(.4)	8.6(.4)	74.1(.3)	22.4(.9)
800	11.0(.9)	3.6(.4)	9.4(.7)	77.9(.4)	24.1(1.3)
900	11.7(.3)	3.7(.4)	10.3(1.1)	80.1(.4)	25.8(1.8)

Hedenbergite

250	15.3(1.6)	13.8(5.3)	-6.2(1.1)	-41.0(.3)	22.9(1.7)
300	14.2(1.3)	14.2(.5)	-5.1(.8)	-40.8(.2)	23.3(1.3)
400	12.4(.7)	14.9(.4)	-3.2(.5)	-40.0(.1)	24.1(.8)
500	10.9(.4)	15.5(.3)	-1.5(.2)	-39.3(.1)	25.0(.5)
600	9.9(.3)	16.2(.2)	-1.2(.2)	-38.8(.1)	26.0(.4)
700	4.1(.4)	16.9(.2)	0.9(.5)	-38.8(.2)	27.0(.5)
800	8.9(.5)	17.6(.1)	1.7(.3)	-39.8(.2)	28.2(.5)

900	8.9(.5)	18.2(.2)	2.2(.3)	-41.8(.3)	29.3(.5)
1000	9.4(.3)	18.9(.2)	2.3(.2)	-44.4(1.2)	30.6(.4)
1100	10.3(.5)	19.6(.3)	2.1(.3)	-46.8(.4)	32.0(.6)
1200	11.6(1.0)	20.2(.4)	1.5(.5)	-48.6(.3)	33.4(.9)
1300	13.3(1.6)	20.9(.5)	0.6(.9)	-49.7(.3)	35.2(1.5)

Diopside

250	7.8(.2)	14.4(.4)	5.4(.1)	-42.8(0.5)	27.6(0.5)
300	7.8(.2)	14.7(.4)	5.4(.1)	-42.8(0.5)	27.9(0.4)
400	7.8(.2)	15.3(.3)	5.4(.1)	-42.7(0.5)	28.4(0.4)
500	7.7(.2)	15.9(.2)	5.4(.1)	-42.7(0.5)	29.0(0.3)
600	7.7(.2)	16.4(.2)	5.4(.1)	-42.7(0.5)	29.5(0.3)
700	7.7(.2)	17.0(.1)	5.4(.1)	-42.7(0.5)	30.2(0.2)
800	7.7(.2)	17.6(.1)	5.4(.1)	-42.7(0.5)	30.7(0.2)
900	7.7(.1)	18.2(.2)	5.4(.1)	-42.7(0.5)	31.3(0.3)
1000	7.7(.1)	18.7(.2)	5.4(.1)	-42.7(0.5)	31.9(0.3)
1100	7.7(.2)	19.3(.3)	5.4(.1)	-42.6(0.5)	32.4(0.4)
1200	7.7(.2)	19.9(.4)	5.4(.1)	-42.6(0.5)	33.0(0.4)
1300	7.7(.2)	20.5(.5)	5.4(.1)	-42.6(0.5)	33.6(0.5)

Results obtained using the Ohashi-Burnham method are given in Table 1-10. These results are also plotted on Figures 1-19 and 1-20 for the purpose of comparison. It is easily seen that the two techniques give comparable results.

The volume coefficient of thermal expansion, and the rates of thermal expansion parallel to the $\underset{\sim}{b}^*$- and the $\underset{\sim}{c}$-axis were also computed. The results are given in Figures 1-21-a, 1-21-b, and 1-21-c. The principal thermal expansion coefficients of these substances may be characterized in the following way.

Figures 1-19 and 1-20 indicate that ε_2, the rate of expansion parallel to the b-axis, is the largest principal coefficient of thermal expansion in every case. This particular principal direction is symmetry fixed in the monoclinic system and must therefore coincide with the b-axis (second setting) at all temperatures. Figure 1-20 indicates that for hedenbergite and diopside ε_2 increases slowly with increasing temperature. Deganello (1973) concluded that the magnitude of ε_2 in diopside was essentially temperature independent with a magnitude of 17.3×10^{-6}. This is in fairly good agreement with our result. The results of Deganello are shown as dotted lines in Figure 1-20. The temperature dependence of ε_2 in spodumene, jadeite and acmite is somewhat different. Figure 1-19 shows that there is an initial increase in the value of ε_2 with increasing temperature followed by a subsequent decrease at high temperatures.

This difference in the temperature dependence of ε_2 may reflect the fact that both the M1 and M2 cations in diopside have a formal charge of +2 while M1 has a formal charge of M1 and M2 a formal charge of +3 in spodumene, jadeite, acmite and ureyite. The data

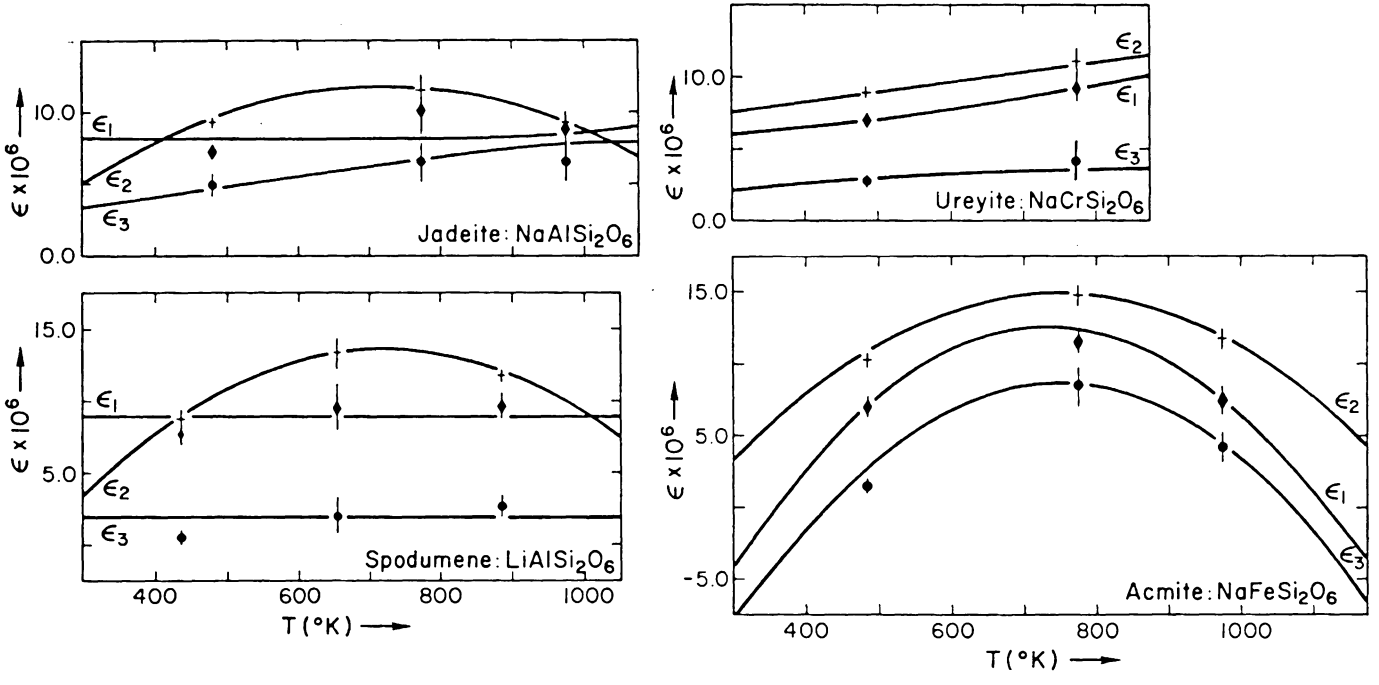

Figure 1-19: Principal coefficients of thermal expansion of jadeite, ureyite, spodumene, and acmite as a function of temperature. Plotted values were obtained using the Ohashi-Burnham equations.

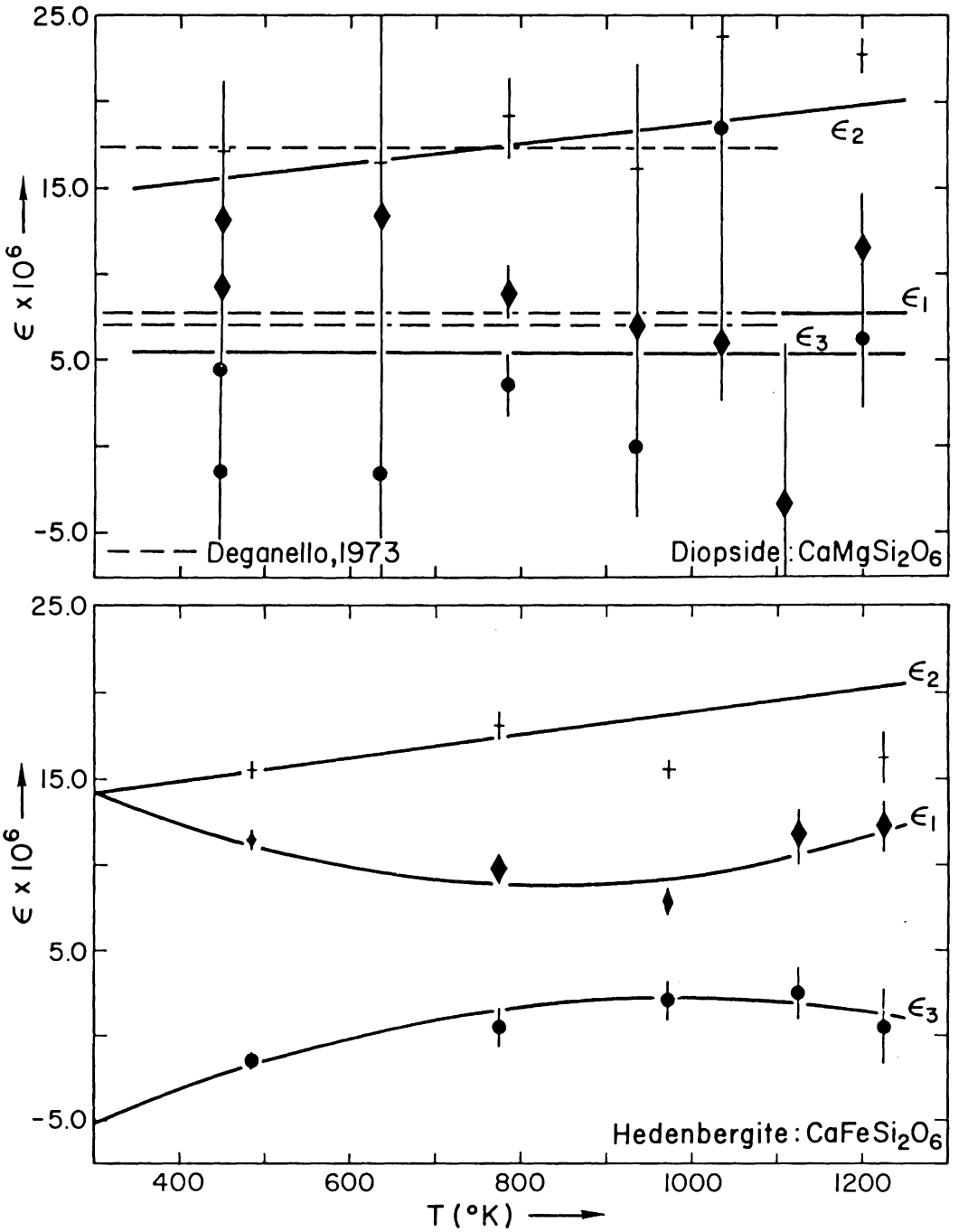

Figure 1-20: Principal coefficients of thermal expansion of diopside and hedenbergite as a function of temperature. Dashed lines on diopside plot represent the values obtained by Deganello (1973). Plotted points were obtained using the Ohashi-Burnham equations.

Table 1-10

Tabulation of the Thermal Expansion Coefficients of Spodumene, Jadeite, Acmite, Ureyite, Hedenbergite, and Diopside as Obtained from Ohashi-Burnham Equations.

Spodumene	Temperature	$\alpha_1 x10^6$ (error)	$\alpha_2 x10^6$ (error)	$\alpha_3 x10^6$ (error)	θ (error)
297.16- 573.16	435.16	7.78(0.92)	08.64(0.60)	0.62(0.56)	45.3(4.7)
573.16- 733.16	653.16	9.60(1.64)	13.37(1.04)	2.07(1.24)	43.9(8.7)
733.16-1033.16	883.16	9.68(0.83)	11.86(0.56)	2.74(0.68)	60.1(5.2)
Jadeite					
297.16- 673.16	485.16	07.63(0.64)	09.32(0.43)	4.93(0.75)	-76.0(7.4)
673.16- 873.16	773.16	10.14(1.54)	11.64(0.82)	6.60(1.39)	-81.2(10.5)
873.16-1073.16	973.16	8.82(0.91)	09.29(0.82)	6.60(1.2)	-19.0(19.8)
Acmite					
297.16- 673.16	485.16	07.04(0.79)	10.28(0.67)	1.51(0.65)	72.5(5.3)
673.16- 873.16	773.16	11.64(0.82)	14.72(0.79)	8.49(1.33)	90.2(12.0)
873.16-1073.16	973.16	7.43(0.99)	11.86(0.79)	4.28(1.09)	68.3(13.8)
Ureyite					
297.16- 673.16	485.16	6.94(0.64)	08.84(0.43)	2.75(0.57)	64.4(6.5)
673.16- 873.16	773.16	9.26(0.95)	10.86(0.80)	4.38(1.17)	74.3(8.6)
Hedenbergite					
297.16- 673.16	485.16	11.50(0.47)	15.62(0.41)	-1.49(0.59)	-37.9(1.8)
673.16- 873.16	773.16	09.80(0.84)	18.18(0.77)	0.64(1.15)	-42.0(4.9)
873.16-1073.16	973.16	07.83(0.78)	15.37(0.67)	2.08(1.21)	-47.0(7.6)
1073.16-1173.16	1123.16	11.75(1.66)	28.45(1.53)	2.56(1.66)	-42.3(9.7)
1173.16-1273.16	1223.16	12.35(1.5)	16.37(1.53)	0.57(2.44)	-48.9(7.4)

Table 1-10 (continued)

Diopside

297.16- 598.16	447.66*	9.20(3.87)	17.12(4.16)	4.28(4.98)	-42.4(48.0)
297.16- 298.16	447.66**	13.06(4.13)	26.51(4.18)	-1.51(5.10)	-40.3(16.7)
518.16- 673.16	635.66***	16.43(17.88)	13.38(14.93)	-1.58(13.32)	-27.18(45.4)
673.16- 898.16	785.16****	09.08(1.61)	19.30(2.03)	3.68(1.80)	-50.02(12.5)
898.16- 973.16	935.66***	06.94(5.82)	16.26(6.08)	-0.14(3.77)	-82.00(31.0)
973.16-1098.16	1035.66***	06.29(1.89)	23.92(1.25)	18.44(15.55)	-82.0(4.8)
1098.16-1123.16	1110.66***	-3.25(9.35)	-26.5(6.20)	-46.24(11.00)	-82.0(6.8)
1123.16-1273.16	1198.16*****	11.60(3.23)	22.84(1.04)	6.26(3.86)	+84.5(22.4)

* Nolan and Edgar (1963) to Deganello (1973)
** Clark et al. (1969) to Deganello (1973)
*** Deganello (1973) to Cameron et al. (1973)
**** Cameron et al. to Deganello (1973)
***** Cameron et al. (1973) to Cameron et al. (1973)

available for ureyite is not sufficient to indicate whether or not the magnitude of ε_2 eventually begins to decrease as the temperature is raised.

The two remaining principal coefficients of thermal expansion are constrained by symmetry to lie in the ac-plane, however, the orientation of the principal axes of thermal expansion in this plane is not symmetry fixed and is consequently a function of temperature. Figures 1-19 and 1-20 indicate, that, with the exception of diopside, jadeite, and acmite, ε_1 and ε_3 tend initially to converge with increasing temperature and then subsequently diverge as the temperature is increased still further. This result agrees with that of Deganello (1973) who concluded that the magnitudes of ε_1 and ε_3 for diopside were essentially temperature independent. Finger and Ohashi (1976) come to a similar conclusion. They found that in diopside "within the resolution of the available data the linear and volume coefficients are independent of temperature for the range studied."

Figure 1-19 indicates that the temperature dependence of ε_1 and ε_3 for acmite are completely different from those obtained for the other minerals in this group. Since these results are based on only four measurements of the cell parameters of acmite more data appears to be necessary before it can be concluded that the results obtained correspond to reality. In particular, it appears that the measurements of the cell parameters made at room temperature and at 673.16°K should be checked.

Orientation of the Representation Quadric for Thermal Expansion.

The representation quadric for the monoclinic minerals studied here has two distinct orientations. For acmite, ureyite, and spodumene the direction of maximum expansion in the ac-plane is roughly independent of temperature and lies at an angle which approximately bisects the obtuse angle (β) between the positive ends of the a- and c- crystallographic axes. In hedenbergite, jadeite, and diopside, however, the direction of maximum expansion is rotated approximately 90 degrees and lies approximately mid-way between the +c- and -a-axes. For hedenbergite and jadeite the magnitude of θ for jadeite at higher temperatures appears to be strongly temperature dependent. It should be noted that in no case do the principal directions of thermal expansion coincide with any simple structural feature of these substances. This observation was also made by Finger and Ohashi (1976). They concluded, however, that the direction of minimum expansion in diopside corresponded closely to the direction of the M2-02C2 bond--a bond whose length apparently decreases as the crystal is heated from room temperature to 700°C (973.16°K). This is the shortest bond in the coordination polyhedron about M2. Our results indicate that this observation is also valid for hedenbergite.

Although the principal directions of expansion of the clinopyroxenes do not coincide with any simple structural features of these substances an examination of the rates of expansion in some specially selected direction is nevertheless interesting.

A comparison of the rate of thermal expansion parallel to the c-axis (parallel to the infinite chains of silicate tetrahedra) is

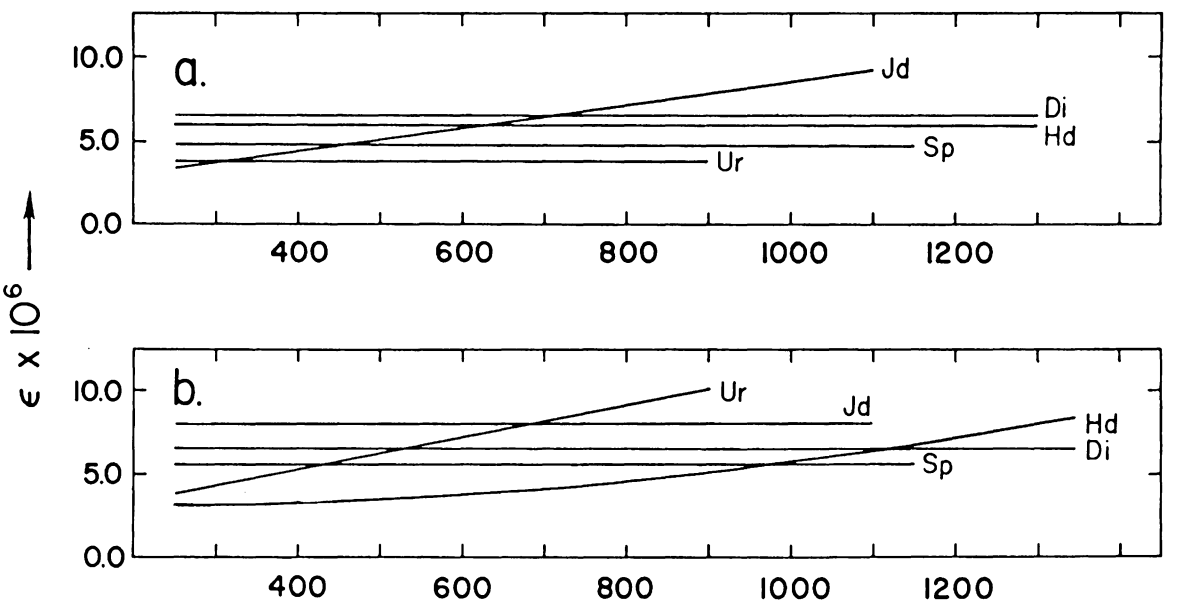

Figure 1-21-a (top): The coefficient of thermal expansion of the clinopyroxenes spodumene, jadeite, acmite, ureyite, hedenbergite, and diopside along the c-axis. Because of the similarity in the magnitudes of the values of $\varepsilon^{[001]}$ the silicate chain running along the c-axis can be said to "control" the expansion in this direction.

Figure 1-21-b (bottom): Thermal expansion coefficients for the minerals spodumene, jadeite, ureyite, hedenbergite, and diopside along the direction [010]. These are also very similar. This reflects the arrangement of alternating sheets of tetrahedral chains and MI and MII cations common to all these materials.

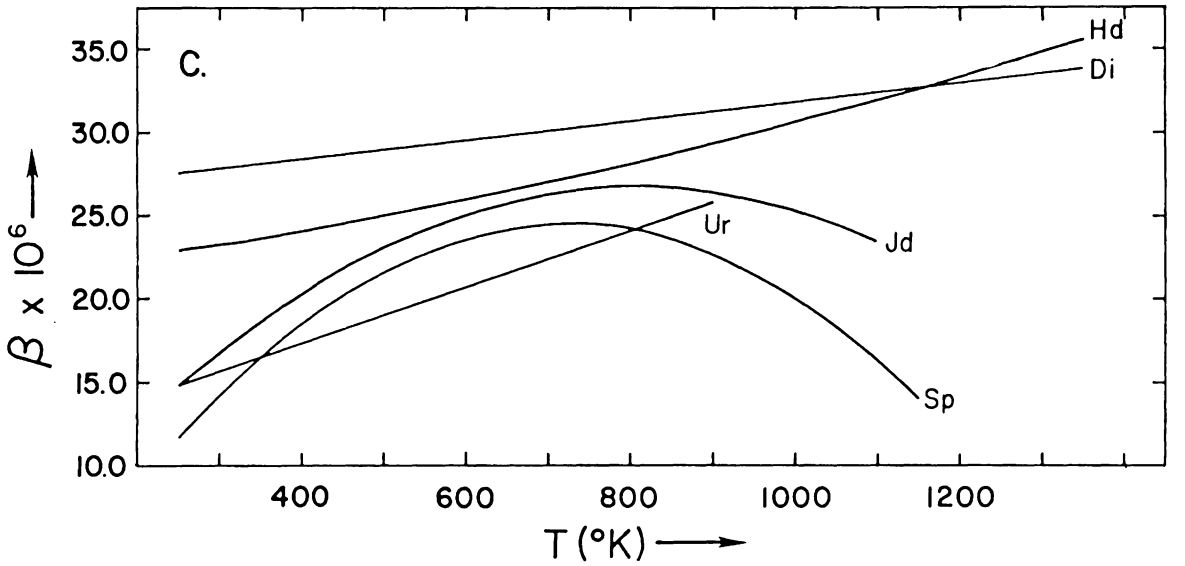

Figure 1-21-c: Volume coefficients of thermal expansion of spodumene, jadeite, ureyite, hedenbergite, and diopside. Note that the volume coefficient of thermal expansion of hedenbergite and diopside exceeds that of other clinopyroxenes examined here. The temperature dependence is also different. (There is insufficient information to determine if the volume coefficient of thermal expansion of ureyite begins to decrease at high temperatures.)

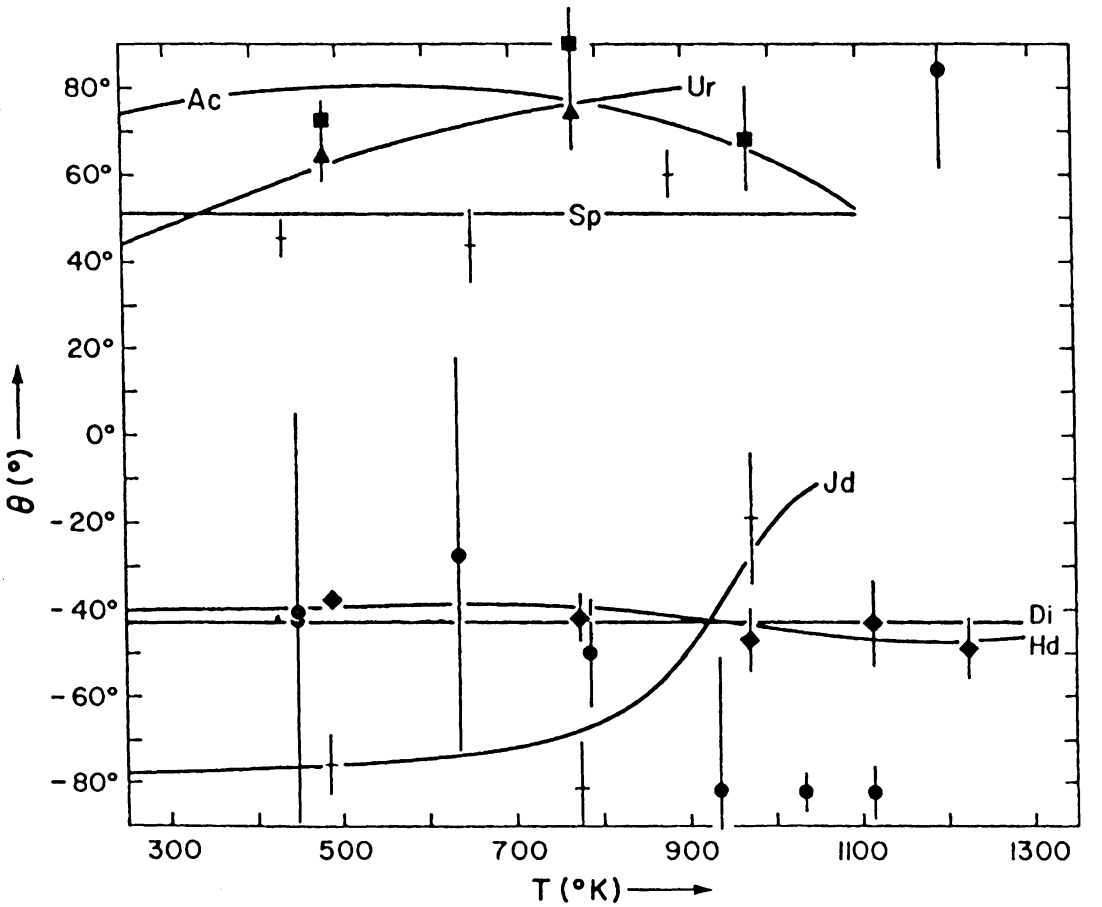

Figure 1-22: Orientation of the representation quadric for the principal directions of thermal expansion in spodumene, jadeite, acmite, ureyite, hedenbergite, and diopside. The angle θ is the angle the principal direction of expansion ε_1 makes with the positive end of the c-axis (see text for discussion).

given in Figure 1-21-a. It is seen that (except for acmite, which is omitted) the rate of expansion along the c-axis is almost identical for all the clinopyroxenes studied here. Thus it can be said that the silicate chain "controls" the rate of expansion in this direction. This however is a very vague statement. Figure 1-21-b indicates that the rates of expansion along a*, that is perpendicular to the alternating sheets of cations and silicate chains, is also very similar. Again the result for acmite is anoamolous.

Volume coefficients of thermal expansion are given in Figure 1-21-c. The results here indicate that the volume coefficient of thermal expansion tends to be larger when both M1 and M2 ions have a charge of +2.

The Grüneisen Equations in a Monoclinic Crystal

In a monoclinic crystal the extended Grüneisen relation takes the form

$$(1\text{-}318)\qquad \begin{bmatrix} \varepsilon_1 \\ \varepsilon_2 \\ \varepsilon_3 \\ 0 \\ \varepsilon_5 \\ 0 \end{bmatrix} = \frac{C_v}{V} \begin{bmatrix} S_{11} & S_{12} & S_{13} & 0 & S_{15} & 0 \\ S_{12} & S_{22} & S_{23} & 0 & S_{25} & 0 \\ S_{13} & S_{23} & S_{33} & 0 & S_{35} & 0 \\ 0 & 0 & 0 & S_{44} & 0 & S_{46} \\ S_{15} & S_{25} & S_{35} & 0 & S_{55} & 0 \\ 0 & 0 & 0 & S_{46} & 0 & S_{66} \end{bmatrix} \begin{bmatrix} \gamma_1 \\ \gamma_2 \\ \gamma_3 \\ 0 \\ \gamma_5 \\ 0 \end{bmatrix}$$

The number of calculations of Grüneisen parameters for crystals of monoclinic symmetry appears to be very small. The only other calculation which could be located was that of Küppers for the ammonium and potassium oxyalates (1971).

Since elastic constants (Simmons and Wong, 1971) and heat capacities (see Fig. 1-22) are available for diopside (see Table 1-11) a calculation of the components of the Grüneisen tensor is possible. Because the macroscopic Grüneisen tensor for a monoclinic crystal has the same form as the thermal expansion tensor it can be diagonalized using formulas identical to those used to diagonalize the thermal expansion tensor.

The principal components of the macroscopic Grüneisen tensor for diopside are given in Figure 1-24. The magnitudes of γ_1, γ_2 and γ_3 are about equal in magnitude to those previously obtained by other researches for crystals of higher symmetry and to those obtained by Küppers (1974). All are well behaved and none are negative (negative Grüneisen parameters tend to bring about negative thermal expansion). The magnitudes of γ_1 and γ_2 are very nearly equal in magnitude. This indicates that although the expansion in the direction of the b-axis is larger than ε_1 and ε_2 the strain dependence of the normal modes is not especially large for this direction. The orientation of the representation quadric for the Grüneisen tensor is plotted in Figure 1-25. There appears to be a definite tendency for the orientation of the representation quadric of the Grüneisen tensor to follow the orientation of the representation quadric of the thermal expansion. This may be a significant result since such parallelism of orientation it is not

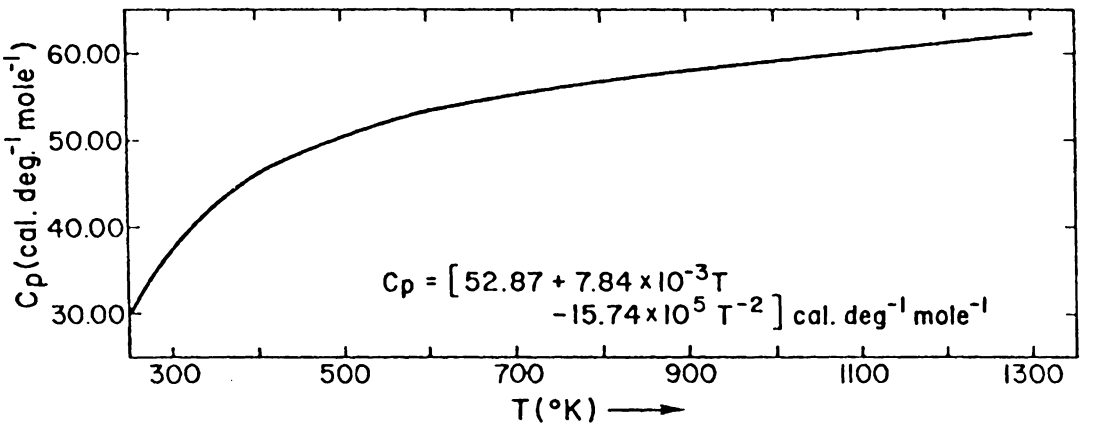

Figure 1-23: Heat capacity of diopside (Cp) as a function of temperature.

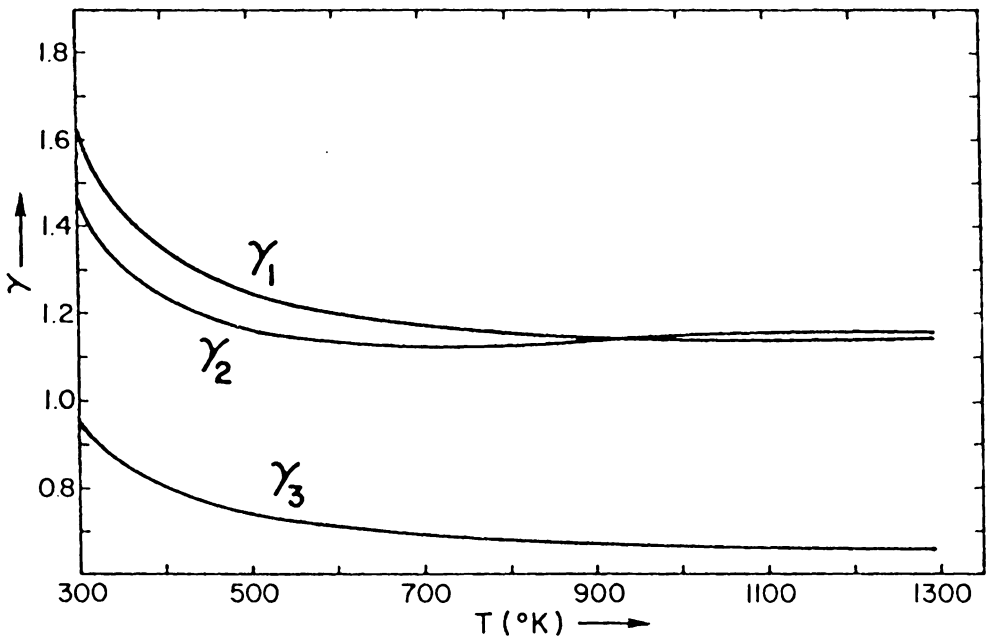

Figure 1-24: Principal components of the macroscopic Grüneisen tensor for diopside. These are all positive and well behaved. The reason for the increase near room temperature is not known.

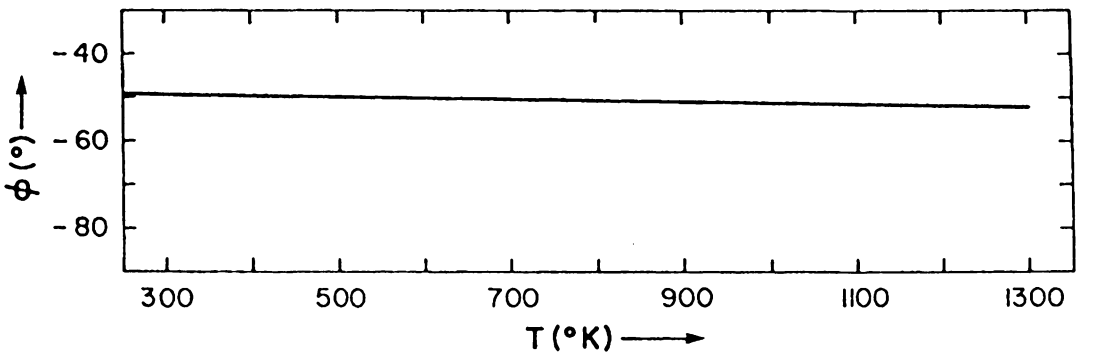

Figure 1-25: Orientation of the representation quadric for the principal directions of the macroscopic Grüneisen tensor for diopside. Note there appears to be some tendency for the orientation of this representation quadric to follow the orientation of the representation quadric of the thermal expansion. This would indicate that the crystal is expanding in those directions in which the strain had the largest effect on the frequencies of the normal modes. This result is not "built into" the equations.

Table 1-11
Principal Thermal Expansion Coefficients of Diopside
(after Finger and Ohashi, 1976)

Temperature Range °C	Reference*	Principal Linear Thermal Expansion Coefficients x 10^{-6} per degree			Volume Expansion Coefficients x 10^{-6} per degree	Orientations**		
		ε_1	ε_2	ε_3		ε_1	ε_2	ε_3
24–100	1	20.6(63)	9.6(53)	-0.6(76)	30(12)	b	153(27)	63(27)
100–200	1	15.7(56)	12.6(55)	1.9(51)	30(10)	b	127(20)	37(20)
200–300	1	16.1(86)	4.5(90)	-2.3(70)	18(15)	49(18)	b	-41(18)
300–400	1	27.9(90)	14.9(76)	3.1(79)	46(14)	b	33(26)	123(26)
400–500	1	20.0(50)	11.8(49)	1.6(46)	33(8)	b	129(19)	39(19)
500–600	1	20.0(31)	11.9(36)	7.8(38)	40(6)	b	130(37)	40(37)
600–700	1	16.6(40)	9.5(54)	4.4(49)	31(9)	b	120(40)	30(40)
700–800	1	26.6(74)	7.8(65)	0.1(76)	34(13)	b	134(40)	44(40)
24–400	2	23.9(15)	13.6(20)	-1.4(25)	36(4)	b	143(7)	53(7)
400–700	2	18.6(5)	8.2(5)	3.1(9)	30(1)	b	121(5)	31(5)
700–850	2	15.5(10)	7.6(18)	4.7(10)	28(2)	b	8(17)	98(17)
850–1000	2	22.8(10)	11.6(30)	6.3(39)	41(5)	b	84(22)	-6(22)
25–325†	3	17.2(5)	9.2(8)	4.3(13)	31(1)	b	138(6)	48(6)
325–625	3	17.8(15)	10.6(13)	2.7(18)	31(2)	b	142(6)	52(6)
625–825	3	21.1(23)	11.5(14)	6.5(24)	39(4)	b	8(17)	98(17)
Weighted mean††		18.5(22)	8.9(14)	3.7(20)	31(3)			

*References: (1) This study, (2) Cameron et al. (1973), (3) Deganello (1973).

**One of the principal axes is constrained to be parallel to *b*. The angles for the other principal axes are measured from *c* toward *a* in (010).

†The value of b at room temperature was taken as 8.924 Å (Deganello, pers. comm.).

"built into" the equations. This observation, however, is based on the single result obtained here.

Conclusion

The results of the last two sections indicate that the method of calculating thermal expansion coefficient of cubic crystals introduced by Owen, Roberts, Stokes, Wilson and others at the beginning of this century can be successfully extended to those crystal systems of lower symmetry. This approach appears to be superior to finite differencing methods in at least two respects:

1) The smoothing of the data inherent in the obtaining of the regression equations eliminates the rapid fluctuations in the values obtained for successive temperature intervals in finite differencing approaches (see Table 3-11). and

2) It is easily possible to easily obtain the best value for a thermal expansion coefficient at any desired temperature.

The disadvantages of the method are:

1) It is more difficult to use because regression equations must first be obtained using weighted least squares.

2) It is unsuitable for those situations where the cell parameters do not vary continuously with temperature and

3) The thermal expansion coefficients will not approach zero as $T \rightarrow 0$ if, as was done here, the cell parameters are expressed as a power series in the temperature.

CHAPTER II

A REFINEMENT OF THE CRYSTAL STRUCTURES OF THE SYNTHETIC CLINOPYROXENES $CaCoSi_2O_6$ AND $CaNiSi_2O_6$

The crystal structures of the synthetic clinopyroxenes $CaCoSi_2O_6$ and $CaNiSi_2O_6$ have been refined to final R-factors of .051 and .077 respectively. As expected, both compounds belong to the space group C2/c. All bond lengths and angles compare well with those previously found in structures of this type.

Although the basic structure of the clinopyroxenes was determined over 45 years ago by Warren and Bragg (1928), very few structural details of these compounds were known before 1959. Since that time, however, a large number of modern refinements have been carried out. Two of the most extensive studies of this type are the eight refinements by Clark, Appleman, and Papike (1969) and the recent high temperature work of Cameron, Sueno, Prewitt, and Papike (1973). In this study we have refined the structures of the two synthetic clinopyroxenes $CaNiSi_2O_6$ and $CaCoSi_2O_6$.

Experimental Data

Cobalt diopside ($CaCoSi_2O_6$), which is bluish in color, was synthesized from a mix prepared from reagent grade $CaCO_3$, $CoCO_3$, and SiO_2 glass. Approximately 50 mg. of the mix was loaded into a Pt capsule which was slightly crimped and then suspended in a vertical Pt-wound furnace. The temperature was raised to 1290°C over a period of 6 hours, cooled to 1035°C at a constant rate of approximately 1°C/min., and then

quenched to room temperature. This procedure yielded a hard, polycrystalline mass from which a single crystal was selected after crushing.

A portion of the charge was ground and unit cell parameters were determined from a least squares refinement (Evans *et al.*, 1963) of x-ray powder diffraction data using synthetic spinel ($MgAl_2O_4$ with a_o = 8.0831 Å) as an internal standard. Peaks were located at the midpoint of the interval corresponding to 2/3's peak height on 4 scans (2 oscillations) at 0.25° 2θ/minute on diffraction patterns obtained using a graphite monochromator-equipped Norelco diffractometer (CuKα radiation). The results (Table I, column a) are in good agreement with those subsequently obtained (column b) from the crystal fragment used in the structure refinement.

The crystal fragment used in the refinement was a cylinder approximately 0.05 mm. in diameter and 0.10 mm. long. Crystal orientation and lattice parameters were determined by a least-squares fitting of 22 hand centered reflections using a modification of B-101 (Gvildys, 1966). Intensity data were collected on a Picker card-controlled four-circle diffractometer using Nb-filtered MoKα radiation. Data reduction was carried out using program ACACA (Guggenberger and Prewitt, 1967). Due to the small sample size ($\mu r_{max} \simeq 0.7$ and $\mu r_{min} \simeq 0.3$), no absorption correction was made during data reduction. Weights for use in subsequent least-squares refinement were computed as

$$\omega = 1/\sigma(F_o) \quad \text{where} \tag{2-1}$$

$$\sigma(F_o^2) = [\sigma^2(I) + (kI^2)]^{1/2} \quad \text{and} \tag{2-2}$$

$$\sigma(F_o) = 1/2F_o\sigma(F_o^2) \tag{2-3}$$

During later stages of refinement, the intensity dependent term (kI) was adjusted to make $|F - F_o|/\sigma(F_o)$ independent of F_o. The final value

of k was 0.035. Full matrix least squares refinement using the Busing, Martin, and Levy (1962) program ORFLS converged with the following residuals:

$$(2\text{-}4)\quad R(F) = \Sigma(F_o - F_c)/\Sigma F_o = .051\ ,$$

$$(2\text{-}5)\quad WR(F) = \Sigma W(F_o - F_c)^2/\Sigma W F_o^2 = .052$$

for 627 reflections having $F_o^2 > \sigma(F_o^2)$.

Nickel diopside ($CaNiSi_2O_6$), synthesized by the procedure of Higgins and Gilbert (1973), was light green in color. Cell parameters from the previous preparation and from a least-squares fitting of 28 hand centered reflections using B-101 are given in Table I. The crystal used in data acquisition was rod-shaped and had dimensions of 0.12 mm. (diameter) by 0.20 mm. (length). A total of 1222 reflections were measured (Nb-filtered MoKα radiation) of which 1173 observations having $F_o^2 > \sigma(F_o^2)$ were used in least-squares refinement. Corrections for absorption and path lengths for subsequent extinction corrections were computed using program DTALIB (Brown, 1971). Final residuals obtained from refinement for $CaNiSi_2O_6$ (weights determined as with $CaCoSi_2O_6$, final value of k = 0.035) are:

$$(2\text{-}6)\quad R(F) = 0.077,$$

$$(2\text{-}7)\quad WR(F) = 0.071.$$

An isotropic extinction parameter was allowed to vary during the final stages of refinement and converged to a value of

$$(2\text{-}8)\quad g = 8.6(27) \times 10^{-6}.$$

Approximately 40 reflections were significantly affected by extinction (greater than 3%). Bond distances, angles, and standard deviations for

both structures ($CaCoSi_2O_6$ and $CaNiSi_2O_6$) were obtained using ORFFE3, the Johnson and Thiessen (1971) modification of Busing, Martin, and Levy's (1964) program ORFFE. The results are given in Tables II through VII. The nomenclature used in these tables is that suggested by Burnham, Clark, Papike, and Prewitt (1967).

Discussion

The general features of the clinopyroxene structure are too well known to warrant discussion here. Therefore our remarks will be confined to a discussion of some structural details.

As is well known both M1 and M2 affect the β angle in clinopyroxenes with M2 exerting the dominant influence and M1 a small perturbing effect. The value of β for calcium clinopyroxenes is approximately 105.5°. The values of 105.40 for $CaCoSi_2O_6$ and 105.92 for $CaNiSi_2O_6$ are consistent with this observation. As expected the M2 site is eight-coordinated with six nearest neighbors and two at a slightly larger distance. The observation that structures with a large cation in the M2 site (calcium in this case) have C2/c symmetry is again confirmed. There is further evidence that the amount of kinking of the chain, ∢03A2-03A1-03A2, is characteristic of the cation in the M2 site. This angle is 164.79 in $CaCoSi_2O_6$ and 165.11 in $CaNiSi_2O_6$ as compared to an average value of 165.08 for $CaMnSi_2O_6$ and $CaMgSi_2O_6$. The M1 octahedra are, as expected, fairly regular.

Certain features of the silicate chain are constant in clinopyroxenes. For example, the Si-O2 bond length has been observed to be the shortest bond of the Si-O tetrahedron with lengths between 1.585 Å and 1.598 Å

and with a mean of 1.598 Å for the eight clinopyroxenes studied by Clark, Appleman and Papike (1960). This observation is verified here with Si-O2 equal to 1.590 for $CaCoSi_2O_6$ and 1.586 for $CaNiSi_2O_6$. The O1-Si-O2 angle has always been observed to be the largest angle of the tetrahedra. This is also the case here (∢O1-Si-O2 equals 117.28 for $CaCoSi_2O_6$ and 117.53 for $CaNiSi_2O_6$). The largest oxygen-oxygen separation of the tetrahedron is O1-O2 as expected (2.723 for $CaCoSi_2O_6$ and 2.730 for $CaNiSi_2O_6$).

In addition the M1-O2 bond has always been observed to be the shortest bond of the octahedron. This is also the case here. (M1-O2 is 2.068 for $CaCoSi_2O_6$ and 2.060 for $CaNiSi_2O_6$.) Note that these constant features all involve O2 which has a charge imbalance.

The thermal vibration parameters are small and not highly anisotropic (see Tables VI and VII). It has been proposed (Clark, Appleman and Papike, 1969) that silicon and oxygens in end-member clinopyroxenes have isotropic temperature factors of about 0.3 ± 0.1 Å^2 and 0.4 ± 0.1 Å^2, respectively. Our results tend to confirm this statement although our temperature factors tend to be slightly higher than these proposed values. The tendency of O2 (the only oxygen in the structure which is coordinated by three cations instead of four) to have a slightly larger thermal vibration is also observed here.

Table 2-1. Single Crystal Data for the Clinopyroxenes $CaCoSi_2O_6$ and $CaNiSi_2O_6$†

	$CaCoSi_2O_6$[a]	$CaCoSi_2O_6$[b]	$CaNiSi_2O_6$[c]	$CaNiSi_2O_6$[d]
a(Å)	9.800(2)	9.7971(13)	9.733(6)	9.737(2)
b(Å)	8.954(2)	8.9541(12)	8.896(5)	8.899(2)
c(Å)	5.257(5)	5.2431(7)	5.230(12)	5.231(1)
β(Å)	105.43 (5)	105.40(2)	105.82(12)	105.92(1)
Cell volume ($Å^3$)	444.67	443.43	435.68	435.88
Space group	---	C2/c	---	C2/c
Calculated density	3.751	3.761	3.825	3.824
Z	4	4	4	4
Source	Synthetic	Synthetic	Synthetic	Synthetic

[a] Popp (this study)

[c] Higgins and Gilbert (1973)

[b,d] Schlenker, Popp, Ross, and Gibbs (this study)

† values in parenthesis are standard deviations

Table 2-2. Atomic Parameters for $CaCoSi_2O_6$ and $CaNiSi_2O_6$[†]

Atom	Parameter	$CaCoSi_2O_6$	$CaNiSi_2O_6$
SiA1	x	0.2874(1)	0.2871(1)
	y	0.0926(1)	0.0929(1)
	z	0.2306(2)	0.2273(2)
	<μ>	0.1237(40)	0.1198(30)
O1A1	x	0.1180(3)	0.1157(4)
	y	0.0884(3)	0.0861(3)
	z	0.1470(6)	0.1429(5)
	<μ>	0.1430(86)	0.1391(61)
O2A1	x	0.3609(3)	0.3601(3)
	y	0.2490(4)	0.2505(3)
	z	0.3207(7)	0.3189(6)
	<μ>	0.1666(84)	0.1642(66)
O3A1	x	0.3503(3)	0.3517(3)
	y	0.0196(3)	0.0192(3)
	z	0.9938(6)	0.9916(5)
	<μ>	0.1550(85)	0.1435(81)
M1 (Co or Ni)	x	0.0000	0.0000
	y	0.90761(9)	0.9090(1)
	z	0.2500	0.2500
	<μ>	0.1253(29)	0.0943(25)
M2 (Ca)	x	0.0000	0.0000
	y	0.2990(1)	0.2978(1)
	z	0.2500	0.2500
	<μ>	0.1540(34)	0.1541(25)

[†] Values in parentheses are standard deviations.

Table 2-3. Bond Lengths (Å) and Some Angles (°) for the M2 Cations in $CaCoSi_2O_6$ and $CaNiSi_2O_6$[†]

Atoms (Oxygens of M2-O)	$CaCoSi_2O_6$	$CaNiSi_2O_6$
O1A1, O1B1	2.349(3)	2.341(3)
O2C2, O2D2	2.340(3)	2.332(3)
O3C1, O3D1	2.609(3)	2.593(3)
O3C2, O3D2	2.724(3)	2.708(3)
Mean of 6	2.433	2.422
Mean of 8	2.506	2.494
Angles		
Si-O1A1-M2	117.15(16)	115.84(13)
Si-O2C2-M2	103.10(16)	102.94(13)
Si-O3C1-M2	100.55(14)	100.54(12)
Si-O3D1-M2	90.26(13)	90.41(12)
Si-O3C2-M2	118.02(15)	117.84(14)
Si-O3D2-M2	95.56(14)	95.73(12)

[†] Values in parentheses are standard deviations.

Table 2-4. Bond Lengths (Å) and Angles (°) for the M1 Octahedra of $CaCoSi_2O_6$ and $CaNiSi_2O_6$†

Atoms	$CaCoSi_2O_6$	$CaNiSi_2O_6$
M1-O1A1,B1	2.140(3)	2.101(3)
-O1A2,B2	2.097(3)	2.055(3)
-O2C1,D1	2.068(3)	2.060(3)
Mean of 6	2.102	2.072
O1A1-O1B1	2.799(6)	2.778(7)
O2C1-O2D1	3.007(6)	3.004(7)
(2)O1A1-O2C1	3.047(4)	2.998(3)
(2)O1A1-O1A2	3.062(3)	3.031(2)
(2)O1A2-O2C1	2.907(4)	2.884(4)
(2)O1A2-O2D1	3.016(4)	2.978(4)
(2)O1A1-O1B2	2.888(6)	2.794(5)
Mean of 12	2.970	2.929
M1-M1(1)	3.100(1)	3.077(1)
M1-S1A1	3.290(1)	3.269(1)
M1-S1A2	3.241(1)	3.197(1)
O-M1-O Angles		
O1A2,O1B2	178.03(17)	177.55(14)
(2)O1A1,O2D1	172.00(12)	171.49(10)
O1A1,O1B1	81.71(16)	82.78(18)
O2C1,O2D1	93.27(12)	93.58(18)
(2)O1A1,O2C1	92.77(12)	92.20(13)
(2)O1A1,O1A2	92.57(12)	93.67(10)
(2)O1A1,O1B2	85.43(12)	84.49(11)
(2)O1A2,O2C1	88.54(12)	88.99(11)
(2)O1A2,O2D1	92.82(12)	92.68(12)
Si-O1A1-M1	122.64(18)	123.20(14)
Si-O1A2-M1	121.99(17)	121.14(20)
Si-O2C1-M1	145.13(20)	144.65(21)

†Values in parentheses are standard deviations.

Table 2-5. Bond Lengths (Å) and Angles (°) for the Clinopyroxenes $CaCoSi_2O_6$ and $CaNiSi_2O_6$[†]

Atoms	$CaCoSi_2O_6$	$CaNiSi_2O_6$
Si-O1	1.599(3)	1.606(3)
Si-O2	1.590(3)	1.586(3)
<Si-O(nbr)>	1.594	1.596
Si-O3A1	1.661(3)	1.665(3)
Si-O3A2	1.686(3)	1.681(3)
<Si-O(br)>	1.674	1.673
<Si-O>	1.634	1.634
O1-O2	2.723(4)	2.730(4)
O1-O3A1	2.680(4)	2.681(4)
O1-O3A2	2.688(4)	2.694(4)
O2-O3A1	2.660(4)	2.664(4)
O2-O3A2	2.582(4)	2.573(4)
O3-O3A2	2.645(1)	2.638(1)
<O-O>	2.663	2.663
Si-SiA2	2.101(1)	
O1-Si-O2	117.28(16)	117.53(16)
O1-Si-O3A1	110.56(16)	110.91(15)
O1-Si-O3A2	109.78(16)	109.27(15)
O2-Si-O3A1	109.84(16)	110.06(18)
O2-Si-O3A2	104.01(16)	103.91(14)
O3A1-Si-O3A2	104.43(11)	104.08(11)
<O-Si-O>	109.32	109.29
Si-O3-SiA2	135.88(19)	135.30(20)
O3A2-O3A1-O3A2	164.79(26)	165.11(24)

[†] Values in parentheses are standard deviations.

Table 2-6

Magnitudes and Orientations of the Thermal Ellipsoids of $CaCoSi_2O_6$†

Atom	Axis	rms Displacement	Angle with Respect to +a	+b	+c
Ca	r_1	.0726(36)	077.2(6.8)	090.0(0.0)	028.2(6.8)
	r_2	.0957(38)	167.2(6.8)	090.0(0.0)	061.8(6.8)
	r_3	.0963(28)	090.0(0.0)	000.0(0.0)	090.0(0.0)
Co	r_1	.0602(45)	034.3(7.4)	090.0(0.0)	139.7(7.4)
	r_2	.0764(21)	124.3(7.4)	090.0(0.0)	130.3(7.4)
	r_3	.0789(24)	090.0(0.0)	000.0(0.0)	090.0(0.0)
Si	r_1	.0542(66)	022.5(8.7)	089.9(7.0)	127.9(8.7)
	r_2	.0747(30)	112.5(8.7)	091.3(18.2)	142.1(8.7)
	r_3	.0824(33)	90.6(8.5)	001.3(17.9)	091.0(15.7)
O1	r_1	.0654(135)	18.4(14.8)	096.8(19.3)	122.3(15.5)
	r_2	.0879(78)	89.9(32.9)	157.9(71.5)	068.7(61.3)
	r_3	.0919(69)	71.6(14.9)	69.0(75.5)	040.2(44.7)
O2	r_1	.0799(119)	64.1(14.1)	50.3(19.0)	136.6(18.5)
	r_2	.1000(78)	92.9(41.6)	133.2(31.3)	133.4(19.0)
	r_3	.1067(69)	26.1(14.1)	110.5(34.3)	088.9(36.3)
O3	r_1	.0549(183)	40.8(10.8)	098.4(7.8)	144.6(10.6)
	r_2	.0916(63)	130.4(10.9)	92.5(13.4)	124.1(10.9)
	r_3	.1124(66)	85.2(10.5)	008.8(8.4)	098.4(10.0)

† Values in parentheses are standard deviations.

Table 2-7

Magnitudes and Orientations of the Thermal Ellipsoids of $CaNiSi_2O_6$†

Atom	Axis	rms Displacement	Angle with respect to +a	+b	+c
Ca	r_1	.0822(21)	111.8(6.5)	090.0(0.0)	142.3(6.5)
	r_2	.0857(19)	090.0(0.0)	180.0(0.0)	090.0(0.0)
	r_3	.0983(33)	158.2(6.5)	090.0(0.0)	052.3(6.5)
Ni	r_1	.0415(49)	154.1(4.6)	090.0(0.0)	048.2(4.6)
	r_2	.0541(19)	090.0(0.0)	180.0(0.0)	090.0(0.0)
	r_3	.0651(17)	115.9(4.6)	090.0(0.0)	138.2(4.6)
Si	r_1	.0545(57)	157.4(4.6)	097.8(13.5)	053.2(6.8)
	r_2	.0669(25)	089.2(12.9)	161.4(8.3)	108.1(10.3)
	r_3	.0831(21)	112.6(4.6)	073.2(5.9)	137.6(5.0)
O1	r_1	.0650(93)	156.7(15.7)	113.1(15.3)	072.1(13.5)
	r_2	.0828(53)	068.9(15.2)	140.0(26.1)	065.6(24.3)
	r_3	.0909(55)	099.5(16.6)	059.4(23.8)	031.0(21.8)
O2	r_1	.0580(113)	051.2(6.1)	039.5(7.0)	106.3(8.1)
	r_2	.0999(65)	108.4(10.6)	067.5(12.2)	022.9(13.3)
	r_3	.1167(49)	135.5(8.6)	059.5(6.8)	105.6(14.2)
O3	r_1	.0403(173)	150.7(5.8)	087.0(8.1)	045.0(5.2)
	r_2	.0840(80)	109.4(8.9)	142.5(11.3)	113.6(10.3)
	r_3	.1091(48)	111.1(5.7)	052.6(11.3)	125.7(6.8)

† Values in parentheses are standard deviations.

REFERENCES

Amorós, J. L. and M. Canut de Amorós (1968) Molecular Crystals; their transforms and diffuse scattering. John Wiley and Sons, Inc., New York.

Auld, B. A. (1973) Acoustic Fields and Waves in Solids, Volume I. John Wiley and Sons, Inc., New York.

Austin, J. B. (1952) Thermal expansion of nonmetallic crystals. J. Am. Ceramic Soc. 35, 243-253.

Baily, A. C. and B. Yates (1970) Anisotropic thermal expansion of graphite at low temperatures. J. Appl. Phys. 41, 5088-5090.

Barr, A. J. and J. H. Goodnight (1972) SAS Statistical Analysis System. Department of Statistics, North Carolina State University, Raleigh, North Carolina.

Barron, T. H. K. (1970) Vibrational effects in the thermal expansion of noncubic solids. J. Appl. Phys. 41, 5044-5050.

Bhagavantam, S. (1966) Crystal Symmetry and Physical Properties. Academic Press, London, England.

Bollmann, W. (1970) Crystal Defects and Crystalline Interfaces. Springer-Verlag, New York.

Born, Max (1963) Reminiscences of my work on the dynamics of crystal lattices. Proceedings of the International Conference on Lattice Dynamics. Pergamon Press, New York.

Born, Max and Kun Huang (1968) Dynamical Theory of Crystal Lattices. Oxford at the Clarendon Press, London, England.

Bouvaist, J. and D. Weigel (1970) Seisquioxyde de plomb, Pb_2O_3 II. Étude de la dilation thermique d'un monocristal. Acta Crystallogr. A26, 510-514.

Brown, F. C. (1967) The Physics of Solids: Ionic Crystals, Lattice Vibrations, and Imperfections. W. A. Benjamin Inc., New York, New York.

Brown, G. M. (1971) Oak Ridge National Laboratory, Oak Ridge, Tennessee. Private communication.

Burnham, Charles W., Joan R. Clark, J. J. Papike, and G. T. Prewitt (1967) A proposed crystallographic nomenclature for clinopyroxene structures. Z. Kristallogr. 125, 109-119.

Busing, W. R., K. O. Martin, and H. A. Levy (1962) A fortran crystallographic least squares program. U. S. Atomic Energy Commission Report ORNL-TM-305.

Busing, W. R., K. D. Martin, and H. A. Levy (1964) A fortran crystallographic function and error program ORNL-TM-306. Oak Ridge National Laboratory. Oak Ridge, Tennessee.

Cady, W. G. (1946) Piezoelectricity. McGraw-Hill Book Company, New York.

Cameron, Maryellen, Shigeho Sueno, C. T. Prewitt and J. J. Papike (1973) High-temperature crystal chemistry of acmite, diopside, hedenbergite, jadeite, spodumene, and ureyite. Am. Mineral. 58, 594-618.

Clark, J. R., D. E. Appleman, and J. J. Papike (1969) Crystal-chemical characterization of clinopyroxenes based on eight new structure refinements. Mineral. Soc. Amer. Spec. Pap. 2, 31-50.

Connell, Jr., L. F. and H. C. Martin, Jr. (1951) Concerning reported discrepancies between x-ray and macroscopic measurements of thermal expansion of some alkali halides. Acta. Crystallogr. 4, 75.

Daniels, W. B. (1963) The pressure derivatives of elastic constants: microscopic Grüneisen parameters. Proceedings of the International Conference on Lattice dynamics. Pergamon Press, New York.

Deganello, Sergio (1973) The thermal expansion of a diopside. Z. Kristallogr. 137, 127-131.

Deganello, Sergio (1973) Atomic vibrations and thermal expansion of some silicates at high temperatures. Z. Crystallogr. 139, 297-315.

Deshpande, V. T., and V. M. Mudholker (1961) On the evaluation of the coefficients of thermal expansion from x-ray data. Ind. J. Phys. 35, 434-436.

Evans, H. T., D. E. Appleman, and D. S. Handwerker (1963) The least squares refinement of crystal unit cells with powder diffraction data by an automated computer indexing method. Prog. Abstr. Amer. Cryst. Assoc. Meet., Cambridge, Mass.

Finger, L. W. and Y. Ohashi (1976) The thermal expansion of diopside to 800°C, and a refinement of the crystal structure at 700°C. Am. Mineral. 61, 303-310.

Fischer, G. (197) The crystal lattice thermal expansion of cordierite ($2MgO \cdot 2Al_2O_3 \cdot 5SiO_2$). Corning Research Laboratories, Corning, New York. (unpublished manuscript)

Frederick, Daniel, and Sun Tien Chang (1965) Continuum Mechanics. Allyn and Bacon, Boston.

Ghatak, A. K. and L. S. Kothari (1972) An Introduction to Lattice Dynamics. Addison-Wesley Publishing Company, Inc. London, England.

Gott, A. (1942) Thermische Gitterdehnung und Makroskopische Ausdehnung von Alkalihalogenidschmelzflußkristallen. Annal. der Phy- 41 520-536.

Guggenberger, L. and C. T. Prewitt (1967), Program ACACA. E. I. DuPont de Nemours and Company, Wilmington, Delaware.

Gvildys J. (1966) Orientation angles setting generation program, Applied mathematics program library B-101 Argonne National Laboratory, Argonne, Illinois.

Higgins, B. B. and M. C. Gilbert (1973) High pressure stability of nickel diopside. Am. Sci., Cooper Vol. 273-a, 511-521.

Kelly, K. K. (1960) Contributions to the Data on Theoretical Metallurgy XIII. High-Temperature Heat-Content, Heat-Capacity, and Entropy Data for the Elements and Inorganic Compounds. Bulletin 584 United States Government Printing Office, Washington D.C.

Kempter, Charles P., and Reed O. Elliott (1959) Thermal expansion of <UN>, $<UO_2>$, $<UO_2 \cdot ThO_2>$, and $<ThO_2>$. J. Chem. Phys. 30, 1524-1526.

Küppers, H. (1974) Anisotropy of thermal expansion of ammonium and potassium oxylates. Z. Crystallogr. 140, 393-398.

Levy, Robert A. (1968) Principles of Solid State Physics. Academic Press, New York.

Mase, George E. (1970) Theory and Problems of Continuum Mechanics. McGraw Hill Book Co., New York.

McMillan, Jaun A. (1968) Lectures on Point Symmetry: Symmetry and Properties of crystals. NSF-AEC Short Course in "Symmetry and Group Theory." Solid State Science Division. Argonne National Laboratory. Argonne, Illinois.

Megaw, H. (1973) Crystal Structures: A Working Approach. W. B. Saunders Company, Philadelphia, Pennsylvania.

Morosin, B. (1972) Structure and thermal expansion of beryl. Acta Crystallogr. B28. 1899-1903.

Munn, R. W. (1970) On the thermal expansion of indium. Acta. Crystallogr. A26, 161.

Nolan, J. and A. D. Edgar (1963) An x-ray investigation of synthetic pyroxenes in the system acmite-diopside-water at 1000 pg/cm^2 water vapor pressure. Mineral. Mag. 33. 625-634.

Nye, J. F. (1960) Physical Properties of Crystals. Oxford University Press, London, England.

Ohashi, Y. and Charles W. Burnham (1973) Clinopyroxene lattice deformations: The roles of chemical substition and temperature. Am. Mineral. 58, 843-849.

Owen, E. A. and T. LL. Richards (1936) XXV. On the thermal expansion of beryllium.Phil. Mag. 22, 304-311.

Owen, E. A., and E. W. Roberts (1936) XXIV. The thermal expansion of the crystal lattices of cadmium, osmium, and ruthenium. Phil. Mag. 22, 290-311.

Pathak, P. D. and N. V. Panda (1960a) Thermal expansion of caesium iodide by X-ray diffraction and the Grüneisen's parameters. Current Science. 29, 14.

Pathak, P. D. and N. V. Panda (1960b) Thermal expansion of some alkali halides by x-ray diffraction. Ind. J. Sci. 34 No. 9, 416-423.

Pathak, P. D., and N. G. Vasavada (1970) Thermal expansion of NaCl, KCl, and CsBr by X-ray diffraction and the law of corresponding states. Acta. Crystallogr. A26, 655-658.

Pillars, W. W. and D. R. Peacor (1973) The crystal structure of beta eucryptite as a function of temperature. Am. Mineral. 58, 681-690.

Rutstein, Martin S. and Richard A. Yund, (1969) Unit cell parameters of synthetic diopside-hedenbergite solid solutions. Am. Mineral. 54, 238-245.

Schlenker, J. L., M. B. Boisen, Jr., and G. V. Gibbs (1975) Thermal expansion coefficients for monoclinic crystals: A phenomenological approach. Am. Mineral. 60, 828-833.

Simmons, Gene and Herbert Wang (1971) Single Crystal Elastic Constants and Calculated Aggregate Properties: A handbook. The M.I.T. Press. Cambridge, Massachusetts.

Slater, J. C. (1939) Introduction to Chemical Physics. McGraw-Hill, New York.

Smith, Charles S. (1958) Macroscopic Symmetry and Properties of Crystals. Solid State Physics Vol. 6 Academic Press, New York.

Stokes, A. R. and A. J. C. Wilson (1941) The thermal expansion of lead from 0°C to 320°C. Proc. Phys. Soc. 53, 658-662.

Warren, B. and W. L. Bragg (1928) The structure of diopside $CaMgSi_2O_6$. Z. Kristallogr. 69, 168-173.

Warner, Richard D., and Luth, William C. (1974) The diopside-orthoenstatite two-phase region in the system $CaMgSi_2O_6$-$Mg_2Si_2O_6$. Am. Mineral. 59, 98-109.

Wallace, D. C. (1972) Thermodynamics of Crystals. John Wiley and Sons, Inc., New York.

Wayman, C. M. (1964) Introduction to the Crystallography of Martensitic Transformations. The Macmillan Company, New York.

Whittier, John Greenleaf (1927) The Complete Poetical Works of John Greenleaf Whittier. Houghton Mifflin Company, The Riverside Press, Cambridge.

Willaime, C., W. L. Brown, and M. C. Perucaud (1974) On the orientation of the thermal and compositional strain ellipsoids in feldspars. Am. Mineral. 59, 457-464.

Willis, B. T. M. and A. W. Pryor (1975) Thermal Vibrations in Crystallography. Cambridge University Press, New York..

Wilson, A. J. C. (1940) Thermal expansion of aluminum from 0°C to 650°C. Proc. Phy. Soc. (London) 53, 235-244.

Winch, Ralph P. (1957) Electricity and Magnetism. Prentice-Hall, Inc. Englewood Cliffs, N. J.

Wooster, W. A. (1973) Tensors and Group theory for the Physical Properties of Crystals. The Clarendon Press, London, England.

Yoon, H. S. and R. E. Newnham (1973) The elastic properties of beryl. Acta. Crystallogr. A29, 507-509.

Zhdanov, C. S. (1965) Crystal Physics.Academic Press, New York.

APPENDIX A

A SHORT INTRODUCTION TO THE CONCEPT OF STRESS

"Take from our souls the strain and stress..."
-John Greenleaf Whittier

Unless one is familiar with the concept of stress it is difficult if not impossible to understand such physical phenomena as piezo- and pyroelectricity, elasticity and so forth. Therefore, the stress concept is of central importance. Stress has the dimensions of force per unit area, newtons/m^2, and the simplest example is that of hydrostatic pressure where a force of P newtons/m^2 acts normally to the surface under consideration. When your hand presses against a table you are exerting a stress; however, the resulting stress vector is not normal to the surface. The concepts of strain and stress belong to the science of continuum mechanics. The basic postulate of this science is the Cauchy Stress Principle. This may be stated as follows:

Cauchy Stress Principle: When a body is acted upon by external forces, the state of stress at every point (X_1, X_2, X_3), in the body may be defined by a second rank symmetric tensor called a stress tensor, σ_{ij}. Given any surface in the body it is possible to construct a unit normal $\hat{n} = n_1\hat{i} + n_2\hat{j} + n_3\hat{k}$ to the surface such that the force per unit area acting on that surface is defined by the stress vector

$$(A\text{-}1) \quad \vec{t}^{\hat{n}} = t_1^{\hat{n}}\hat{i} + t_2^{\hat{n}}\hat{j} + t_3^{\hat{n}}\hat{k} \ ,$$

where the components of $\vec{t}^{\hat{n}}$ are given by the relation

$$(A\text{-}2) \quad t_i^{\hat{n}} = n_j\sigma_{ji} \ .$$

This principle will now be examined in detail. Consider the potato-shaped lump of matter in Figure A-1. It is possible to draw a unit vector $\hat{n}$ perpendicular to each point on its surface. In fact, it is possible to construct unit vectors normal to any surface passing through the interior of the body as well. These normals constitute the $\hat{n}$ referred to in the Cauchy Stress Principle, which states that a stress tensor

$$[\sigma_{ij}] = \begin{bmatrix} \sigma_{11} & \sigma_{12} & \sigma_{13} \\ \sigma_{21} & \sigma_{22} & \sigma_{23} \\ \sigma_{31} & \sigma_{32} & \sigma_{33} \end{bmatrix}$$

is defined at each point in the material body. The σ_{ij} may be constants; for example both

$$\begin{bmatrix} 7 & -5 & 0 \\ -5 & 3 & 1 \\ 0 & 1 & 2 \end{bmatrix} \quad \text{and} \quad \begin{bmatrix} 3X_1X_2 & 5X_2^2 & 0 \\ 5X_2^2 & 0 & 2X_3 \\ 0 & 2X_3 & 0 \end{bmatrix}$$

are perfectly acceptable as stress tensors. Note that the stress tensor is symmetric, i.e. $\sigma_{ij} = \sigma_{ji}$.

Finally the Cauchy Stress Principle permits the calculation of the force per unit area acting on any surface at a point within the body. The components of this force are simply

$$(A\text{-}3) \quad t_i^{\hat{n}} = n_j \sigma_{ji} \ .$$

Several examples will now be described to clarify the principles which have been discussed. Consider the plane (Figure A-2) defined by the equation

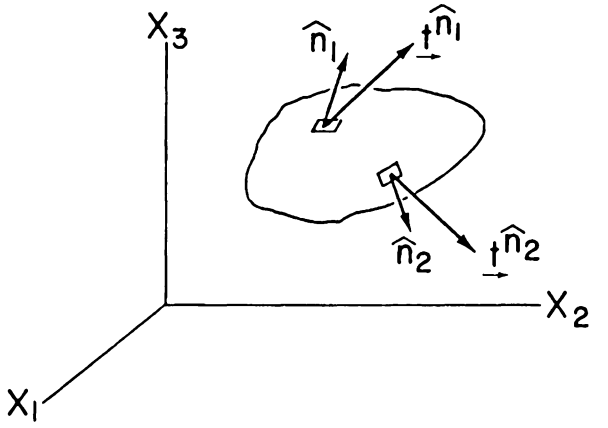

Figure A-1: A material medium of arbitrary shape (see text for discussion).

(A-4) $3X_1 + 6X_2 + 2X_3 = 12$.

We wish to find the unit normal to this flat surface. From (A-4) we obtain

(A-5) $3X_1 + 6X_2 + 2X_3 - 12 = 0$.

We operate on this with $\underset{\rightarrow}{\nabla} = \partial/\partial X_1\hat{i} + \partial/\partial X_2\hat{j} + \partial/\partial X_3\hat{k}$ to obtain

(A-6) $$\underset{\rightarrow}{\nabla}(3X_1 + 6X_2 + 2X_3 - 12) = (\partial/\partial X_1\hat{i} + \partial/\partial X_2\hat{j} + \partial/\partial X_3\hat{k})(3X_1 + 6X_2 + 2X_3 - 12)$$
$$= 3\hat{i} + 6\hat{j} + 2\hat{k} .$$

The resulting vector is perpendicular to the surface shown in Figure A-2. The normal to any surface can always be found by operating on the equation of that surface with the $\underset{\rightarrow}{\nabla}$ operator. Next we normalize this vector to obtain $\hat{n}$:

(A-7) $(3\hat{i} + 6\hat{j} + 2\hat{k})\cdot(3\hat{i} + 6\hat{j} + 2\hat{k}) = 9 + 36 + 4 = 49$

and

(A-8) $\hat{n} = 3/7\hat{i} + 6/7\hat{j} + 2/7\hat{k}$.

To find the stress vector (i.e., the force per unit area acting on the plane) we use $t_i^{\hat{n}} = n_j\sigma_{ji}$. Therefore

(A-9) $$t_1^{\hat{n}} = n_1\sigma_{11} + n_2\sigma_{21} + n_3\sigma_{31} = (3/7)(7) + (6/7)(-5) + (2/7)(0)$$
$$= -9/7$$

(A-10) $$t_2^{\hat{n}} = n_1\sigma_{12} + n_2\sigma_{22} + n_3\sigma_{32} = (3/7)(-5) + (6/7)(3) + (2/7)(1)$$
$$= 5/7$$

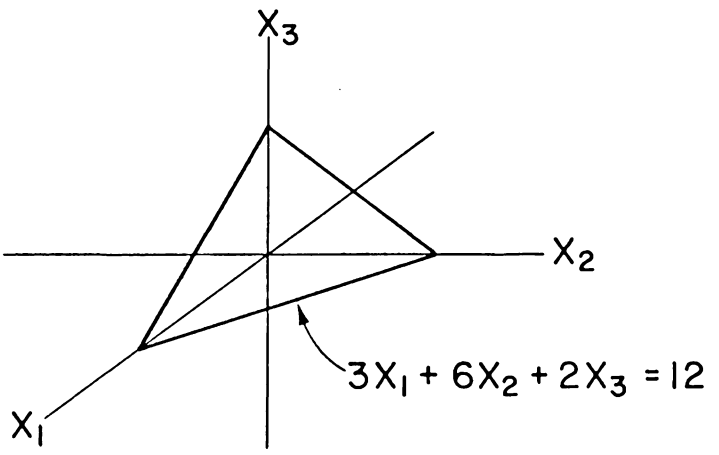

Figure A-2: A flat surface with the equation $3X_1 + 6X_2 + 2X_3 = 12$ (see text for discussion).

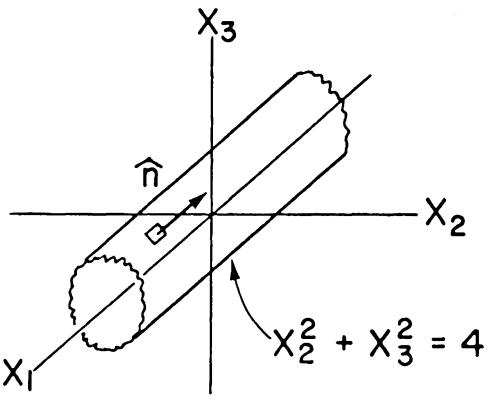

Figure A-3: A cylinder coaxial with the X_1-axis (see text for discussion).

$$(A\text{-}11)\quad t_3^{\hat{n}} = n_1\sigma_{13} + n_2\sigma_{23} + n_3\sigma_{33} = (3/7)(0) + (6/7)(1) + (2/7)(2) = 10/7 \ .$$

Hence, the force acting on this surface is

$$(A\text{-}12)\quad \underset{\sim}{t}^{3/7\hat{i} + 6/7\hat{j} + 2/7\hat{k}} = [-9/7\hat{i} + 5/7\hat{j} + 10/7\hat{k}]\text{newtons/m}^2 \ .$$

Obviously this force is independent of our position on the plane; it is the same everywhere. As a more involved example, we will calculate the stress vector acting at point $(2,1,\sqrt{3})$ on a cylindrical surface whose equation is

$$(A\text{-}13)\quad x_2^2 + x_3^2 = 4 \ .$$

The normal to the surface is

$$(A\text{-}14)\quad \underset{\rightarrow}{\nabla}(X_2^2 + X_3^2 - 4) = 2X_2\hat{j} + 2X_3\hat{k}$$

which, when normalized becomes

$$(A\text{-}15)\quad \hat{n} = X_2\hat{j}/(X_2^2 + X_3^2)^{1/2} + X_3\hat{k}/(X_2^2 + X_3^2)^{1/2} \ .$$

Obviously this is dependent on our position on the surface but at $(2,1,\sqrt{3})$ it becomes

$$(A\text{-}16)\quad \hat{n} = 1/2\hat{j} - \sqrt{3}/2\hat{k} \ .$$

Next we will consider the stress tensor

$$\begin{bmatrix} 3X_1X_2 & 5X_2^2 & 0 \\ 5X_2^2 & 0 & 2X_3 \\ 0 & 2X_3 & 0 \end{bmatrix}$$

at the point $(2,1,\sqrt{3})$; this tensor becomes

$$\begin{bmatrix} 6 & 5 & 0 \\ 5 & 0 & 2\sqrt{3} \\ 0 & 2\sqrt{3} & 0 \end{bmatrix} .$$

The components of $\underset{\sim}{t}^{\hat{n}}$ are calculated exactly as was done previously:

(A-17) $t_1^{\hat{n}} = (0)(6) + (1/2)(5) + (\sqrt{3}/2)(0) = 5/2$

(A-18) $t_2^{\hat{n}} = (0)(5) + (1/2)(0) + (\sqrt{3}/2)(2\sqrt{3}) = 3$

(A-19) $t_3^{\hat{n}} = (0)(0) + (1/2)(2\sqrt{3}) + (\sqrt{3}/2)(0) = \sqrt{3}$.

Therefore the force per unit area acting on the surface at this point is

(A-20) $\underset{\sim}{t}^{\hat{j}/2 + \sqrt{3}/2\hat{k}} = [5/2\hat{i} + 3\hat{j} + \sqrt{3}\hat{k}]\text{newtons/m}^2$.

It is possible that some of the components of the strain tensor are zero. For example, for a hydrostatic pressure, P, the strain tensor is given by

$$\begin{bmatrix} -P & 0 & 0 \\ 0 & -P & 0 \\ 0 & 0 & -P \end{bmatrix} .$$

Let us now see that our procedures give reasonable results in an easily visualized situation. Suppose we have a galena crystal, PbS, bounded by forms {100} and {111} and subjected to a hydrostatic pressure P. Let us calculate the stress vector acting on (100) and (111). Since the normal to (100) is $\hat{i}$, then

(A-21) $t_1^{\hat{i}} = 1\sigma_{11} = -P$

(A-22) $t_2^{\hat{i}} = 1\sigma_{12} = 0$

(A-23) $t_3^{\hat{i}} = 1\sigma_{13} = 0,$

or

(A-24) $\underset{\rightarrow}{t}^{\hat{i}} = [-P\hat{i}]\text{newtons/m}^2$, results.

This tells us there is a force per unit area of P acting in the minus direction, pushing in, on face (100). This is what we expect from a hydrostatic pressure. The normal to face (111) is

(A-25) $\hat{n} = 1/\sqrt{3}(\hat{i} + \hat{j} + \hat{k})$.

Therefore

(A-26) $t_1^{[111]} = 1/\sqrt{3}(\sigma_{11} + \sigma_{12} + \sigma_{13}) = -P/\sqrt{3}$

(A-27) $t_2^{[111]} = 1/\sqrt{3}(\sigma_{12} + \sigma_{22} + \sigma_{23}) = -P/\sqrt{3}$

(A-28) $t_3^{[111]} = 1/\sqrt{3}(\sigma_{13} + \sigma_{23} + \sigma_{33}) = -P/\sqrt{3}$

or

(A-29) $\underset{\rightarrow}{t}^{[111]} = [-(\hat{i} + \hat{j} + \hat{k})P/\sqrt{3}]\text{newtons/m}^2$.

The magnitude of this force is

(A-30) $(\underset{\rightarrow}{t}^{[111]} \cdot \underset{\rightarrow}{t}^{[111]})^{1/2} = -3P/\sqrt{3}\sqrt{3} = -P$.

Thus we see that we have a force of -P newtons/m^2 pushing in perpendicularly on [111]. Again this is what intuition would lead one to expect.

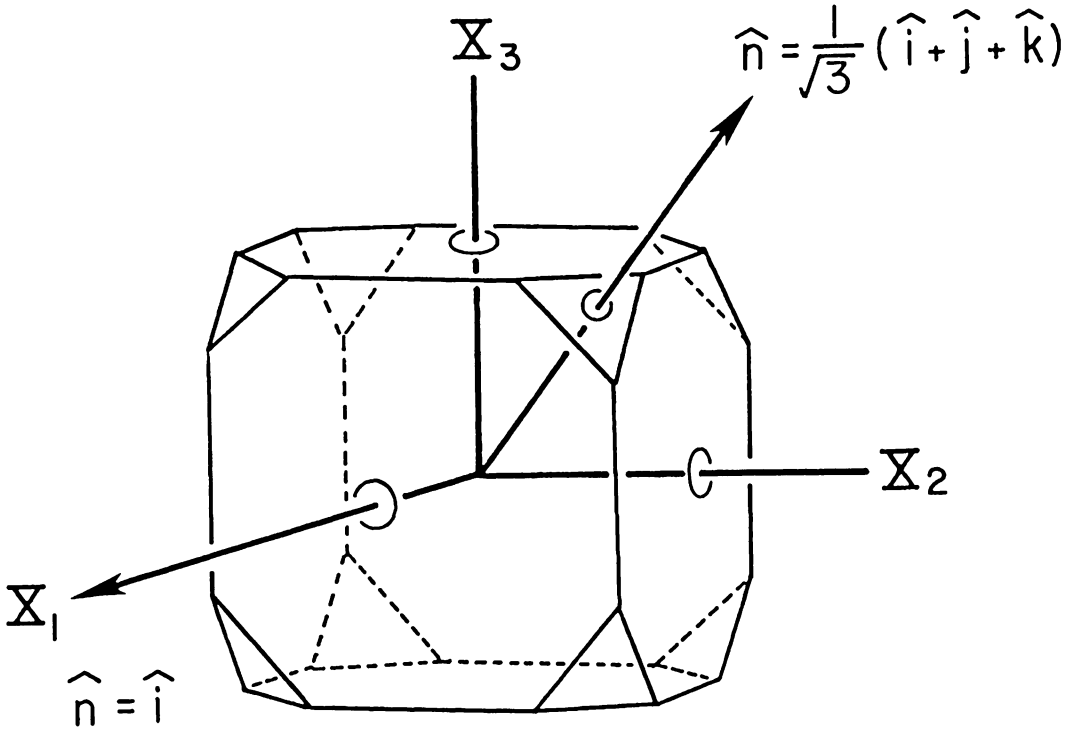

Figure A-4: Galena crystal with cubic, {100}, and octahedral, {111}, forms. The unit normals perpendicular to (100) and (111) are shown (see text for discussion).

APPENDIX B

AN INTRODUCTION TO THE THEORY OF STRAIN

Introduction

Strain, or deformation theory, is a much more difficult subject than stress because of the mathematical approximations used in the formulation of the theory. It is therefore necessary to be very clear and to define terms carefully. In particular, the meaning of the word "point" must be very carefully defined since it can be taken to be a "point" in space or a "point" which is a part of the continuum and which moves in space as the continuum is deformed. It is the fixed (never moving) location in space which will be denoted by the word point here. The expression "material particle" will denote a "point" in the continuum which moves from point to point in space as the continuum is deformed.

The Lagrangian and Eulerian Formulations of a Deformation

Figure B-1 shows a continuum at some time, t = 0, (before deformation) and at a later time, t = t (after a deformation has occurred). The material particle initially at P (at t = 0) has moved to point Q during the deformation. The initial position of this material particle is denoted here by

$$(B\text{-}1) \quad X = X_1\hat{i} + X_2\hat{j} + X_3\hat{k}$$

while the final position is denoted by

$$(B\text{-}2) \quad x = x_1\hat{i} + x_2\hat{j} + x_3\hat{k}$$

It is obvious from the diagram that the displacement of the

material particle initially at P is given by the vector equation

$$(B\text{-}3) \quad \underset{\rightarrow}{u} = u_1\hat{i} + u_2\hat{j} + u_3\hat{k} = \underset{\rightarrow}{x} - \underset{\rightarrow}{X} .$$

This equation can be writtin in component form as

$$(B\text{-}4) \quad u_i = x_i - X_i$$

As a continuum is deformed, the movements of the material particles along certain paths in space can be expressed by equations such as

$$(B\text{-}5) \quad x_i = x_i(X_1,X_2,X_3,t)$$

which give the location at time t of the material particle initially located (at t = 0) at (X_1,X_2,X_3). The coordinates of a material particle before the medium was deformed are called its initial coordinates. Its coordinates after deformation of the continuum are called its final coordinates. Equation (B-5) which gives the final coordinates (x_1,x_2,x_3) as functions of the initial ones (X_1,X_2,X_3), is called the "Lagrangian formulation of the deformation." An inverse formulation, termed the "Eulerian formulation of the deformation," may be written as

$$(B\text{-}6) \quad X_i = X_i(x_1,x_2,x_3,t) .$$

Essentially equation (B-6) tells us where a particle located at (x_1,x_2,x_3) at time t started out from at t = 0.

For example, a possible Lagrangian description of a deformation is

$$(B\text{-}7) \quad x_1 = X_1 + X_2(e^t - 1),$$

$$(B\text{-}8) \quad x_2 = X_1(e^{-t} - 1) + X_2 ,$$

and

$$(B\text{-}9) \quad x_3 = X_3$$

while the corresponding Eulerian description of the same deformation (obtained by solving the previous equations for X_1, X_2, and X_3) is

$$(B\text{-}10) \quad X_1 = [-x_1 + x_2(e^t - 1)]/(1 - e^t - e^{-t}) ,$$

$$(B\text{-}11) \quad X_2 = [x_1(e^{-t} - 1) - x_2]/(1 - e^t - e^{-t}) ,$$

and

$$(B\text{-}12) \quad X_3 = x_3.$$

This example is taken from Mase (1970).

Formulation of the Displacement Field Vector $\underset{\sim}{u}$ in Terms of (X_1,X_2,X_3) and (x_1,x_2,x_3)

We know that $x_i = x_i(X_1,X_2,X_3)$ in the Lagrangian description of the deformation and that $u_i = x_i - X_i$. This means that

$$(B\text{-}13) \quad u_i = x_i(X_1,X_2,X_3) - X_i$$

or that

$$(B\text{-}14) \quad u_i = u_i(X_1,X_2,X_3) ,$$

that is, the amount of displacement a given material particle undergoes during a deformation of the continuum is a function of the initial position, (X_1,X_2,X_3), of that particle before the deformation occurred. Similarly since $X_i = X_i(x_1,x_2,x_3)$ in the Eulerian description of the deformation we have

$$(B\text{-}15) \quad u_i = x_i - X_i(x_1,x_2,x_3)$$

or

$$(B\text{-}16) \quad u_i = u_i(x_1,x_2,x_3).$$

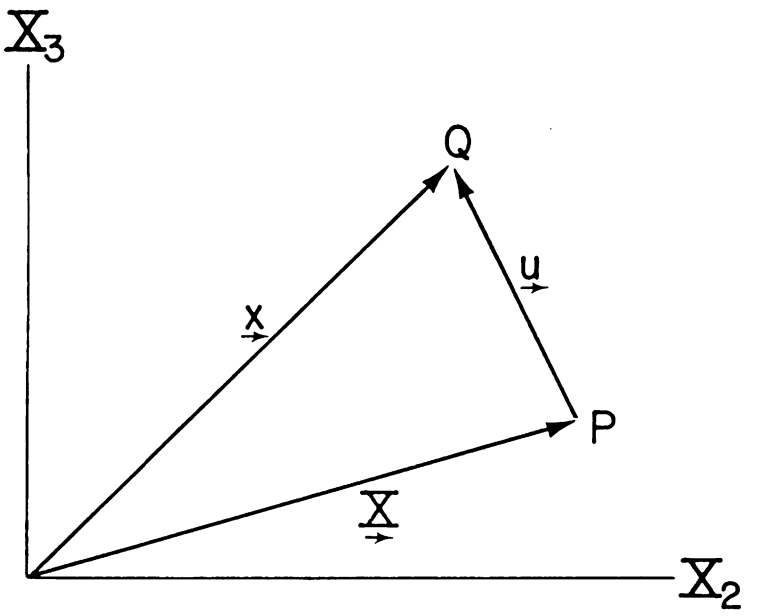

Figure B-1: Deformation of a material medium.

The Deformation - Δ

A material is deformed when the material particles which constitute that medium are displaced relative to each other. Suppose we want to design some mathematical criteria which will enable us to decide unambiguously whether or not a given material body has been deformed from its initial state. We might at first be tempted to say that knowing $u_i = u_i(X_1,X_2,X_3)$ or $u_i = u_i(x_1,x_2,x_3)$ will enable us to decide this immediately. However this is not the case since the values of u_i will be nonzero for all the material points of a continuum if that continuum undergoes a rigid translation. Of course if the continuum does undergo a translation of this type the values of u_i will be the same for every particle, that is independent of (X_1,X_2,X_3) or (x_1,x_2,x_3), the initial and final coordinates of the particle. Under such conditions it is obvious that the elements of

$$\text{(B-17)} \quad \begin{bmatrix} I_{11} & I_{12} & I_{13} \\ I_{21} & I_{22} & I_{23} \\ I_{31} & I_{32} & I_{33} \end{bmatrix} = \begin{bmatrix} \frac{\partial u_1}{\partial X_1} & \frac{\partial u_1}{\partial X_2} & \frac{\partial u_1}{\partial X_3} \\ \frac{\partial u_2}{\partial X_1} & \frac{\partial u_2}{\partial X_2} & \frac{\partial u_2}{\partial X_3} \\ \frac{\partial u_3}{\partial X_1} & \frac{\partial u_3}{\partial X_2} & \frac{\partial u_3}{\partial X_3} \end{bmatrix}$$

and

$$(B\text{-}18)\quad \begin{bmatrix} J_{11} & J_{12} & J_{13} \\ J_{21} & J_{22} & J_{23} \\ J_{31} & J_{32} & J_{33} \end{bmatrix} = \begin{bmatrix} \frac{\partial u_1}{\partial x_1} & \frac{\partial u_1}{\partial x_2} & \frac{\partial u_1}{\partial x_3} \\ \frac{\partial u_2}{\partial x_1} & \frac{\partial u_2}{\partial x_2} & \frac{\partial u_2}{\partial x_3} \\ \frac{\partial u_3}{\partial x_1} & \frac{\partial u_3}{\partial x_2} & \frac{\partial u_3}{\partial x_3} \end{bmatrix}$$

will all be zero. These two tensors are referred to as the *material displacement gradient* and *spacial displacement gradient* tensors, respectively. It therefore appears that we have succeeded at our task; however, such is not the case as the following example shows. Consider a rigid rotation of the continuum by an amount ρ about an axis with direction cosines (ℓ_1,ℓ_2,ℓ_3), which for simplicity is assumed to pass through the origin of the coordinate system. We have for the general case

$$(B\text{-}19)\quad \begin{bmatrix} x_1 \\ x_2 \\ x_3 \end{bmatrix} = \begin{bmatrix} \ell_1^2(1-\cos\rho) + \cos\rho & \ell_1\ell_2(1-\cos\rho) - \ell_3\sin\rho \\ \ell_2\ell_1(1-\cos\rho) + \ell_3\sin\rho & \ell_2^2(1-\cos\rho) + \cos\rho \\ \ell_3\ell_1(1-\cos\rho) - \ell_2\sin\rho & \ell_3\ell_2(1-\cos\rho) + \ell_1\sin\rho \end{bmatrix}$$

$$\begin{bmatrix} \ell_1\ell_3(1-\cos\rho) + \ell_2\sin\rho \\ \ell_2\ell_3(1-\cos\rho) - \ell_1\sin\rho \\ \ell_3^2(1-\cos\rho) + \cos\rho \end{bmatrix} \begin{bmatrix} X_1 \\ X_2 \\ X_3 \end{bmatrix}$$

or

$$(B\text{-}20)\quad \begin{bmatrix} u_1 \\ u_2 \\ u_3 \end{bmatrix} = \begin{bmatrix} x_1 \\ x_2 \\ x_3 \end{bmatrix} - \begin{bmatrix} X_1 \\ X_2 \\ X_3 \end{bmatrix} = \begin{bmatrix} \ell_1^2(1-\cos\rho) + \cos\rho - 1 \\ \ell_2\ell_1(1-\cos\rho) + \ell_3\sin\rho \\ \ell_3\ell_1(1-\cos\rho) - \ell_2\sin\rho \end{bmatrix}$$

$$\begin{bmatrix} \ell_1\ell_2(1-\cos\rho) - \ell_3\sin\rho & \ell_1\ell_3(1-\cos\rho) + \ell_2\sin\rho \\ \ell_1^2(1-\cos\rho) + \cos\rho - 1 & \ell_2\ell_3(1-\cos\rho) - \ell_1\sin\rho \\ \ell_3\ell_2(1-\cos\rho) + \ell_1\sin\rho & \ell_3^2(1-\cos\rho) + \cos\rho - 1 \end{bmatrix} \begin{bmatrix} X_1 \\ X_2 \\ X_3 \end{bmatrix}$$

Therefore we have

$$(B\text{-}21)\quad I_{ij} = \delta_{ij}\cos\rho + \ell_i\ell_j(1-\cos\rho) - \varepsilon_{ijk}\ell_k\sin\rho - \delta_{ij}$$

which is, in general not zero even though no true deformation has occurred.

It is obvious that we must approach this problem somewhat differently. Consider the material point of the continuum which was located at $\underset{\rightarrow}{X} = X_1\hat{i} + X_2\hat{j} + X_3\hat{k}$ before the medium was deformed. We now increment this vector by a small amount

$$(B\text{-}22)\quad \delta\underset{\rightarrow}{X} = \delta X_1\hat{i} + \delta X_2\hat{j} + \delta X_3\hat{k} \ .$$

We see that

$$(B\text{-}23)\quad \delta X^2 = \delta\underset{\rightarrow}{X} \cdot \delta\underset{\rightarrow}{X} = \delta X_i\delta X_i = \delta X_1^2 + \delta X_2^2 + \delta X_3^2 \ .$$

During the deformation the point initially at $\underset{\rightarrow}{X}$ moves to $\underset{\rightarrow}{x} = x_1\hat{i} + x_2\hat{j} + x_3\hat{k}$ while the point initially located at $\underset{\rightarrow}{x} + \delta\underset{\rightarrow}{x}$, where δx is a slight increment of the vector $\underset{\rightarrow}{x}$ denoted by

$$(B\text{-}24)\quad \delta\underset{\rightarrow}{x} = \delta x_1\hat{i} + \delta x_2\hat{j} + \delta x_3\hat{k} \ .$$

We see that the square of the length of $\delta\underset{\rightarrow}{x}$, denoted by δx^2 is given by

$$(B\text{-}25)\quad \delta x^2 = \delta\underset{\rightarrow}{x} \cdot \delta\underset{\rightarrow}{x} = \delta x_1^2 + \delta x_2^2 + \delta x_3^2 \ .$$

Let us now define a function Δ', termed the deformation, as

$$(B\text{-}26) \quad \Delta' = \delta x^2 - \delta X^2$$

where the value of Δ' depends on the magnitudes of δX_1, δX_2, δX_3, X_1, X_2, X_3 and the functional form of the deformation. It is obvious that if the medium is translated or undergoes a rigid rotation then we will have

$$(B\text{-}27) \quad |\delta \underset{\rightarrow}{x}| = \delta x = |\delta \underset{\rightarrow}{X}| = \delta X$$

and Δ' will be zero. For any true deformation, however, Δ' will have a nonzero value for some choice of δX_1, δX_2, δX_3. In Δ' therefore we have an infallible guide as to whether a deformation has occurred.

The Finite Lagrangian and Eulerian Strain Tensor

Let us now develop a criterion for determining whether or not a deformation has occurred in the neighborhood of a point (X_1,X_2,X_3). We know from equation (B-5), that

$$(B\text{-}28) \quad x_k = X_k(X_1,X_2,X_3) \ .$$

The differential of (B-28) is

$$(B\text{-}29) \quad dx_k = \partial x_k/\partial X_i dX_i$$

or on changing the dummy subscript i to j

$$(B\text{-}30) \quad dx_k = \partial x_k/\partial X_j dX_j \ .$$

By analogy with equation (B-26) we may define a parameter Δ, called the *deformation*, as

$$(B\text{-}31) \quad \Delta = dx^2 - dX^2 = \frac{\partial x_k}{\partial X_i}\frac{\partial x_k}{\partial X_j} dX_i dX_j - dX^2$$

or, on using the identity

$$(B\text{-}32) \quad dX_i = \delta_{ij} dX_j$$

$$(B\text{-}33) \quad \Delta = \left(\frac{\partial x_k}{\partial X_i}\frac{\partial x_k}{\partial X_j} - \delta_{ij}\right) dX_i dX_j$$

This tensor with components

$$(B\text{-}34) \quad G_{ij} = \frac{\partial x_k}{\partial X_i}\frac{\partial x_k}{\partial X_j}$$

is often called *Green's deformation tensor*. Using this definition we can write equation (B-33) as

$$(B\text{-}35) \quad \Delta = (G_{ij} - \delta_{ij}) dX_i dX_j \ .$$

We also know from equation (B-6) that

$$(B\text{-}36) \quad X_k = X_k(x_1, x_2, x_3) \ .$$

In differential form this becomes

$$(B\text{-}37) \quad dX_k = \frac{\partial X_k}{\partial x_i} dx_i$$

or on changing the dummy index i to j

$$(B\text{-}38) \quad dX_k = \frac{\partial X_k}{\partial x_j} dx_j \ .$$

Using equations (B-37) and (B-38) the expression for Δ becomes

$$(B\text{-}39) \quad \Delta = dx^2 - \frac{\partial X_k}{\partial x_i}\frac{\partial X_k}{\partial x_j} dx_i dx_j$$

or

$$(B\text{-}40) \quad \Delta = \left(\delta_{ij} - \frac{\partial X_k}{\partial x_i}\frac{\partial X_k}{\partial x_j}\right) dx_i dx_j \ .$$

The tensor

$$(B\text{-}41)\quad C_{ij} = \frac{\partial X_k}{\partial x_i}\frac{\partial X_k}{\partial x_j}$$

is called *Cauchy's deformation tensor*. Using equation (B-41) we can write

$$(B\text{-}42)\quad \Delta = (\delta_{ij} - C_{ij})dx_i dx_j \ .$$

Thus we have two expressions for the deformation, Δ, that is

$$(B\text{-}43)\quad \Delta = (G_{ij} - \delta_{ij})dX_i dX_j = (\delta_{ij} - C_{ij})dx_i dx_j \ .$$

It is useful at this point to define the *Lagrangian finite strain tensor* as

$$(B\text{-}44)\quad L_{ij} = \frac{1}{2}[G_{ij} - \delta_{ij}] = \frac{1}{2}[\frac{\partial x_k}{\partial X_i}\frac{\partial x_k}{\partial X_j} - \delta_{ij}]$$

and the *Eulerian finite strain tensor* as

$$(B\text{-}45)\quad E_{ij} = \frac{1}{2}[\delta_{ij} - C_{ij}] = \frac{1}{2}[\delta_{ij} - \frac{\partial X_k}{\partial x_i}\frac{\partial X_k}{\partial x_j}]$$

The Lagrangian and Eulerian finite strain tensors are also referred to as Green's finite strain tensor and Almonsi's finite strain tensor respectively. We can now write

$$(B\text{-}46)\quad \Delta = 2L_{ij}dX_i dX_j = 2E_{ij}dx_i dx_j = (dx - dX)(dx + dX)$$
$$\simeq 2dX(dx - dX) \simeq 2dx(dx - dX) \ .$$

An especially useful form of the finite Lagrangian and Eulerian strain tensors is one in which they appear as functions of the displacement gradients. We recall that $u_k = x_k - X_k$ so that

$$(B\text{-}47)\quad \partial x_k/\partial X_i = \delta_{ki} + \partial u_k/\partial X_i$$

and

$$(B\text{-}48) \quad \partial x_k/\partial X_j = \delta_{kj} + \partial u_k/\partial X_j$$

We substitute equations (B-47) and (B-48) into (B-44) to obtain

$$(B\text{-}49) \quad L_{ij} = \frac{1}{2}[(\delta_{ki} + \frac{\partial u_k}{\partial X_i})(\delta_{kj} + \frac{\partial u_k}{\partial X_j}) - \delta_{ij}]$$

$$= \frac{1}{2}[\delta_{ki}\delta_{kj} + \delta_{ki}\frac{\partial u_k}{X_j} + \delta_{kj}\frac{\partial u_k}{\partial X_i} + \frac{\partial u_k}{\partial X_i}\frac{\partial u_k}{\partial X_j} - \delta_{ij}] \ .$$

However since

$$(B\text{-}50) \quad \delta_{ki}\frac{\partial u_k}{\partial X_j} = \frac{\partial u_i}{\partial X_j}$$

and

$$(B\text{-}51) \quad \delta_{ki}\frac{\partial u_k}{\partial X_j} = \frac{\partial u_i}{\partial X_j} \ ,$$

we obtain

$$(B\text{-}52) \quad L_{ij} = \frac{1}{2}[\delta_{ij} + \frac{\partial u_i}{\partial X_j} + \frac{\partial u_j}{\partial x_i} + \frac{\partial u_k}{\partial X_i}\frac{\partial u_k}{\partial X_j} - \delta_{ij}]$$

or

$$(B\text{-}53) \quad L_{ij} = \frac{1}{2}[\frac{\partial u_i}{\partial X_j} + \frac{\partial u_j}{\partial X_i} + \frac{\partial u_k}{\partial X_i}\frac{\partial u_k}{\partial X_j}] \ .$$

This is the desired result and equation (B-53) is a form of the finite Lagrangian strain tensor which is seen quite frequently. In a similar manner it can be shown that

$$(B\text{-}54) \quad E_{ij} = \frac{1}{2}[\frac{\partial u_i}{\partial x_j} + \frac{\partial u_j}{\partial x_i} + \frac{\partial u_k}{\partial x_i}\frac{\partial u_k}{\partial x_j}] \ .$$

The Linear Lagrangian and Linear Eulerian Strain Tensors

The "small deformation theory" of continuum mechanics has as a basic condition the requirement that the displacement gradients be small compared to unity, that is $I_{ij} << 1$ and $J_{ij} << 1$. Since most solid materials will fracture or undergo plastic deformation when the displacement gradients exceed $\approx 10^{-4}$ (dimensionless) this condition is almost always satisfied. We see that under such conditions

$$(B\text{-}55) \quad \frac{\partial u_k}{\partial X_i}\frac{\partial u_k}{\partial X_j} << \frac{\partial u_i}{\partial X_j} \quad (\text{i.e. } I_{ki}I_{kj} << I_{ij})$$

and

$$(B\text{-}56) \quad \frac{\partial u_k}{\partial x_i}\frac{\partial u_k}{\partial x_j} << \frac{\partial u_k}{\partial x_j} \quad (\text{i.e. } J_{ki}J_{kj} << J_{ij})$$

so that to a very good approximation we can say

$$(B\text{-}57) \quad \Delta = 2\ell_{ij}dX_i dX_j = 2e_{ij}dx_i dx_j$$

where

$$(B\text{-}58) \quad \ell_{ij} = \frac{1}{2}\left(\frac{\partial u_i}{\partial X_j} + \frac{\partial u_j}{\partial X_i}\right)$$

and

$$(B\text{-}59) \quad e_{ij} = \frac{1}{2}\left(\frac{\partial u_i}{\partial x_j} + \frac{\partial u_j}{\partial x_i}\right) .$$

$[\ell_{ij}]$ and $[e_{ij}]$ are second rank symmetric tensors which are called the *linear Lagrangian* and *linear Eulerian strain tensors* respectively.

Conditions Under Which $\ell_{ij} \approx e_{ij}$

Using the chain rule we obtain

$$\text{(B-60)} \quad \frac{\partial u_i}{\partial X_j} = \frac{\partial u_i}{\partial x_k} \frac{\partial x_k}{\partial X_j}$$

and since $x_k = X_k + u_k$ also the following:

$$\text{(B-61)} \quad \frac{\partial x_k}{\partial X_j} = \frac{\partial X_k}{\partial X_j} + \frac{\partial u_k}{\partial X_j} = \delta_{kj} + \frac{\partial u_k}{\partial X_j}$$

therefore

$$\text{(B-62)} \quad \frac{\partial u_i}{\partial X_j} = \frac{\partial u_i}{\partial x_k}(\delta_{kj} + \frac{\partial u_k}{\partial X_j})$$

or

$$\text{(B-63)} \quad \frac{\partial u_i}{\partial X_j} = \delta_{kj} \frac{\partial u_i}{\partial x_k} + \frac{\partial u_i}{\partial x_k} \frac{\partial u_k}{\partial X_j} = \frac{\partial u_i}{\partial x_j} + \frac{\partial u_i}{\partial x_k} \frac{\partial u_k}{\partial X_j}$$

If the components of the material displacement gradient tensor $I_{ij} = \partial u_i/\partial X_j$ and the spacial displacement gradient tensor $J_{ij} = \partial u_i/\partial x_j$ are very small then

$$\text{(B-64)} \quad \frac{\partial u_i}{\partial X_j} >> \frac{\partial u_i}{\partial x_k} \frac{\partial u_k}{\partial X_j}$$

and we can write

$$\text{(B-65)} \quad \frac{\partial u_i}{\partial X_j} \simeq \frac{\partial u_i}{\partial x_j} .$$

This implies, however, that

$$\text{(B-66)} \quad \ell_{ij} \simeq e_{ij}$$

when the displacement gradients are very small. In this situation there is no difference between a linear Lagrangian strain tensor component and the corresponding element of the linear Eulerian strain tensor. Thus no distinction need be made between them.

The Role of the Deformation Gradients in the Theory of Linear Strain

We recall that

$$\text{(B-67)}\qquad \begin{bmatrix} du_1 \\ du_2 \\ du_3 \end{bmatrix} = \begin{bmatrix} I_{11} & I_{12} & I_{13} \\ I_{21} & I_{22} & I_{23} \\ I_{31} & I_{32} & I_{33} \end{bmatrix} \begin{bmatrix} dX_1 \\ dX_2 \\ dX_3 \end{bmatrix}$$

or

$$\text{(B-68)}\qquad \begin{bmatrix} du_1 \\ du_2 \\ du_3 \end{bmatrix} = \begin{bmatrix} \frac{\partial u_1}{\partial X_1} & \frac{\partial u_1}{\partial X_2} & \frac{\partial u_1}{\partial X_3} \\ \frac{\partial u_2}{\partial X_1} & \frac{\partial u_2}{\partial X_2} & \frac{\partial u_2}{\partial X_3} \\ \frac{\partial u_2}{\partial X_1} & \frac{\partial u_3}{\partial X_2} & \frac{\partial u_3}{\partial X_3} \end{bmatrix} \begin{bmatrix} dX_1 \\ dX_2 \\ dX_3 \end{bmatrix} .$$

We see that the latter expression is equivalent to

$$\text{(B-69)}\qquad \begin{bmatrix} du_1 \\ du_2 \\ du_3 \end{bmatrix} = \begin{bmatrix} \frac{\partial u_1}{\partial X_1} & \frac{1}{2}\left(\frac{\partial u_1}{\partial X_2} + \frac{\partial u_2}{\partial X_1}\right) & \frac{1}{2}\left(\frac{\partial u_1}{\partial x_3} + \frac{\partial u_3}{\partial X_1}\right) \\ \frac{1}{2}\left(\frac{\partial u_2}{\partial X_1} + \frac{\partial u_1}{\partial X_2}\right) & \frac{\partial u_2}{\partial X_2} & \frac{1}{2}\left(\frac{\partial u_2}{\partial X_3} + \frac{\partial u_3}{\partial X_2}\right) \\ \frac{1}{2}\left(\frac{\partial u_3}{\partial X_1} + \frac{\partial u_1}{\partial X_3}\right) & \frac{1}{2}\left(\frac{\partial u_3}{\partial X_2} + \frac{\partial u_3}{\partial X_2}\right) & \frac{\partial u_3}{\partial X_3} \end{bmatrix} \begin{bmatrix} dX_1 \\ dX_2 \\ dX_3 \end{bmatrix}$$

$$+ \begin{bmatrix} 0 & \frac{1}{2}\left(\frac{\partial u_1}{\partial X_2} - \frac{\partial u_2}{\partial X_1}\right) & \frac{1}{2}\left(\frac{\partial u_1}{\partial X_3} - \frac{\partial u_3}{\partial X_1}\right) \\ \frac{1}{2}\left(\frac{\partial u_2}{\partial X_1} - \frac{\partial u_1}{\partial X_2}\right) & 0 & \frac{1}{2}\left(\frac{\partial u_2}{\partial X_3} - \frac{\partial u_3}{\partial X_2}\right) \\ \frac{1}{2}\left(\frac{\partial u_3}{\partial X_1} - \frac{\partial u_1}{\partial X_3}\right) & \frac{1}{2}\left(\frac{\partial u_3}{\partial X_2} - \frac{\partial u_3}{\partial X_2}\right) & 0 \end{bmatrix} \begin{bmatrix} dX_1 \\ dX_2 \\ dX_3 \end{bmatrix}$$

Thus the material displacement gradient tensor can be broken up into

two parts, the first part of which is symmetric while the second part is antisymmetric. We see that the elements of the first tensor are identical with those of the linear Lagrangian strain tensor. Let us denote the elements of the second tensor by

$$\text{(B-70)} \quad \omega_{ij} = \frac{1}{2}\left(\frac{\partial u_i}{\partial X_j} - \frac{\partial u_j}{\partial X_i}\right).$$

We can then write

$$\text{(B-71)} \quad \begin{bmatrix} du_1 \\ du_2 \\ du_3 \end{bmatrix} = \begin{bmatrix} \ell_{11} & \ell_{12} & \ell_{13} \\ \ell_{21} & \ell_{22} & \ell_{23} \\ \ell_{31} & \ell_{32} & \ell_{33} \end{bmatrix} \begin{bmatrix} dX_1 \\ dX_2 \\ dX_3 \end{bmatrix} + \begin{bmatrix} 0 & \omega_{12} & \omega_{13} \\ \omega_{21} & 0 & \omega_{23} \\ \omega_{31} & \omega_{32} & 0 \end{bmatrix} \begin{bmatrix} dX_1 \\ dX_2 \\ dX_3 \end{bmatrix}$$

or

$$\text{(B-72)} \quad du_i = (\ell_{ij} + \omega_{ij})dX_j \ .$$

A "pure deformation" is defined as a deformation having all $\omega_{ij} = 0$. In a similar way it is possible to show (by starting with the definition of the spacial displacement gradient tensor) that

$$\text{(B-73)} \quad \begin{bmatrix} du_1 \\ du_2 \\ du_3 \end{bmatrix} = \begin{bmatrix} e_{11} & e_{12} & e_{13} \\ e_{21} & e_{22} & e_{23} \\ e_{31} & e_{32} & e_{33} \end{bmatrix} \begin{bmatrix} dx_1 \\ dx_2 \\ dx_3 \end{bmatrix} + \begin{bmatrix} 0 & \tilde{\omega}_{21} & \tilde{\omega}_{13} \\ \tilde{\omega}_{21} & 0 & \tilde{\omega}_{23} \\ \tilde{\omega}_{31} & \tilde{\omega}_{32} & 0 \end{bmatrix} \begin{bmatrix} dx_1 \\ dx_2 \\ dx_3 \end{bmatrix}$$

or

$$\text{(B-74)} \quad du_i = (e_{ij} + \tilde{\omega}_{ij})dx_j$$

where

$$\text{(B-75)} \quad \tilde{\omega}_{ij} = \frac{1}{2}\left(\frac{\partial u_i}{\partial x_j} - \frac{\partial u_j}{\partial x_i}\right) .$$

The Physical Significance of ℓ_{ij}, e_{ij}, ω_{ij} and $\tilde{\omega}_{ij}$

At this point it is possible to give simple physical interpretations of ℓ_{ij}, e_{ij}, ω_{ij}, and $\tilde{\omega}_{ij}$. Let us consider three line elements of initial length dX', dX'', and dX''' located, before deformation of the medium, along (1,0,0), (0,1,0) and (0,0,1) respectively. Let dx', dx'', and dx''' denote the final length (after deformation) of these line segments. On noting that $dX_i = n_i dX$ we see that equation (B-46) becomes, in the linear approximation, $(dX - dx)/dX = \ell_{ij} n_j n_j$. Using this result we obtain:

(B-76) $(dx' - dX')/dX' = \ell_{11}$,

(B-77) $(dx'' - dX'')/dX'' = \ell_{22}$,

and

(B-78) $(dx''' - dX''')/dX''' = \ell_{33}$.

Thus the diagonal elements ℓ_{11}, ℓ_{22} and ℓ_{33} of the linear Lagrangian strain tensor represent the change in length per unit initial length of line segments initially, before deformation, located along (1,0,0), (0,1,0) and (0,0,1) respectively. In order to see the significance of the off diagonal terms we may proceed as follows. Consider a line segment

(B-79) $d\underset{\rightarrow}{X} = dX_1\hat{i} + dX_2\hat{j} + dX_3\hat{k}$

which becomes after deformation

(B-80) $d\underset{\rightarrow}{x} = dx_1\hat{i} + dx_2\hat{j} + dx_3\hat{k}$.

Using equation (B-72) we write for a pure deformation

(B-81) $du_k = \ell_{ki} dX_i = \ell_{kj} dX_j$

or

$$(B\text{-}82)\quad dx_k = dX_k + du_k = dX_k + \ell_{ki}dX_i = (\delta_{ki} + \ell_{ki})dX_i$$
$$= (\delta_{kj} + \ell_{kj})dX_j$$

We therefore have

$$(B\text{-}83)\quad dx^2 = d\underset{\rightarrow}{x} \cdot d\underset{\rightarrow}{x} = (\delta_{ki} + \ell_{ki})(\delta_{kj} + \ell_{kj})dX_i dX_j$$
$$= (\delta_{ki}\ell_{kj} + \delta_{ki}\ell_{kj} + \ell_{ki}\delta_{kj} + \ell_{ki}\ell_{kj})dX_i dX_j$$
$$= (\delta_{ij} + \ell_{ij} + \ell_{ji} + \ell_{ki}\ell_{kj})dX_i dX_j$$
$$= (\delta_{ij} + \ell_{ij} + \ell_{ji} + \ell_{ki}\ell_{kj})n_i n_j dX^2$$

For the line segments dX', and dX'' initially located along (1,0,0) and (0,1,0) equation (B-83) becomes

$$(B\text{-}84)\quad dx'^2 = (1 + 2\ell_{11} + \ell_{k1}\ell_{k1})dX'2$$

and

$$(B\text{-}85)\quad dx''^2 = (1 + 2\ell_{22} + \ell_{k2}\ell_{k2})dX''^2$$

and since

$$(B\text{-}86)\quad \ell_{k1}\ell_{k1} << 2\ell_{11} << 1$$

and

$$(B\text{-}87)\quad \ell_{k2}\ell_{k2} << 2\ell_{22} << 1$$

equations (B-84) and (B-85) reduce to

$$(B\text{-}88)\quad dx' \simeq dX'$$

and

$$(B\text{-}89)\quad dx'' \simeq dX'' .$$

Using the relation given in equation (B-82) we see that

$$(B\text{-}90)\quad d\vec{x}' = dx_1'\hat{i} + dx_2'\hat{j} + dx_3'\hat{k} = (1 + \ell_{11})dX'\hat{i} + \ell_{12}dX'\hat{j} + \ell_{13}dX'\hat{k}$$

$$(B\text{-}91)\quad d\vec{x}'' = dx_1''\hat{i} + dx_2''\hat{j} + dx_3''\hat{k} = \ell_{21}dX''\hat{i} + (1 + \ell_{22})dX''\hat{j} + \ell_{23}dX''\hat{k}$$

Taking the dot product of equations (B-90) and (B-91) gives

$$(B\text{-}92)\quad d\vec{x}' \cdot d\vec{x}'' = |d\vec{x}'||d\vec{x}''|\cos\Theta = dX'dX''\cos\Theta$$
$$= [(1 + \ell_{11})\ell_{21} + \ell_{12}(1 + \ell_{22}) + \ell_{13}\ell_{23}]dX'dX''$$

This gives

$$(B\text{-}93)\quad \cos\Theta = (\ell_{21} + \ell_{11}\ell_{21} + \ell_{12} + \ell_{12} + \ell_{22} + \ell_{13}\ell_{23}) \simeq \ell_{12} + \ell_{21}$$

Here Θ is the angle between $d\vec{x}'$ and $d\vec{x}''$.

Let us define

$$(B\text{-}94)\quad \gamma_{12} = \frac{\pi}{2} - \Theta$$

where γ_{12} represents the change in the angle between the line segments originally oriented along $\hat{i}$ and $\hat{j}$. We see that

$$(B\text{-}95)\quad \cos\Theta = \cos(\frac{\pi}{2} - \gamma_{12}) = \cos\frac{\pi}{2}\cos\gamma_{12} + \sin\frac{\pi}{2}\sin\gamma_{12} = \sin\gamma_{12} \simeq \gamma_{12}$$

since γ_{12} is very small (generally $\gamma_{12} \simeq 10^{-4}$ radians) we now write

$$(B\text{-}96)\quad \gamma_{12} = \ell_{12} + \ell_{21} = 2\ell_{12} = 2\ell_{21}$$

(since $\ell_{12} = \ell_{21}$). Thus we see that

$$(B\text{-}97)\quad \ell_{12} = \ell_{21} = 1/2\gamma_{12}\ .$$

This means that ℓ_{12} and ℓ_{21} represent 1/2 the change in angle between two line segments in the medium initially oriented along (1,0,0) and (0,1,0). This is the standard engineering interpretation of this off diagonal element of the linear Lagrangian strain tensor. The significance of the other off diagonal elements is similar. Let us now consider the significance of the term, e_{ij}, of the linear Eulerian strain

tensor. We can begin, after the deformation is complete, by looking at three infinitesimal line segments dx', dx", and dx"' which are oriented along (1,0,0), (0,1,0) and (0,0,1). Initially, before the deformation occurred, these line segments had lengths dX', dX", and dX"'. Using the equation $(dx - dX)/dx = e_{ij}\bar{n}_i\bar{n}_j$ we see that

(B-98) $(dx' - dX')/dx' = e_{11}$

(B-99) $(dx" - dX")/dx" = e_{22}$

(B-100) $(dx"' - dX"')/dx"' = e_{33}$.

Thus the diagonal elements e_{11}, e_{22}, and e_{33} of the linear Eulerian strain tensor therefore represent the change in length per unit final length of line segments which, after the deformation is complete, are oriented along (1,0,0), (0,1,0) and (0,0,1) respectively. We know that

(B-101) $dX_k = dx_k - du_k$

and that for a pure strain where $\tilde{\omega}_{ij} = 0$, we have

(B-102) $dX_k = dx_k - e_{ki}dx_i = (\delta_{ki} - e_{ki})dx_i = (\delta_{kj} - e_{kj})dx_j$

Therefore

(B-103) $$dX^2 = dX_k dX_k = (\delta_{ki} - e_{ki})(\delta_{kj} - e_{kj})dx_i dx_j$$
$$= (\delta_{ki}\delta_{kj} - \delta_{ki}e_{kj} - e_{ki}\delta_{kj} + e_{ki}e_{kj})dx_i dx_j$$
$$= (\delta_{ij} - e_{ij} - e_{ji} + e_{ki}e_{kj})dx_i dx_j$$

For the line segment dx' we have

(B-104) $dX'^2 = (1 - 2e_{11} + e_{k1}e_{k1})dx'^2$

and for the line segment

(B-105) $dX"^2 = (1 - 2e_{22} + e_{k2}e_{k2})dx"^2$

and since

$$(B\text{-}106)\quad e_{k1}e_{k1} << 2e_{11} << 1$$

and

$$(B\text{-}107)\quad e_{k2}e_{k2} << 2e_{11} << 1$$

the expressions given in equations (B-104) and (B-105) reduce to

$$(B\text{-}108)\quad dX' \simeq dx'$$

and

$$(B\text{-}109)\quad dX'' \simeq dx''$$

Using equation (B-102) we see that

$$(B\text{-}110)\quad d\vec{X}' = dX_1'\hat{i} + dX_2'\hat{j} + dX_3'\hat{k} = (1 - e_{11})dx'\hat{i} - e_{21}dx'\hat{j} - e_{31}dx'\hat{k}$$

and

$$(B\text{-}111)\quad d\vec{X}'' = dX_1''\hat{i} + dX_2''\hat{j} + dX_3''\hat{k} = -e_{12}dx''\hat{i} + (1 - e_{22})dx''\hat{j} - e_{32}dx''\hat{k}\ .$$

On taking the dot product of the two previous expressions we obtain

$$(B\text{-}112)\quad d\vec{X}' \cdot d\vec{X}'' = |d\vec{X}'||d\vec{X}''|\cos\Theta = |d\vec{x}'||d\vec{x}''|\cos\Theta = [-(1 - e_{11})e_{12} - e_{21}(1 - e_{22}) + e_{31}e_{32}]dx'dx''$$

or

$$(B\text{-}113)\quad \cos\Theta = (-e_{12} + e_{11}e_{12} - e_{21} + e_{21}e_{22} + e_{31}e_{32}) \simeq -e_{12} - e_{21}$$

We now define the change in the angle between the two line segments which, after the deformation, are located along (1,0,0) and (0,1,0) as

$$(B\text{-}114)\quad \gamma_{12} = \Theta - \pi/2$$

where Θ is, of course, the initial angle between these line segments. We now consider the expression

$$\text{(B-115)} \quad \cos\Theta = \cos(\gamma_{12} + \pi/2) = \cos\gamma_{12}\cos\pi/2 - \sin\gamma_{12}\sin\pi/2$$

$$= -\sin\gamma_{12} \simeq -\gamma_{12}$$

since γ_{12} is very small. Therefore from equation (B-111) we have

$$\text{(B-116)} \quad -\gamma_{12} = -e_{12} - e_{21}$$

or

$$\text{(B-117)} \quad e_{12} = e_{21} = 1/2\gamma_{12} \ .$$

Therefore e_{12} and e_{21} represent the one half the change in angle between two line segments which, after the deformation is complete, are oriented ninety degrees apart along (1,0,0) and (0,1,0). It is important to realize that before the deformation occurred these two line segments were not separated by 90° and were not (except in special cases) oriented along $\hat{i}$ and $\hat{j}$. The interpretation of the other off diagonal elements of $[e_{ij}]$ is similar.

We must now consider the significance of the elements of the linear Lagrangian rotation tensor $[\omega_{ij}]$. In general the elements of this tensor will be functions of the initial coordinates, (X_1,X_2,X_3), of the material particle, that is

$$\text{(B-118)} \quad \omega_{ij} = \omega_{ij}(X_1,X_2,X_3) \ .$$

Let us assume that the elements of the linear Lagrangian strain tensor are zero so that the components of the relative displacement vector, $d\underset{\rightarrow}{u}$, are given by

$$\text{(B-119)} \quad du_i = \omega_{ij}dX_j \ .$$

From equation (B-101) we obtain

$$(B\text{-}120)\quad dx_k = (\delta_{ki} + \omega_{ki})dX_i = (\delta_{kj} + \omega_{kj})dX_j$$

Therefore

$$(B\text{-}121)\quad dx^2 = (\delta_{ki} + \omega_{kj})(\delta_{kj} + \omega_{kj})dX_i dX_j$$

$$= (\delta_{ij} + \omega_{ij} + \omega_{ji} + \omega_{ki}\omega_{kj})dX_i dX_j$$

$$= (\delta_{ij} + \omega_{ki}\omega_{kj})dX_i dX_j \simeq dX^2$$

Equation (B-121) is important because it indicates that, to the first order, the linear Lagrangian rotation tensor does not change the length of any element $d\underset{\rightarrow}{X}$. This result should be compared with that of equation (B-80) where we see that $[\ell_{ij}]$ does cause a first order change in the length of a line element $d\underset{\rightarrow}{X}$. We can also form the dot product

$$(B\text{-}122)\quad d\underset{\rightarrow}{u} \cdot d\underset{\rightarrow}{X} = du_i dX_i = \omega_{ij} dX_i dX_j = 0$$

This indicates that $d\underset{\rightarrow}{u}$ is perpendicular to $d\underset{\rightarrow}{X}$. This behavior is illustrated by Figure B-2. Essentially what occurs (to the first order) is a rotation about the point with material coordinates (X_1, X_2, X_3). After the deformation this particle has moved to (x_1, x_2, x_3) so that from the point of view of an observer fixed to the material point (X_1, X_2, X_3), Maxwell's demon or some such creature, all that has occurred is a rotation of $d\underset{\rightarrow}{X}$ to a new position $d\underset{\rightarrow}{x}$ with $|d\underset{\rightarrow}{x}| = |d\underset{\rightarrow}{X}|$ (again equal to the first order).

To gain more insight into the nature of $[\omega_{ij}]$ let us return to the generalized Cartesian rotation matrix used in equation (B-19). We wish to consider a rotation of the point $(X_1 + dX_1,\ X_2 + dX_2,\ X_3 + dX_3)$ about point (X_1, X_2, X_3) followed by a rigid body translation of

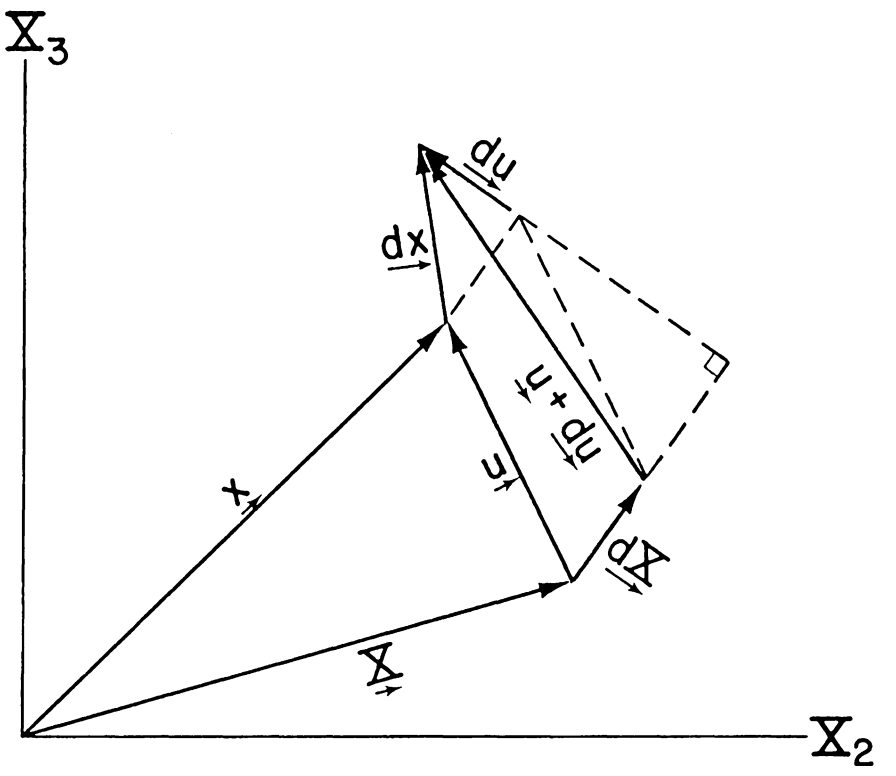

Figure B-2: The effect of the antisymmetric linear Lagrangian rotation tensor on the line segment $d\underset{\rightarrow}{X}$ (see text for discussion).

(u_1,u_2,u_3). Therefore we write

$$(B\text{-}123)\quad \begin{bmatrix} x_1 + dx_1 \\ x_2 + dx_2 \\ x_3 + dx_3 \end{bmatrix} = \begin{bmatrix} \ell_1^2(1 - \cos\rho) + \cos\rho \\ \ell_2\ell_1(1 - \cos\rho) + \ell_3\sin\rho \\ \ell_3\ell_1(1 - \cos\rho) - \ell_2\sin\rho \end{bmatrix}$$

$$\begin{bmatrix} \ell_1\ell_2(1 - \cos\rho) - \ell_3\sin\rho & \ell_1\ell_3(1 - \cos\rho) + \ell_2\sin\rho \\ \ell_1^2(1 - \cos\rho) + \cos\rho & \ell_1\ell_3(1 - \cos\rho) - \ell_1\sin\rho \\ \ell_3\ell_2(1 - \cos\rho) + \ell_1\sin\rho & \ell_3^2(1 - \cos\rho) + \cos\rho \end{bmatrix}$$

$$\begin{bmatrix} X_1 + dX_1 - X_1 \\ X_2 + dX_2 - X_2 \\ X_3 + dX_3 - X_3 \end{bmatrix} + \begin{bmatrix} X_1 \\ X_2 \\ X_3 \end{bmatrix} + \begin{bmatrix} u_1 \\ u_2 \\ u_3 \end{bmatrix}$$

We now assume that ρ is very small (i.e. $\rho \leq 10^{-4}$ radians).

$$(B\text{-}124)\quad \cos\rho = 1 - \frac{\rho^2}{2!} + \frac{\rho^4}{4!} - \frac{\rho^6}{6!} + \cdots$$

$$(B\text{-}125)\quad \sin\rho = \rho - \frac{\rho^3}{3!} + \frac{\rho^5}{5!} - \frac{\rho^7}{7!} \cdots$$

We retain the first terms of these expansions to obtain

$$(B\text{-}126)\quad \begin{bmatrix} x_1 + dx_1 \\ x_2 + dx_2 \\ x_3 + dx_3 \end{bmatrix} = \begin{bmatrix} 1 & -\rho\ell_3 & \rho\ell_2 \\ \rho\ell_3 & 1 & -\rho\ell_1 \\ -\rho\ell_2 & \rho\ell_1 & 1 \end{bmatrix} \begin{bmatrix} dX_1 \\ dX_2 \\ dX_3 \end{bmatrix}$$

$$+ \begin{bmatrix} X_1 \\ X_2 \\ X_3 \end{bmatrix} + \begin{bmatrix} u_1 \\ u_2 \\ u_3 \end{bmatrix}$$

We see that the matrix in the expression given above is similar in form to $[\omega_{ij}]$. It is for this reason that $[\omega_{ij}]$ is termed the linear

Lagrangian rotation matrix. We note, however, that since the above matrix has diagonal values equal to 1 it is not quite correct to refer to $[\omega_{ij}]$ as a "rotation" matrix. Since

$$u_i = x_i - X_i \tag{B-127}$$

equation (B-126) may also be written in the form

$$\begin{bmatrix} dx_1 \\ dx_2 \\ dx_3 \end{bmatrix} + \begin{bmatrix} 1 & -\rho\ell_3 & \rho\ell_2 \\ \rho\ell_3 & 1 & -\rho\ell_1 \\ -\rho\ell_2 & \rho\ell_1 & 1 \end{bmatrix} \begin{bmatrix} dX_1 \\ dX_2 \\ dX_3 \end{bmatrix} \tag{B-128}$$

We can now write (using $du_i = dx_i - dX_i$)

$$\begin{bmatrix} du_1 \\ du_2 \\ du_3 \end{bmatrix} = \begin{bmatrix} 0 & \omega_{12} & \omega_{13} \\ -\omega_{12} & 0 & \omega_{23} \\ -\omega_{13} & -\omega_{23} & 0 \end{bmatrix} \begin{bmatrix} dX_1 \\ dX_2 \\ dX_3 \end{bmatrix} \tag{B-129}$$

$$= \begin{bmatrix} 0 & \rho\ell_3 & \rho\ell_2 \\ \rho\ell_3 & 0 & -\rho\ell_1 \\ -\rho\ell_2 & \rho\ell_1 & 0 \end{bmatrix} \begin{bmatrix} dX_1 \\ dX_2 \\ dX_3 \end{bmatrix}$$

We see that the effect of $[\omega_{ij}(X_1,X_2,X_3)]$ is to rotate all infinitesimal line segments $d\vec{X}$ which have their origin at (X_1,X_2,X_3), through an angle ρ about a line with direction cosines

$$\vec{\ell} = \ell_1\hat{i} + \ell_2\hat{j} + \ell_3\hat{k} \ . \tag{B-130}$$

Note that in general we will have

$$\ell_i = \ell_i(X_1,X_2,X_3), \tag{B-131}$$

that is, the amount of rotation and the axis about which the rotation occurs will change from point to point in the medium. We note also that

$$(B\text{-}132)\quad \omega_{12}^2 + \omega_{13}^2 + \omega_{23}^2 = \rho^2\ell_3^2 + \rho^2\ell_2^2 + \rho^2\ell_1^2 = \rho^2(\ell_3^2 + \ell_2^2 + \ell_1^2) = \rho^2$$

or

$$(B\text{-}133)\quad \rho = \sqrt{\omega_{12}^2 + \omega_{13}^2 + \omega_{23}^2}$$

so that it is possible to find the amount of rotation ρ from a knowledge of the magnitudes of the elements of $[\omega_{ij}]$. Once ρ has been found it is easy to obtain (ℓ_1,ℓ_2,ℓ_3).

To summarize the effect of $[\omega_{ij}]$ is to rotate all points in the neighborhood of a material particle with initial coordinates (X_1,X_2,X_3) by an amount ρ about an axis $\underset{\rightarrow}{\ell}$. In a similar way it can be shown that the elements $[\omega_{ij}]$ of the linear Eulerian rotation tensor are related to the amount of rotation which has taken place about a material particle whose final coordinates are (x_1,x_2,x_3).

Homogeneous Strain: A Special Case

We know that $u_i = u_i(X_1,X_2,X_3)$. Let us expand this function in a Taylor series expansion about the arbitrarily selected point $(X_1^\circ,X_2^\circ,X_3^\circ)$. We obtain

$$(B\text{-}134)\quad u_i(X_1,X_2,X_3) = \frac{u_i(X_1^\circ,X_2^\circ,X_3^\circ)}{0!} + \frac{1}{1!}\left.\frac{\partial u_i}{\partial X_j}\right|_{(X_1^\circ,X_2^\circ,X_3^\circ)}(X_j - X_j^\circ) + \frac{1}{2!}\left.\frac{\partial^2 u_i}{\partial X_j \partial X_k}\right|_{(X_1^\circ,X_2^\circ,X_3^\circ)}(X_j - X_j^\circ)(X_k - X_k^\circ) + \cdots$$

It is traditional to neglect the higher terms. This results in a linear relationship. We can then write

$$(B\text{-}135)\quad u_i(X_1,X_2,X_3) \simeq u_i(X_1^\circ,X_2^\circ,X_3^\circ) + \left.\frac{\partial u_i}{\partial X_1}\right|_{(X_1^\circ,X_2^\circ,X_3^\circ)} (X_j - X_j^\circ) = u_i(X_1^\circ,X_2^\circ,X_3^\circ) + \frac{1}{2}\left[\left.\frac{\partial u_i}{\partial X_j}\right|_{(X_1^\circ,X_2^\circ,X_3^\circ)} + \left.\frac{\partial u_j}{\partial X_i}\right|_{(X_1^\circ,X_2^\circ,X_3^\circ)}\right](X_j - X_j^\circ) + \frac{1}{2}\left[\left.\frac{\partial u_i}{\partial X_j}\right|_{(X_1^\circ,X_2^\circ,X_3^\circ)} - \left.\frac{\partial u_j}{\partial X_i}\right|_{(X_1^\circ,X_2^\circ,X_3^\circ)}\right](X_j - X_j^\circ)$$

We see immediately that this becomes

$$(B\text{-}136)\quad u_i(X_1,X_2,X_3) \simeq u_i(X_1^\circ,X_2^\circ,X_3^\circ) + \ell_{ij}(X_1^\circ,X_2^\circ,X_3^\circ)(X_j - X_j^\circ) + \omega_{ij}(X_1^\circ,X_2^\circ,X_3^\circ)(X_j - X_j^\circ)$$
$$= [u_i(X_1^\circ,X_2^\circ,X_3^\circ) - \ell_{ij}(X_1^\circ,X_2^\circ,X_3^\circ)X_j^\circ - \omega_{ij}(X_1^\circ,X_2^\circ,X_3^\circ)X_j^\circ] + \ell_{ij}(X_1^\circ,X_2^\circ,X_3^\circ)X_j + \omega_{ij}(X_1^\circ,X_2^\circ,X_3^\circ)X_j \ .$$

We now consider the point with material coordinates (0,0,0). Using the above expression we obtain

$$(B\text{-}137)\quad u_i(0,0,0) \simeq [u_i(X_1^\circ,X_2^\circ,X_3^\circ) - \ell_{ij}(X_1^\circ,X_2^\circ,X_3^\circ)X_j^\circ - \omega_{ij}(X_1^\circ,X_2^\circ,X_3^\circ)X_j^\circ] \ .$$

Therefore the term in square brackets in equation (B-136) represents the amount by which the material particle at the origin is moved by the deformation and we can write

$$(B\text{-}138)\quad u_i(X_1,X_2,X_3) \simeq u_i(0,0,0) + \ell_{ij}(X_1^\circ,X_2^\circ,X_3^\circ)X_j + \omega_{ij}(X_1^\circ,X_2^\circ,X_3^\circ)X_j \ .$$

We must now determine the conditions under which equation (B-138)

gives results which are reasonably correct. The neglect of the higher terms in the expansion is justified under several conditions. The most obvious is the so-called homogeneous deformation. The deformations which occur when a material is heated are of this type. A homogeneous deformation has the form

$$u_i = \ell_{ij} X_j \tag{B-139}$$

where the ℓ_{ij} are constants. Under these conditions equation (B-138) is exact since all derivations higher than the first are equal to zero. If the ℓ_{ij} are very small the deformation is termed an "infinitesimal homogeneous deformation." These have additional special properties (Mase, 1970). We are also justified in neglecting the higher terms if they are small or if we confine ourselves to the immediate neighborhood of the point about which the Taylor series expansion was made since in this case the $(X_j - X_j^\circ)$ values are small and in the expansion terms of the type $(X_j - X_j^\circ)(X_k - X_k^\circ)$, etc. may be neglected relative to those containing only one $(X_j - X_j^\circ)$ term. This latter justification is the one which is normally cited in most texts. By making a similar Taylor series expansion of the expression $u_i = u_i(x_1,x_2,x_3)$ it is possible to obtain the equation

$$u_i(x_1,x_2,x_3) \simeq u_i(0,0,0) + e_{ij}(x_1^\circ,x_2^\circ,x_3^\circ)x_j + \tilde{\omega}_{ij}(x_1^\circ,x_2^\circ,x_3^\circ)x_j \tag{B-140}$$

where

$$e_{ij} = \frac{1}{2}\left[\left.\frac{\partial u_i}{\partial x_j}\right|_{(x_1^\circ,x_2^\circ,x_3^\circ)} + \left.\frac{\partial u_j}{\partial x_i}\right|_{(x_1^\circ,x_2^\circ,x_3^\circ)}\right] \tag{B-141}$$

and

$$(B\text{-}142)\quad \tilde{\omega}_{ij} = \frac{1}{2}\left[\left.\frac{\partial u_i}{\partial x_j}\right|_{(x_1^\circ,x_2^\circ,x_3^\circ)} - \left.\frac{\partial u_j}{\partial x_i}\right|_{(x_1^\circ,x_2^\circ,x_3^\circ)}\right] .$$

In equation (B-140) $u_i(0,0,0)$ represents the amount by which the material particle which occupies the origin (after the deformation is complete) has moved. Again the above expression will be completely accurate if the deformation is homogeneous and of the type

$$(B\text{-}143)\quad u_i = e_{ij}x_j$$

or if attention is confined to the neighborhood of the point $(x_1^\circ,x_2^\circ,x_3^\circ)$ about which the expansion was made.

Limitations on the Functional Forms of ℓ_{ij} and e_{ij}:

The Compatibility Equations

Although the components of the linear Lagrangian strain tensor are of the form

$$(B\text{-}144)\quad \ell_{ij} = \ell_{ij}(X_1,X_2,X_3)$$

and the linear Eulerian strain tensor components take the form

$$(B\text{-}145)\quad e_{ij} = e_{ij}(x_1,x_2,x_3)$$

arbitrarily chosen functions of X_1, X_2, and X_3 and x_1, x_2, and x_3 are not usually suitable expressions for ℓ_{ij} and e_{ij} because they lead to displacement fields $\underset{\sim}{u}(X_1,X_2,X_3)$ and $\underset{\sim}{u}(x_1,x_2,x_3)$ which are not physically reasonable, that is, to displacement fields which are not continuous and single valued. The equations that the strain components must satisfy in order to meet the criteria of being physically reasonable are called the compatibility equations. They are both necessary and sufficient conditions. This means that it is necessary

that the ℓ_{ij} and the e_{ij} satisfy these relations in order for the ℓ_{ij} and e_{ij} are to be suitable components of the linear Lagrangian and Eulerian strain tensors and that if the ℓ_{ij} and e_{ij} do satisfy these conditions their suitability is established.

There are 81 of these compatibility relations but only six are independent. They may be written very concisely in the form

$$\ell_{ij,kl} + \ell_{kl,ij} = \ell_{ik,jl} + \ell_{jl,ik} \tag{B-146}$$

(see Frederick and Chang, 1965). The combination of indices of the six independent equations can be obtained from the following tabulation

i	1	3	2	1	2	3
j	1	3	2	1	2	3
k	2	1	3	2	3	1
l	2	1	3	3	1	2

.

For the linear Eulerian strain tensor these relations take the form

$$e_{ij,kl} + e_{kl,ij} = e_{ik,jl} + e_{jl,ik} \cdot \tag{B-147}$$

The vita has been removed from the scanned document

A PHENOMENOLOGICAL TREATMENT OF THERMAL EXPANSION IN CRYSTALS OF THE LOWER SYMMETRY CLASSES AND THE CRYSTAL STRUCTURES OF $CaCoSi_2O_6$ AND $CaNiSi_2O_6$

by

John L. Schlenker

(ABSTRACT)

Thermal expansion in a crystal may be completely described from a phenomenological point of view by a second rank tensor whose elements are defined by

$$\lambda_{ij} = \left(\frac{\partial \ell_{ij}}{\partial T}\right)_\sigma$$

or

$$\varepsilon_{ij} = \left(\frac{\partial e_{ij}}{\partial T}\right)_\sigma$$

where the ℓ_{ij} and the e_{ij} are the elements of the linear Lagrangian and Eulerian strain tensors respectively. These λ_{ij} and ε_{ij} have been formulated in terms of crystal cell parameters. For example, for a monoclinic crystal the λ_{ij} are of the form:

$$\lambda_{11}(T) = \frac{1}{a_o \sin\beta_o} \frac{d[a(T)\sin\beta(T)]}{dT} ,$$

$$\lambda_{13}(T) = \frac{1}{2}\left(\frac{1}{a_o \sin\beta_o} \frac{d[a(T)\cos\beta(T)]}{dT} - \frac{\cot\beta_o}{c_o} \frac{dc(T)}{dT}\right) ,$$

$$\lambda_{22}(T) = \frac{1}{b_o} \frac{db(T)}{dT} ,$$

and

$$\lambda_{33}(T) = \frac{1}{c_o} \frac{dc(T)}{dT}$$

where a_o, b_o, c_o, and β_o are the crystal's cell parameters at some

reference temperature T_o. By expressing the crystal cell parameters as power series expansions in the temperature, thermal expansion coefficients have been computed for indialite (hexagonal cordierite), emerald and beryl and for the clinopyroxenes: diopside, hedenbergite, jadeite, ureyite, acmite, and spodumene. The extended Grüneisen equation has been used to further examine the nature of the thermal expansion in emerald, beryl, and diopside.

The crystal structures of the synthetic clinopyroxenes $CaCoSi_2O_6$ (cobalt diopside) and $CaNiSi_2O_6$ (nickel diopside) have also been determined.